Delft University of Technology
Faculty Electrical Engineering, Mathematics and Computer Science
Delft Institute of Applied Mathematics

Wind derivatives: hedging wind risk

A thesis submitted to the
Delft Institute of Applied Mathematics
in partial fulfillment of the requirements

for the degree of

MASTER OF SCIENCE
in
APPLIED MATHEMATICS

by

STEVEN HOYER

Delft, the Netherlands,
October 2013

MSc THESIS APPLIED MATHEMATICS

"Wind derivatives: hedging wind risk"

STEVEN HOYER

Delft University of Technology

Daily supervisor & responsible professor

Prof.dr. C. W. Oosterlee

Other thesis committee members

dr. ir. J.H.M. Anderluh

dr. H.M. Schuttelaars

J. de Leeuw MSc.

October, 2013

Delft

Preface

Over the last 11 months, I have done research in the field of wind derivatives for my MSc thesis. I performed this research in close cooperation with Mercurious, and my professor Kees Oosterlee. In October 2012 the MSc thesis project was born at CWI in Amsterdam. That day I met with Kees Oosterlee and Jerry de Leeuw (managing director of Mercurious). Mercurious had spotted the opportunity in the market, and services energy producing companies that were looking into wind risk hedging. Kees Oosterlee believed in the idea, and I was looking for a challenging thesis subject. This resulted in the start of the project in December 2012.

Although I have encountered wind for as long as I can remember, it was fun to dive into this phenomenon. Examining wind at this level was totally new for me, but as I noticed throughout the project, many people are interested in wind as a phenomenon. This makes talking about the MSc subject fun, even if it is not to fellow mathematicians. The project proved to be a nice mixture of a some physics, mathematics and a direct application. Combining this with wind turbines being a hot topic made this great project.

As I did the financial track within the MSc program of Applied Mathematics, an MSc thesis in this field was a logical choice. Although I had followed courses in Financial Mathematics and Computational Finance, it increased my understanding of these course significantly. It turned out that not much research had been done into wind derivatives. It was great to be one of the people to have a better look at wind as a statistical phenomenon.

In the first months I maintained a website (`http://www.windderivatives.com`) to keep people who were interested up-to-date. In a weekly update I wrote my progress and what I had done that week. For me, this was a great way to keep a good overview of what I was doing. After a couple of months, I had to focus more on the modeling, no interesting results were booked each week and I decided to stop updating the website.

This document presents an overview of the thesis work I did. The report is written for people who have understanding of basic probability theory, stochastic differential equations and a little mathematical finance. MATLAB was used for all the computations and the code is available upon request.

Acknowledgment

First of all, I want to thank all the members of my thesis committee: Prof. dr. C.W. Oosterlee, dr. ir. J.H.M. Anderluh, dr. H.M. Schuttelaars and Jerry de Leeuw MSc. Specifically, I want to thank my daily supervisor Prof. Kees Oosterlee for all of his continuous support and enthusiasm throughout the entire project. Kees has made me a much better mathematician, learned me to be exact and write pragmatic but also learned me how to apply mathematics and sell it to the industry. Furthermore, Kees made it possible for me to go to Toulouse for a one week wind and solar prediction conference, which brought me loads of inspiration. Additionally, I want to thank the people at CWI for many fruitful discussions about wind, wind energy and wind derivatives.

I owe great gratitude to Mercurious, and all of its staff for the possibility of doing my research in close cooperation with them. This cooperation added an extra angle to the research, a direct application in the market in terms of documentation, exercises and simulations that can directly be used in Mercurious' training and education business. Explicitly, I want to thank Jerry de Leeuw, managing director of Mercurious. Over the last year Jerry proved to be a sharp, smart and helpful person with a great eye for opportunities within the energy markets and a great network of people in the business with valuable thoughts on wind risk and wind derivatives. Moreover, I am grateful to all of the people 'in the business' who gave me endlessly many new insights and motivated me by their enthusiasm for the project. In special, I want to thank Arno Brand from ECN for helping me out on the physics and the wind power part, both areas which I was not very familiar with.

I would like to thank my friends and fellow students for their time and interest in my project. I have had many interesting conversations about wind and especially wind energy. This again showed the direct application, and motivated me to keep on working. Finally I want to thank my family for their unconditional support and confidence.

Contents

Chapter 1

Introduction

1.1 Weather risk

In 1999, Hanley [1] estimated that $ 1 trillion of the US's $ 7 trillion economy is affected by weather. This can be due to extreme cold, heat, rainfall, snowfall, sun, wind, et cetera. Dependence on weather causes weather risk. In this thesis we will focus on the financial weather risk. Financial risk can be defined [2] as the unexpected variability or volatility of returns. Some of this risk is covered by insurances, but the largest portion is not. To manage a part of this weather risk, some organizations apply weather derivatives. These contracts are traded at several exchanges, as well as Over-The-Counter (OTC). OTC transactions are transactions that are done directly between two parties, without any supervision or insurance of an exchange.

Financial products exist to hedge all kinds of risk. Since 1997, there also is a growing market for weather derivatives. These derivative products were introduced to control, hedge and mitigate all forms of weather risk. The specific subset of weather risk that will be of importance for this research is **wind risk**.

Over the last 10 years, there has been a growing awareness of weather risk. Also, worldwide there is an increasing environmental awareness. Governments are forced to think in a sustainable matter, and one consequence of this is government budgets are allocated to stimulate the construction of wind turbines. This yields a strong increase in the wind capacity around the world (Figure 1.1), which at its turn causes greater overall wind risk. The awareness of weather risk in general (and thus wind risk), and the dependence on wind are reasons to look at (possibly new) derivative contracts to handle this kind of risk.

Wind affects many things in life. Wind affects growth of all sorts of agricultural products. It influences wave heights at sea, and sometimes influences the temperature as we sense it. Closer to home, it influences the travel time when using a bike, in a both positive and negative sense, and it affects the way your hair looks after having encountered a storm. In short, wind influences all different things in daily life. Ever since 200 B.C. wind has influenced the output (f.e. kilograms of flour, or MWh of electricity) of windmills and wind turbines. This latter part will be the main interest in this research. Wind affects the production of electricity by wind turbines. As the number of wind turbines has steadily grown over the last couple of years, also the dependence on wind speeds grew over this same period. The uncertainty of generated electricity by wind turbines is getting so substantial, that it is interesting to look at methods to mitigate this uncertainty or

risk in some sense.

Electricity being produced by wind (turbines) is a hot topic these days. Wind is available for free and it is considered renewable. With wind power there are very little marginal costs in place. So once wind capacity is installed power generation is relatively cheap; or at least the variable costs can be ignored (the cost of installing the equipment can be costly, and maintenance should also be considered). Not only wind energy is a hot topic, but also the climate and the environment.

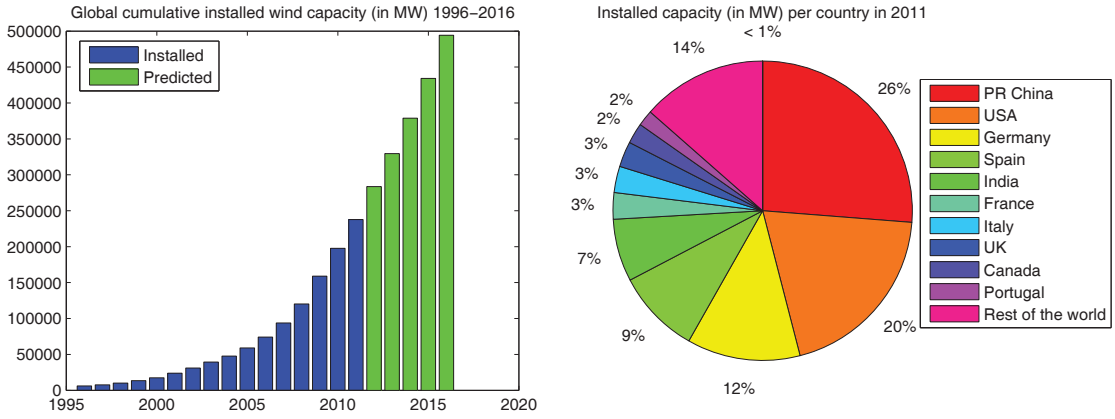

Figure 1.1: The global installed capacity per year (1996-2016) and per country (2011), with courtesy of GWEC

The fast growth over the past decade is clear, but the constantly increasing market also implies constantly increasing risk for the companies investing in these wind turbines. A possibility to decrease this wind risk, is by the use of wind derivatives.

A derivative contract is literally a contract 'around' an underlying product. The underlying will be expressed using a wind index. This wind index is a translation of wind speed or delivered wind power. In the case of wind derivatives, the wind index can be wind speed (f.e. average wind speed per hour, of average wind speed per day), but it can also be the generated amount of electricity (generated electricity per hour, generated electricity per day et cetera). The contract implies that two parties that agree with each other on a certain contract may have certain rights and obligations towards each other during this contract. This can be the right to a certain amount of money if certain criteria with respect to the wind speeds or wind power production are met, or of course the obligation to pay this amount. Since weather is not a tangible asset, most likely payments with respect to weather derivatives contracts will be done in cash. Possibilities for these wind derivative contracts are similar to some financial derivative contracts as they are traded on exchanges and OTC at the moment. As an example interest rate derivatives can be taken. Interest rate as underlying, is also not physically tradable, however there are ways to trade it on an exchange or OTC by means of bonds for example. Some examples of wind derivatives are wind options, wind futures or wind swaps.

1.2 Goal

The pre-defined goal of this research is to design (when necessary and not yet existent) and price several financial derivative products, such that wind risk can be hedged. This can for example be a combination of a wind turbine and a certain wind derivative contract yielding a steady cash flow over some years. A benefit of these derivatives can be that energy companies that produce electricity through wind turbines are financially less dependent of wind, or the lack of wind. Wind derivative contracts can possibly reduce risk for electricity generating companies. Furthermore, prices for certain contracts can be seen as a measure of the risk. Wind derivatives thus can be used as an indication of the price of wind risk, and can be used to financially hedge potential wind risk. Also, quantifying the uncertainty can be used when valuating an investment in a wind turbine park.

Research into this field has also been done by amongst others Alexandridis [3] (2012), Yamada [4] (2008) and A. Leroy [5] (2004). Our addition will be that a larger spectrum of wind derivatives will be considered, that seasonality effects will be modeled in a new way, and that well-known methods for fast and exact computations will be applied to the pricing and calibration of wind derivatives.

1.3 Overview

As the last part of this introduction we give an overview of how this thesis is built up. In Chapter 2 we consider the behavior of wind, wind speed and wind energy. Wind speeds over the last 8 to 50 years for different weather stations located in the Netherlands are analyzed, and the basics of wind energy are laid out. We take a look at seasonality effects and correlations of wind and discuss the prerequisite of wind energy to price wind derivative contracts. The link between wind speed and wind energy is an efficiency function of a certain wind turbine or park. A wind turbine's efficiency function is a curve that links the speed of wind to the power of the wind turbine or the output of a wind farm. This implies that the efficiency function is a mapping of the wind speed in m/s to the amount of power in MWh. Data will usually be measured as average wind speed (in m/s) per hour. This means the efficiency function can also be seen as the mapping of the wind speed to the amount of generated energy (kWh). Note that in this thesis we will use the words power and electricity interchangeably, but they have exactly the same meaning. Our focus will be on offshore wind turbines. Moreover, we do not consider climate change with respect to wind speeds, nor will we consider the effect of varying wind speeds at different heights and the effect this has on the wind turbine.

When the distribution of wind is known, and the efficiency function of a certain wind turbine is known as well, also the distribution of generated wind power is available. We assume that from this process, the price of a wind power derivative can be calculated.

In Chapter 3 we discuss various wind derivative contracts. Using this model for wind, several kinds of wind derivative contracts can be priced. Differently from other literature like [3], [4] and [5], a distinction will be made between wind speed derivative contracts, and wind power derivative contracts. This distinction is shown in more detail in Figure 1.3.

Wind speed derivatives include all derivative contracts with underlying being a wind speed index, and a wind index has unit [m/s]. This wind speed index can for example be a translation of wind speeds over a certain period or a deviation from a seasonal mean. Wind power derivatives include contracts with a wind power index as underlying. This wind power index is a translation

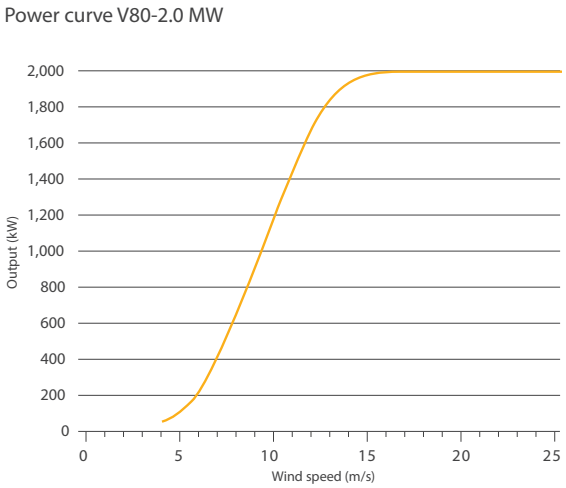

Figure 1.2: The efficiency function of an Vestas V80 2MW wind turbine, with courtesy of Vestas.

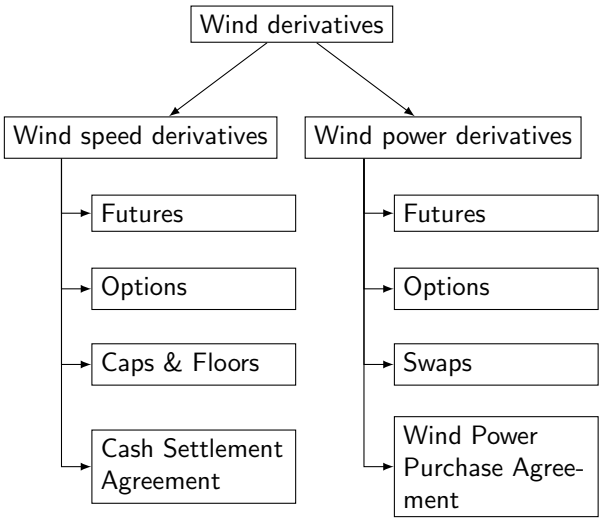

Figure 1.3: Distinction of wind speed and power derivatives.

of the amount of produced electricity by a wind turbine, and the unit of a wind power index is [MWh]. Our focus will be on long term wind derivatives. These are contracts that start at least one month from present, and may have contract durations of one day up to several years. We assume that these contracts can be priced using historical behavior. For short term valuation of derivatives, prediction techniques could be applied. No emphasis will lie on the possible market for wind derivatives. Possible counterparties will shortly be discussed but we will not elaborate on the future of wind derivatives market.

After having examined wind, in Chapter 4 wind is modeled. We consider wind models that in-

corporate seasonal effects and a model that does not incorporate seasonal effects. The goal of Chapter 4 is to reproduce wind speeds as accurate as possible using the available data. This means that when little data is available, wind will have to be modeled without seasonality effects, whereas when sufficient data is available, a seasonality function can be extracted and wind can be modeled in more detail. At the end of Chapter 4, we will suggest one model for modeling wind speeds without seasonality, and one model for reconstructing wind speeds with seasonality.

In Chapter 5 we consider how wind speed and power derivatives can be priced. We discuss on the unavailability of a risk neutral measure, and consider several methods to price wind derivatives. Analytical solutions to derivatives will be given when possible, otherwise pricing is done by the Monte Carlo method, numerical methods or the COS-method. Analytical solutions and the COS-method approach may be useful for calibration purposes. We will not elaborate on the modeling of electricity.

Finally we will conclude and look forward in Chapter 6. The results of this thesis will be summarized, and further recommendations and ideas are given about wind. These ideas are not necessarily in the field of wind derivatives, but also in related fields.

Chapter 2

Wind & wind energy

Before analyzing wind-related financial instruments, the characteristics of wind need to be discussed. A wind speed index (transformed wind speed) may be the direct underlying for wind speed derivatives, and wind speed is a part of the underlying of wind power derivatives, a wind power index. In this chapter, we first look into the 'phenomenon' wind. Furthermore, we look into the volatility of wind speed, the distribution of wind speed, the daily and yearly seasonality, the dependency of wind with respect to other components of the weather and the predictability of wind on the short and long term. This will be done using freely available data as measured in the Netherlands, as detailed below.

2.1 Definition of wind

Wind is nothing but air in motion. It is formed because of the difference in air pressure at different sites. Wind can be defined as air moving in horizontal and vertical directions. So, to be clear, wind doesn't move, but air moves and this causes wind. For this research, we consider only the horizontal wind speeds, and for now we ignore the wind direction. The horizontal wind speed has by far the greatest effect on the electricity production, and also most derivatives that have been traded OTC only considered horizontal wind speeds. In further research it would be very interesting to look at a vector of 2 elements, the wind speed and the wind direction, and model these as one process, but for now this is not our aim.

Although the vertical component in wind speed is assumed to be fairly small and not very influential for the generation of wind energy, the speed of this vertical component is important for the daily weather as we sense and see it. The fact that vertical wind has this influence, is because rising air will cool down, often due to saturation, and can then lead to clouds and precipitation. On the other hand, sinking air warms and thus causes clouds to disappear and this leads to 'good' (warm and dry) weather. The vertical wind speed may thus have influence on other weather components. This may be interesting when looking at other kinds of weather derivatives.

There are three main forces that are the cause of the phenomenon wind. The **pressure gradient force** is a force that equalizes pressure differences. This force causes air to flow from high pressure to low pressure areas. The second force that influences wind is called the **Coriolis force**. This force comes from the Earth turning around its axis. This force also causes objects in the northern hemisphere to turn to the right and objects in the southern hemisphere to turn to the left. As the Earth rotates in a counter-clockwise direction with respect to its axis anything moving over a

long distance above its surface is deflected, because as something moves freely above the Earth's surface, the Earth is moving east under the object at a faster speed. The third force is **friction**. Friction is a force that slows motion and dampens kinetic energy. This force causes wind to blow slower near the ground.

To get familiar with wind, some examples will be provided below. Almost everyone is familiar with a weatherman talking about high and low pressure zones, and nearly everyone knows the red H's and the blue L's on the map to show respectively high and low pressure fields. Below is explained why high pressure fields often causes warm and 'good' (again warm and dry) weather, and why low pressure fields have the opposite effect.

Example

Conservation of mass is a property of air and it refers to the fact that mass cannot be created or destroyed in a given area. What happens to the converging winds near a low pressure field? Air cannot 'pile up' at a given spot. As it rises the air cools off. When air is cooled it can hold less water vapor so some of the vapor condenses, forming clouds and precipitation. Of course, the whole process is more complex, but this is a heuristic insight into why the weather is often considered bad near low pressure areas.

Example

Diverging air near high pressure fields has the opposite effect. As the air spreads away from the high pressure, air from above replaces it. This sinking air warms up, and as air warms it can hold more water vapor, which means that clouds will tend to evaporate. Again a simple heuristic insight into why good, generally accepted as comfortable, weather is often associated with high pressure.

2.2 Data used to analyze wind speed

The data to analyze wind speeds in this thesis has been provided by the Dutch meteorological institute (KNMI). This is publicly available data, downloaded from the KNMI website. The dataset consists of hourly average wind speeds (measured continuously in time [6]), as well as the average wind direction of every hour (also measured continuously in time). Locations of various weather stations, measuring wind speeds, are shown in Figure 2.1. Also, data of some offshore wind locations has been included; these locations lie rather far from the Dutch coast, and are therefore not visible in Figure 2.1, since the map is rather small. Local situations (climate) obviously impact outcomes, but the concepts described apply -more or less- to all areas.

The data that has been used are so called **potential wind data** [7]. This means that all wind data has been corrected for height and local surroundings. Figure 2.2 shows how this translation is done. The measured wind speeds of each station are translated to a height of ten meters above sea level and a surroundings roughness of 0.03 m is taken. The transformation is done using the logarithmic wind speed profile. This profile will be explained below.

Figure 2.1: Geographical location of the weather stations of KNMI, with courtesy of KNMI.

For the translations of wind speed at different heights, our main interest lies in the wind speeds in the so called surface layer. This is the layer of air from the ground up to 100 meters in the air. To use the KNMI data for wind turbine purposes, we must transform the potential wind speed to get representable wind speeds for a height, which can also be done using the logarithmic wind speed profile. The potential wind data is thus translated to a height of 10 meters. Our interest however, lies in the wind speeds at about 80 meters. There is an easy formula to approximate wind speeds $V(h)$ at different heights [7] [8, p.10]:

$$V(\mathrm{h}) = V(\mathrm{h_{ref}}) \frac{\ln(\mathrm{h}/z_0)}{\ln(\mathrm{h_{ref}}/\mathrm{z}_0)}, \tag{2.1}$$

where $V(\mathrm{h})$ is the speed at the chosen height, $V(\mathrm{h_{ref}})$ is the potential wind speed at 10 meters, and z_0 is the roughness length. The greater z_0 is, the more the wind speed is decreased by the surrounding terrain. Popularly said, z_0 can be seen as the height at which wind speed is zero [7]. This translation is considered to be a satisfactory one for both onshore and offshore wind speed. This logarithmic translating is used by the KNMI when translating wind data measurements to potential wind data [9].

The data has been made applicable for this thesis, by using Equation (2.1) in which $h = 80$, $h_{\mathrm{ref}} = 10$. z_0 is equal to 0.03 for onshore wind sites, and 0.002 for offshore wind sites. For this research, three different locations were used to analyze the behavior of wind over the years. These are three different wind sites, with different properties. These three locations are De Bilt, Schaar and Maastricht. For each of the wind sites, data over the last 40 years is available. This data will give a useful insight of how wind behaves at these locations. The analysis of these three sites should also give an indication of how wind behaves at different places in the Netherlands. We have chosen to thoroughly analyze three wind sites with different properties. Of course, wind will be differently at other places on Earth, but the principles will be similar. We shortly introduce

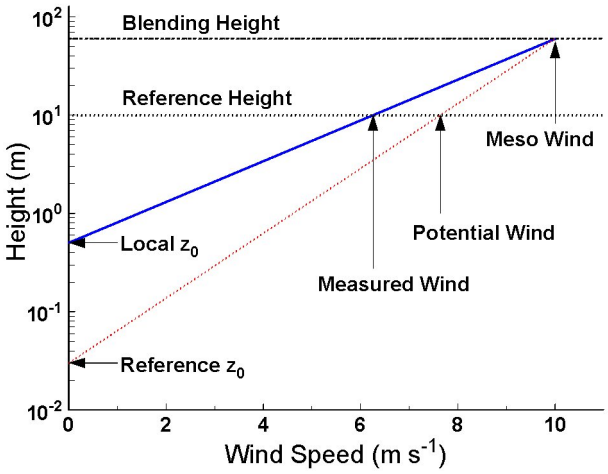

Figure 2.2: The translation of wind measurements to potential wind data, provided by the KNMI.

the wind sites, and explain the differences between these stations.

De Bilt
The KNMI is headquartered in De Bilt. Temperature data has been stored for over 100 years, and wind data for over 50 years. De Bilt is located in the center of The Netherlands, but the country is so small that De Bilt may even have influence of wind from sea.

Schaar
Schaar is an offshore wind site. Comparing this location to two onshore sites clearly shows the differences between on- and offshore wind.

Maastricht
For wind at the east border of the Netherlands, a weather station in the city of Maastricht is used. The Maastricht area is governed by some small hills in its surroundings, and it is also the most in-land site available for KNMI data. This may give different insights than the other two wind sites.

Station location	Measuring height	Roughness surroundings	Latitude, Longitude
De Bilt	20 m	0.03 m	[52.0999, 5.1770]
Schaar	16.5 m	0.002 m	[51.6552, 3.6942]
Maastricht	10 m	0.03 m	[50.9096, 5.7675]

Table 2.1: Specifics of three wind sites in The Netherlands

With respect to these locations, four different aspects were taken into account. First of all, the average development of the wind speed on a single day is considered. After that, the average wind speeds per week, month, and season are discussed to look at seasonality effects. For the pricing of a derivative, a wind speed distribution is a prerequisite, which is considered third. The last part is a part about wind directions and shows how the wind direction is distributed for several sites. While doing this thesis, in cooperation with 3 students from the Hogeschool van Amsterdam, we

designed a software tool which displays the characteristics of wind per wind site. A screen shot of this software can be found in Figure 2.3. Each of the KNMI weather stations can be loaded, a time slot can be chosen, and the software displays graphs of yearly seasonality, the diurnal cycle per month of the year, wind speed distribution and a wind rose.

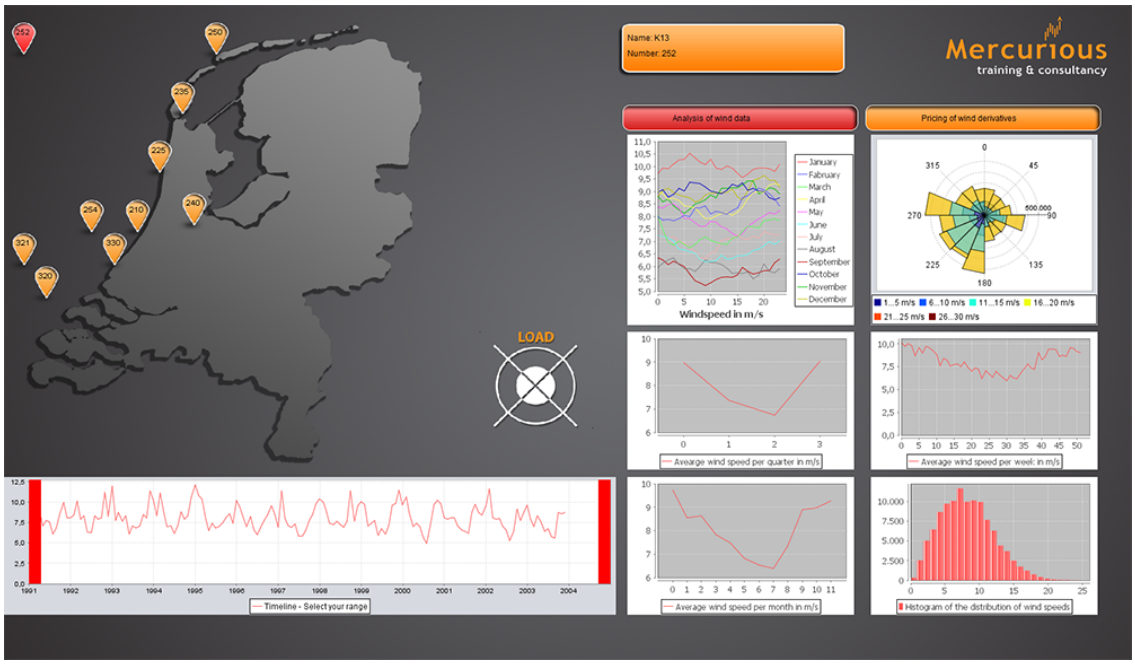

Figure 2.3: A wind speed characteristics tool, made for Mercurious for educational purposes, provided by Mercurious

Leap years

Astronomically, the Earth rotates around the sun four times in 1461 days. The time it takes the Earth to rotate around the sun is thus not exactly 365 days, hence the leap year every four years. This is a small inconvenience with respect to the modeling of wind speeds. When we will consider months, these will be calender months. This means that in leap years, February 29th is taken to be a day of February. When considering weeks, the year is split up into 52 parts. This means that in normal years, the last week of the year incorporates eight days. In leap years, the last week incorporates nine days.

Quality of data

For precise modeling of wind speeds, the wind speed data has to satisfy certain data quality requirements. The used data, supplied by the KNMI, is assumed to be of good quality, however due to varying local surroundings and possible changes in measuring equipment, certain patterns can be found in the data that we think are not representative for the wind behavior. In this thesis we will accept stilling wind speeds and wind speed variability due to changes in local surroundings, but we do not draw conclusions on the actual stilling of the wind climate. The decrease in wind speed and wind variability may be caused by increasing tree or building size, or an increased density of buildings in the near surroundings. Furthermore, we do not account for changes in

measurement equipment. We assume that any change in measurement techniques has improved the quality of the data, but this does not make earlier data negligible.

2.3 Properties of wind

In this section, several properties of wind will be discussed. We start with an explanation about the behavior of wind at different heights. After that we look into the development of wind speed over one day, and over one year. Finally, we discuss the distribution of wind speed. Some smaller issues that we look into are the difference between onshore and offshore wind, the direction of wind, the dependence of wind on other weather components, and the long term prediction of wind speed.

Difference in wind behavior at different heights

The daily development of wind speeds is also called a **diurnal cycle**. The diurnal cycle for all locations is different at different heights. In Figure 2.4 the measurements at Cabauw are shown. Cabauw is a specific wind site located between Utrecht and Rotterdam. At Cabauw, wind speed is measured at different heights at the same time.

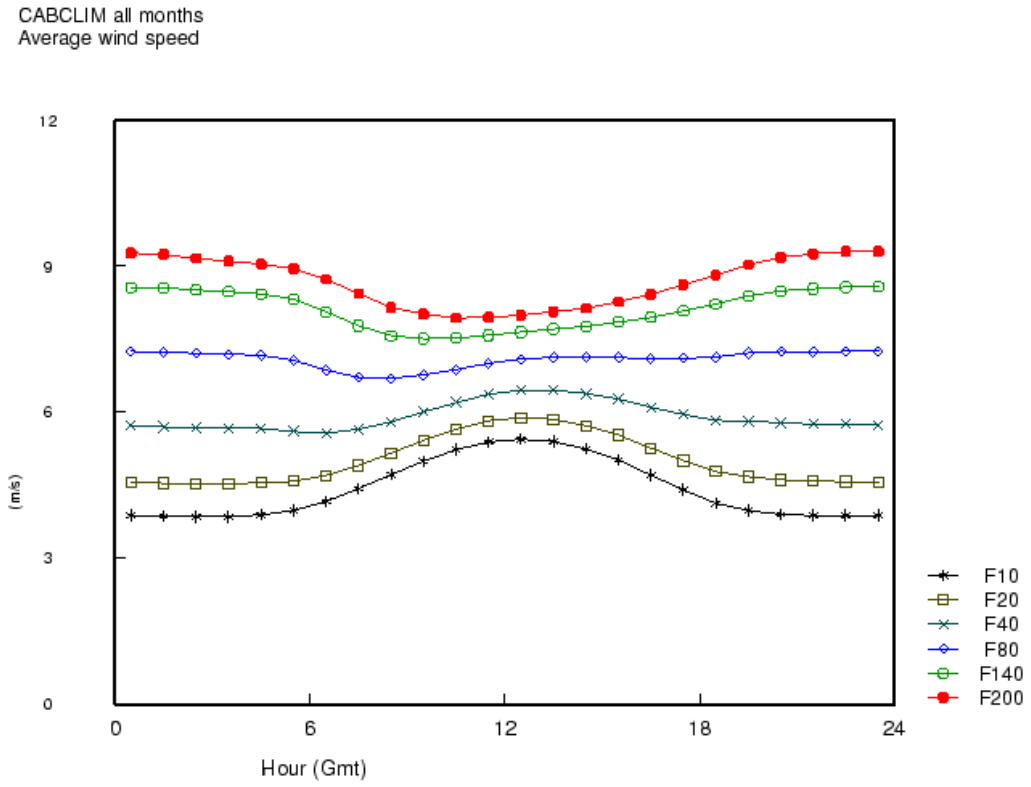

Figure 2.4: The daily wind speeds at different heights at the same wind site, provided by KNMI

Figure 2.4 shows the wind speed at different heights at different times per day. From Figure 2.4 it is clear that the nearer to the ground, the less constant the diurnal cycle is. When going up in altitude, to around 80 meters, there is hardly a diurnal cycle measured, and the behavior is mirrored when going to even greater heights. We conclude that onshore wind has different diurnal cycles at different heights. A second conclusion from Figure 2.4 is that wind speeds increase when the height at which it is measured increases. This has to do with the third important force that has an effect on the wind speed, i.e. friction. What can also be seen from this figure is that the blending height lies around 60 meters. This is the height at which wind speeds on average are most constant throughout a day.

Seasonality in wind speed data

In this section, the seasonality of wind speed data will be discussed. Note here that seasonality does not necessarily mean that we consider the meteorological seasons, but any form of returning pattern within the wind speed data. Recalling, the development of the average wind speeds over a day is called the diurnal cycle.

Diurnal cycle

The diurnal cycle is different for wind speeds over land than for wind speeds over sea. This can best be seen in Figure 2.5, which displays the diurnal cycles for the three wind sites that were mentioned above, and also shows the standard deviation of the wind speed data per hour. Note that since we're considering potential wind data, the height on which these figures are based is 10 meters for all wind sites.

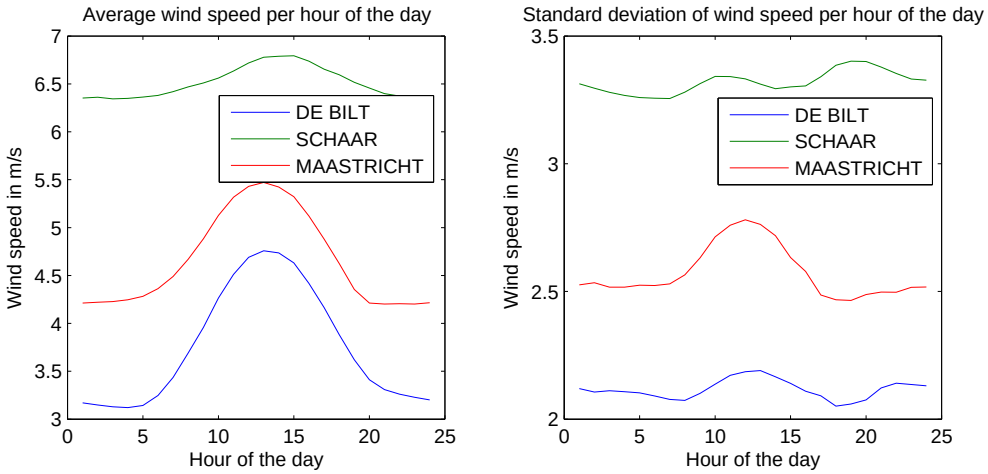

Figure 2.5: The diurnal cycle for the three wind sites from data over the last 40 years

It can be seen that the most constant diurnal cycle is measured at Schaar. Maastricht and De Bilt show a clear daily pattern in their diurnal cycles. At these sites, daily heating and maybe buildings or nature have more effect on the average wind speeds. This has to do with the daily temperature differences being greater when the site is located further away from sea. A direct consequence of this is that offshore diurnal cycles for wind speed will always be more stable than onshore diurnal cycles. The temperature above sea is more stable, due to the constant warming/cooling of the water. The difference between the diurnal cycles of De Bilt and Maastricht can be explained by the fact that the Maastricht station is located higher above sea level (but measured from the same

distance to the ground). Also, the wind speed at Maastricht seems to be 1 m/s higher than the wind speed in De Bilt due to the local surroundings of both wind sites. The KNMI tries to make sure that the surroundings have as little effect on the measurements as possible, but the exact same circumstances are never created. Looking at the standard deviation of the wind speed data per hour, we conclude that over sea the standard deviation is quite constant. However, looking at Maastricht, also the standard deviation appears to exhibit a seasonal pattern.

Yearly cycle

When looking at the daily average wind speed per week or month of the year, the seasonal effect can clearly be seen in Figure 2.6. In the summer, the average wind speeds are lower than the average wind speeds in the winter. This again is connected to the distance of the Netherlands to the sun in different seasons. This makes pressure differences greater in the winter than in the summer. A direct result is that wind speeds are higher on average in the winter than in the summer. In Figure 2.6 the weekly and monthly average wind speeds have been plotted, as well as the weekly and monthly standard deviations.

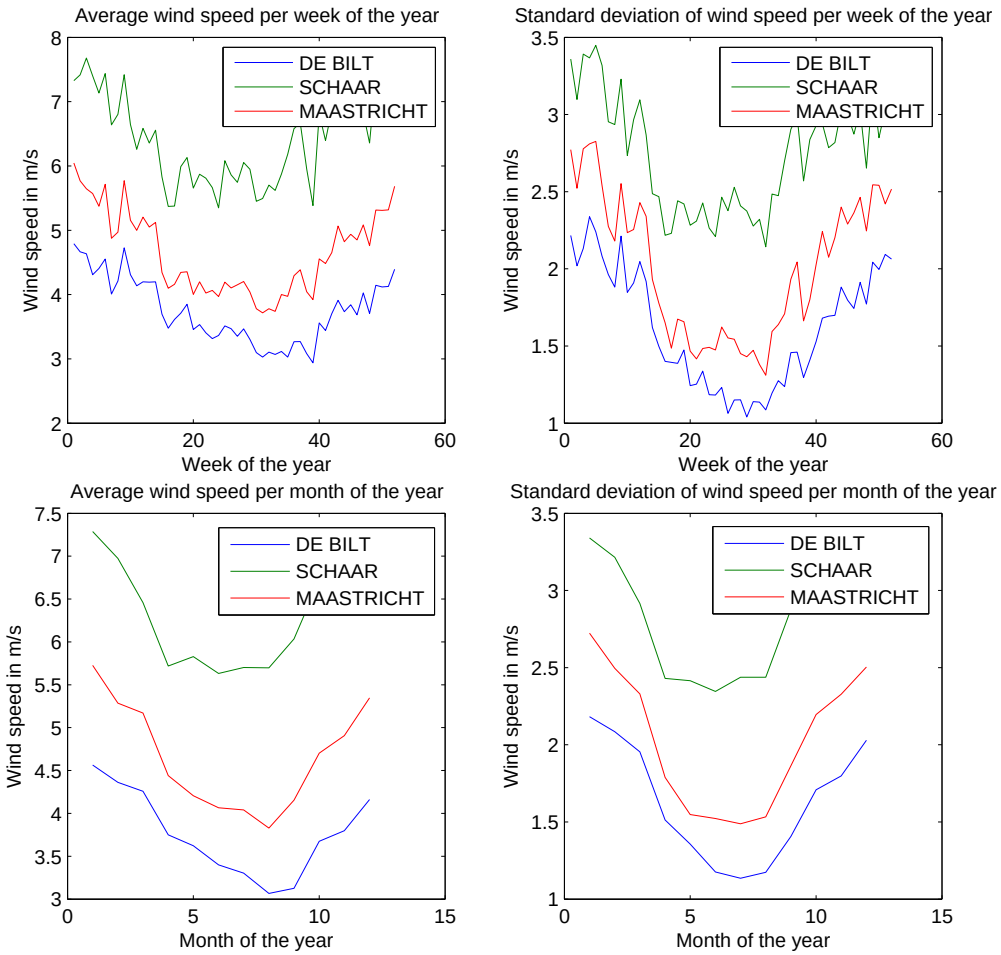

Figure 2.6: The average wind speeds and standard deviations per week and per month of the year

As the wind speed per week or month of the year differs from the average wind speed (wind speed shows a seasonal pattern), it is also interesting to look into the volatility (a measure of variability of wind speeds, higher volatility indicates more variability within the wind speed data) of the wind speed data. To this extent, we plotted the standard deviation of the wind data per month for the station of De Bilt. The result is also shown in Figure 2.6. This figure shows that also the volatility of wind speed is greater in the winter, and smaller in the summer. Here the volatility (σ) is defined as:

$$\sigma = \sqrt{\left(\frac{1}{M-1}\sum_{i=1}^{M}\left(y_i - \sum_{i=1}^{M}\frac{y_i}{M}\right)^2\right)},$$

where y_i is the i-th day of the data set, which consists of M points. When considering weekly volatility of 10 years of data, this data set will consist of $M = 7 \cdot 10 = 70$ data points. If the volatility of wind in a day of the year is considered, the data set will consist of as many points as years are used (in our previous example 10 data points). A period can be one day of the year (f.e. May 23nd), a week of the year (f.e. week 17) or a month (f.e. June).

From the average wind speed per hour of the day and the average wind speed per week/month of the year, we conclude that wind speed is governed by to two seasonal effects: a daily effect and a yearly effect. The first effect is due to the fact that the Earth rotates around its axis. The second effect is caused by the rotation of the Earth around the sun. Also, the standard deviation shows a seasonal pattern when looking at a whole year. When looking at the diurnal cycle, volatility looks almost constant.

Distribution of wind speed

The distribution of wind speeds over the last 40 years in De Bilt are shown in Figure 2.7. This figure shows how daily (upper) and hourly (lower) wind speeds are distributed. First of all we would like to mention something about the quality of the data. Apparently, the measurement system is somewhat imprecise, as the distributions of hourly wind speed data and hourly differences show.

The distribution of wind speeds for Schaar, De Bilt and Maastricht are shown in Figure 2.8. On average, wind speeds are higher at the site of Schaar. The average wind speeds of De Bilt and Maastricht do not differ much. This confirms the difference between onshore and offshore wind speeds.

2.3.1 Dependence of wind speed

As stated earlier, wind is moving air. The speed at which air moves will depend on several elements. It has already been concluded that wind speed depends on the location of the measurement points. This is related to the roughness of the surroundings, as well as the subsoil (ground, sea). Furthermore, it may depend on temperature, location and wind direction.

Using KNMI data, average wind speed over one hour or a day can be tested for correlation against the hourly or daily average of other weather components. We have tested wind direction (in degrees), wind speed (in m/s), temperature (in degrees Celsius), radiation (in J/cm^2), pressure (in hPa), horizontal sight (0 means less than 100m, 1=100-200m, 2=200-300m,..., 49=4900-5000m, 50=5-6km, 56=6-7km, 57=7-8km, ..., 79=29-30km, 80=30-35km, 81=35-40km,..., 89=more than

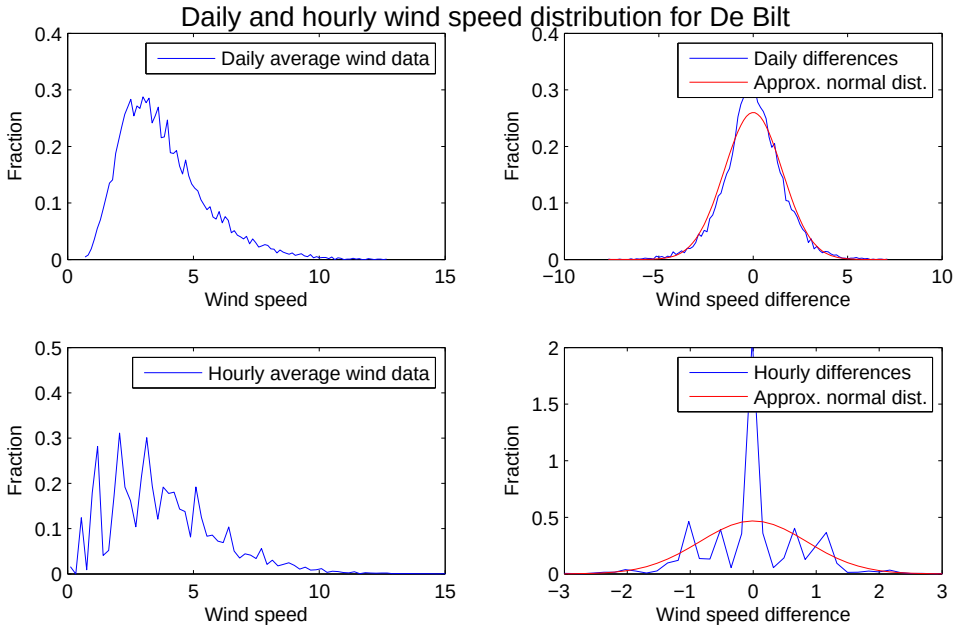

Figure 2.7: Daily (upper) and hourly (lower) wind speeds and differences distributions.

70km), overcast (scale 0-9, where 9 means upper air is not visible), humidity (percentage). To look into correlations we have tested both the measured data vectors, as well as the hourly or daily differences vectors for correlation. The testing is based on computing the correlation for the measured data, and daily or hourly differences of the measured data in MATLAB.

The correlations of the absolute and differentiated hourly and daily averages of these weather components are presented in correlation matrices. To see any (longer term) influence, we also checked lagged correlations until 7 data points away (7 hours/days later). A visual representation of the correlation matrices can be found in Figure A.1 up to Figure A.4. These figures show the correlations of the eight mentioned weather components, for the daily and hourly averages, and the average daily and hourly differences with lags from 0 to 7. Since we look at the correlations of wind speed data with other weather components, we're mainly interested in the second row and second column of these figures.

From these figures we conclude that there is no clear correlation between the daily and hourly differences. However, some weather components seem correlated in the absolute data. We see in Figure A.1 that wind speed and temperature are (slightly) negatively correlated, and the same is concluded for wind speed and radiation and for wind speed and pressure. With respect to the correlation with temperature, this indicates that as temperature goes up, wind speed decreases. This is in accordance with the seasonal effects we have seen. This also implies that in some way, certain wind risk could partly be hedged by considering temperature (dependent) derivatives.

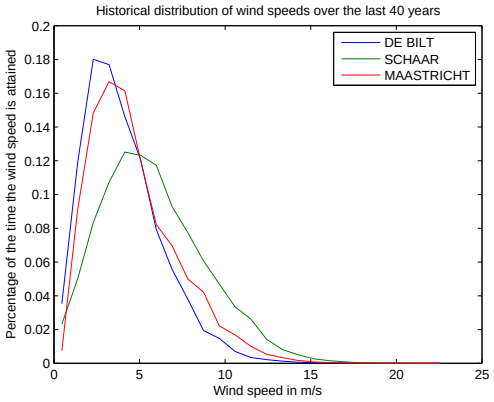

Figure 2.8: The distribution of daily average wind speeds for Schaar, De Bilt and Maastricht.

Temperature

Average wind speed is not directly connected with the temperature. This means that high temperatures do not necessarily guarantees high or low wind speeds. However, we know that temperature also shows a seasonal effect due to the position of the Netherlands and the distance of the Earth in relation to the sun. Around the equator most direct heat is to be found. Temperature on average will be lower in the winter than in the summer, but wind speeds will on average be higher in the winter than in the summer. This would indicate a negative correlation. Figure A.1 shows that this is indeed the case, albeit a slight negative correlation.

Wind direction

As wind is defined as moving air, this means that when standing at a certain point, the wind will arrive at a certain speed and a certain angle. Figure 2.9 shows the distribution of the wind directions for the three stations. Overall, the wind comes mostly from the south west. This is logical for the Netherlands when looking at the major drivers of wind speed, the Coriolis force and the pressure gradient force. An image of the windflows around the world is also included in Figure 2.9.

Local area

Wind behaves differently at different locations. We have already seen that on average wind speeds at sea are higher than wind speeds on land. This is because the wind is not inhibited by its surroundings. Also, the diurnal cycle is different above land than it is above sea. This diurnal cycle differs because temperature on land fluctuates much more than temperature above the sea.

2.3.2 Long term prediction of wind speeds

Scientific articles about the long term trend of wind speeds and wind directions are available. Vautard et al. [10] found a downward trend in observed surface winds for most of the northern Hemisphere between 1979 and 2008. They hypothesized that this is partly due to increasing surface roughness caused by increasing vegetation. This is of course of less interest when looking to offshore wind sites, than it is for onshore wind sites. However, another article by Bakker [11] has doubts about the used methodology in [10]. More research about climate change and its effect on

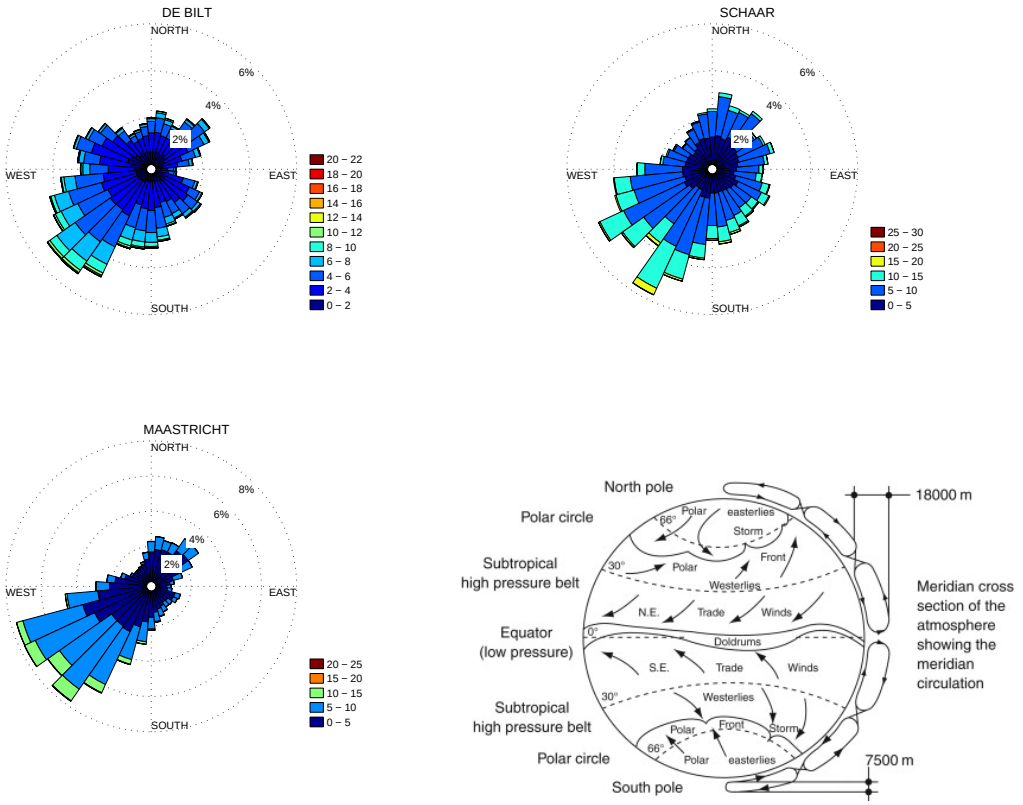

Figure 2.9: The daily wind speeds at different heights at the same wind site, with courtesy of KNMI.

wind speeds is currently performed, however no clear overall conclusion can be drawn.

In this thesis, we will not focus on incorporating or modeling changes of climate or long term trends for wind speeds, so we assume a stable climate. This is a harsh assumption, as we know that climate is (always) changing. Incorporating climate change is however beyond the scope of this thesis.

2.4 Wind power

To price wind power derivatives, we need to have a basic understanding of wind energy. Many good and comprehensive books are written about wind power [12, 13, 14]. We shortly discuss the basics of wind power. Wind power is the conversion of wind energy into electricity. A possible tool to convert the energy of wind into power is a wind turbine. The goal of a wind turbine is to generate as much power from moving air (wind) as possible. To approximate the amount of power that is generated by a wind turbine, we should know how much kinetic energy wind generates, and how much of this energy can be captured by a wind turbine and turned into electricity. Schematically this looks as in Figure 2.10:

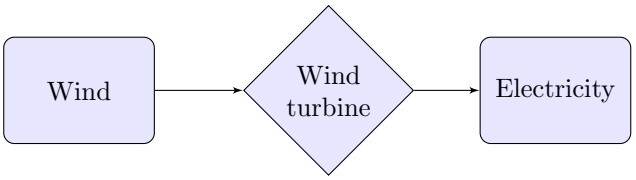

Figure 2.10: Flow chart of the transformation of wind to electricity.

In this section, we discuss approximations of the electricity production from a wind turbine and where this production depends on. We shortly discuss the physical background of power and energy. We then discuss how energy can be extracted from wind, and the wind turbine specifics to calculate how much electricity approximately is generated. A generic function is given by which wind speed can be mapped to generated electricity. This mapping of wind speed to generated wind energy is called the **efficiency function** or the **power curve**.

2.4.1 Kinetic energy

In physical context, the kinetic energy (E) of a system with mass m (in kg) and speed v (in m/s) is defined as:

$$E = \frac{1}{2}mv^2. \tag{2.2}$$

E is expressed in kg $(\text{m/s})^2$, Nm, J or Ws. In our case, we're interested in the kinetic energy of wind. We may express mass m as the total mass of the air that moves through an imaginary area A. Physics laws yield that the mass of moving air can be expressed as follows [12]:

$$m = A\rho tv, \tag{2.3}$$

where A is the imaginary area, ρ is the density of the air, t is the time in seconds that air moves through this area, and v is the speed that the air that moves through the area has. Combining (2.2) and (2.3) gives

$$E = \frac{1}{2}A\rho t v^3.$$

Furthermore, we know that power and energy are related via a time component:

$$P = \frac{E}{t}.$$

So P can be expressed in J/s, or in W. When considering the power that can be extracted from wind, the unit is, for example, kW, whereas the energy that is extracted from wind we talk about kWh. The total power can be expressed as:

$$P = \frac{1}{2}A\rho v^3.$$

The power is extracted by the blades of the wind turbine. For a wind turbine, the area A that was considered above, is equal to the total rotor swept area. This is the area that is covered by the blades of a wind turbine. Assuming a diameter D of the blades of a certain wind turbine, this yields a rotor swept area of $\pi(\frac{D}{2})^2$. This means that the wind power is defined as follows:

$$P = \frac{1}{2}\pi\left(\frac{D}{2}\right)^2\rho v^3$$

2.4.2 Extracting the power from wind

With the power of wind expressed, we look at how this power can be extracted from wind, and how it is converted to electricity. The most basic way to look at the amount of energy that is absorbed by the blades of a wind turbine is to take the difference of the wind power before the wind hits the blades and the wind power after the wind has hit the blades. Let v be the speed at which the wind hits the blades (this is also called the upstream wind speed), and let v_0 be the speed of wind after it hit the blades (the downstream wind speed). We then have the following approximation for the power extracted by the rotor [12]:

$$\begin{aligned} P &= \frac{1}{2}\{\text{mass flow rate per second}\}(v^2 - v_0^2) \\ &= \frac{1}{2}A\rho v(v^2 - v_0^2). \end{aligned}$$

As in [12], we ignore advanced aerodynamics at this stage and take the wind speed to be the average of the upstream wind speed and downstream wind speed: $\frac{v+v_0}{2}$. After rearranging we find the following expression for the power extracted from the blades:

$$P = \frac{1}{2}\rho A\frac{v+v_0}{2}(v^2 - v_0^2) \tag{2.4}$$

$$= \frac{1}{2}\rho A v^3\frac{\left(1+\frac{v_0}{v}\right)\left(1-\left(\frac{v_0}{v}\right)^2\right)}{2}. \tag{2.5}$$

(2.4) expresses the total amount of power that is extracted from the wind. The fraction of the upstream wind power that is captured by the blades can also be expressed by C_p:

$$C_p = \frac{\left(1+\frac{v_0}{v}\right)\left(1-\left(\frac{v_0}{v}\right)^2\right)}{2}. \tag{2.6}$$

C_p, the fraction of the upstream wind that is captured can at most be 0.59. This is also known as the Betz limit or Betz' law [15]. A derivation of this number can be found in Appendix A.1. C_p, the fraction of upstream wind that is captured by the blades is dependent of the upstream downstream wind rate ($\frac{v_0}{v}$). For each wind turbine this function will be a different curve. An image that can often be found in literature to compare different types of wind turbines originates from Eldridge [16]. In Figure 2.11 this image to compare different types of wind turbines is shown. Although this figures dates from 1980, it gives a good idea of wind turbine efficiency functions. In this picture, the rotor efficiency is set out against the ratio of the blade tip speed to wind speed (the speed of a blade tip, divided by the speed of upstream wind). So, the wind turbine efficiency is set out against the ratio $\frac{v_{tip}}{v}$ (v_{tip} is the blade tip speed). The choice to plot the efficiency function against the tip-speed ratio is to get a clear comparison of all wind turbine types.

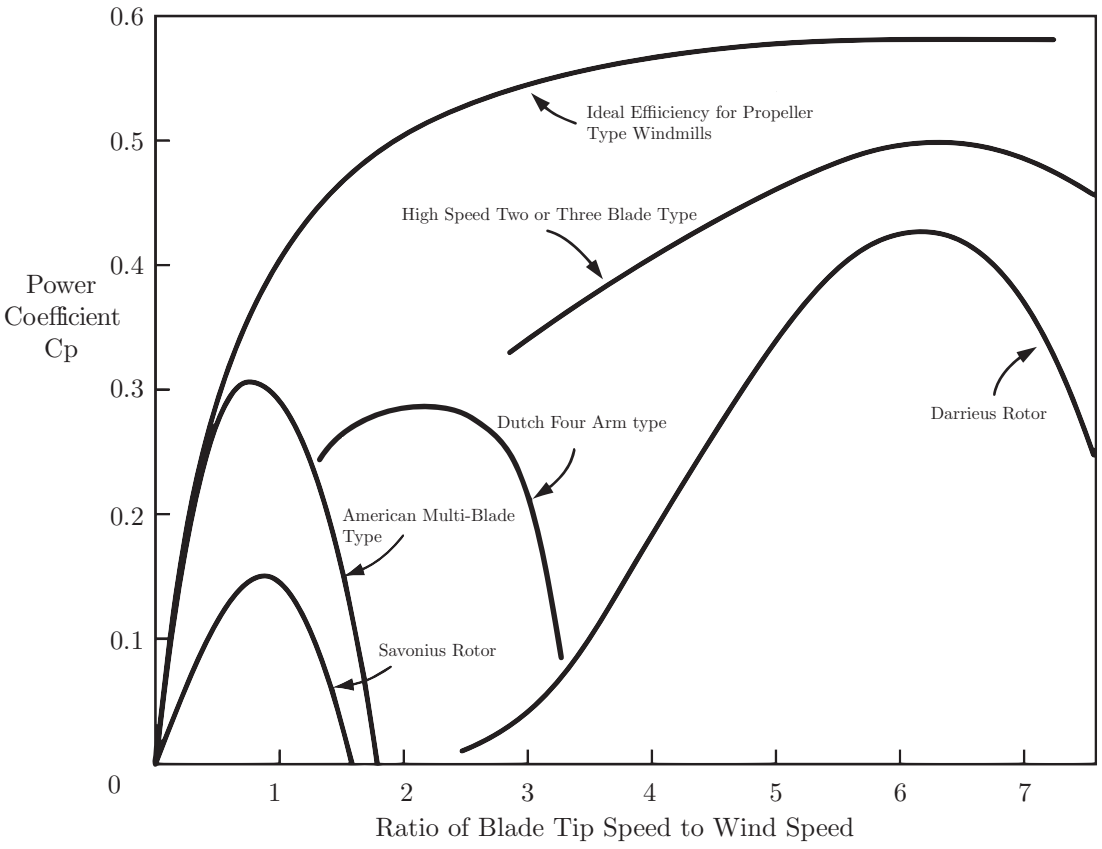

Figure 2.11: Comparison of several types of wind turbines and the maximum power coefficient, with courtesy of Eldridge.

In practice, a continuous curve for $C_p(v)$ will not be given by the supplier (i.e. Vestas, Siemens,

et cetera) of a wind turbine. Instead, an approximation per wind speed in m/s of generated electricity in kWh is given. Of course, an approximation of this function as a continuous time function can be computed. This means that a generic formula is dependent on ρ, D and v. All the above yields the following generic efficiency function for wind turbines:

$$P(\rho, D, v) = \frac{1}{2}\pi D^2 \rho C_p(v) v^3,$$

where D is the diameter of the wind turbine blades, v is the wind speed, ρ is the air density and $C_p(v)$ is the efficiency function. D is a fixed value, which depends only on the model type of wind turbine. v is the wind speed. The wind speed v is the most important variable in the efficiency function. The amount of generated electricity is in relation with the cube of the wind speed. It is important to get an accurate estimate of v before we are able to approximate the amount of generated electricity because of this dependence. Another conclusion that can be drawn, since wind speed is highly volatile, the generated amount of electricity will be as well. This means that the wind speed should not be considered over a too long period. Preferably a period of 10 to 15 minutes is considered for the average wind speed. If such a short period is used, the variation of the wind speed over a small interval of time is obviated. Furthermore, there are constant deviations in wind speed. Wind turbines these days are so tall that the wind speed is constantly different at its lowest and highest points. We translate the wind speed to the wind turbine's shaft height. The translation will be done using the logarithmic wind profile. $C_p(v)$ is the efficiency function of a wind turbine. As was mentioned, the efficiency function is given by the turbine producer as a discrete function. $C_p(v)$ will be dependent of, amongst others, the generator, the gearbox and the blade design of a specific wind turbine. The air density, ρ, is not a constant, but it is dependent of the air pressure (p) and the temperature (T). If the relative humidity is low, ρ can be expressed as [12]:

$$\rho = \frac{p}{T \cdot R},$$

where R is the gas constant. The air pressure and temperature differ, so ρ is not a fixed value, but a variable.

efficiency function in practice

In practice, the efficiency of a wind turbine is not a smooth function, but values follow a pattern. An example of measurements is given in Figure 2.12 [17].

The deviations from the given efficiency function can be explained by quickly varying wind speeds within the measurement times, the wind directions and the differences in air density.

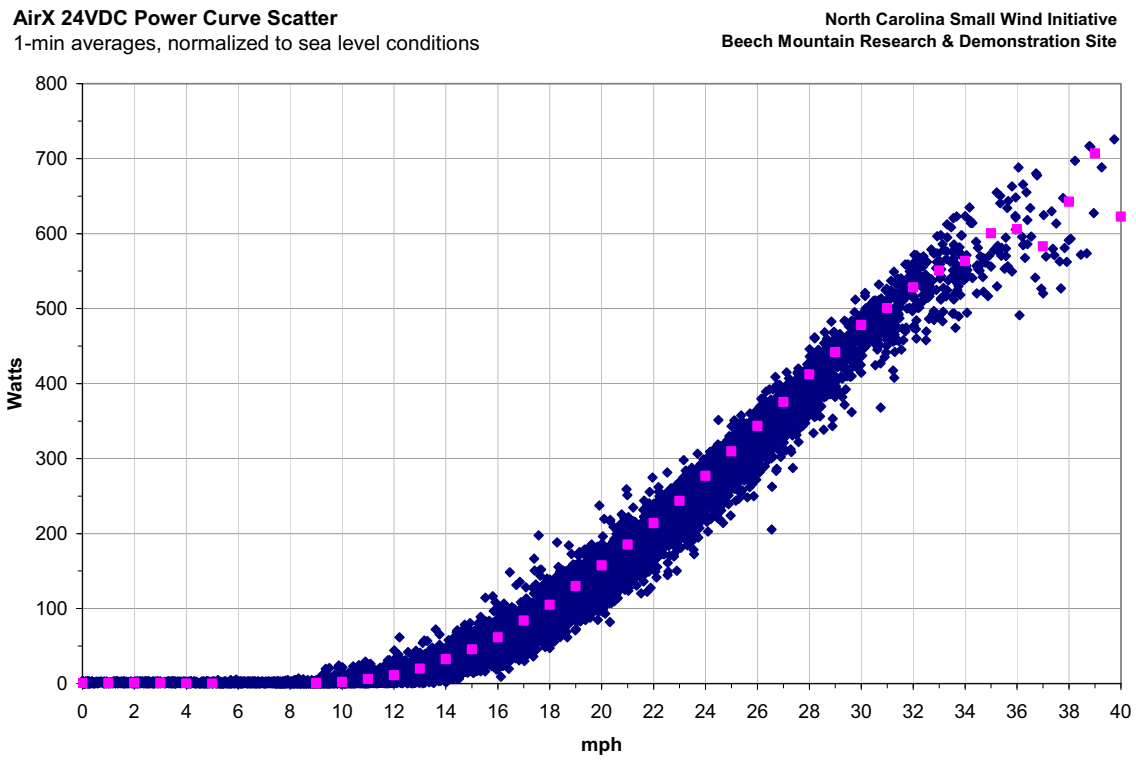

Figure 2.12: Measurements of wind speed vs. electricity production, with courtesy of Western North Carolina Renewable Energy Initiative.

Chapter 3

Hedging instruments for wind risk

After a discussion on wind and wind power, in this chapter various wind derivatives can be discussed. In the introduction, it was already mentioned that in this thesis we consider essentially two types of wind derivatives: wind speed derivatives and wind power derivatives. Academic literature about wind derivatives is mainly about wind speed derivatives. We start with an introduction of wind indices, and after that we consider wind speed and power derivatives of several kinds as mentioned in Figure 1.3. Furthermore, we suggest some other ways to hedge wind risk and elaborate on possible counterparties for wind derivatives.

3.1 Wind indices

The underlyings for wind speed and wind power derivatives will be certain wind indices. For wind indices, the same distinction is made as for wind derivatives, we consider wind speed indices and wind power indices. A wind speed index is a translation of the wind speed or delivered wind power at a certain location. This means that for wind speed derivatives, a wind index is used which is based on wind speed as underlying. A wind speed index can f.e. consist of hourly average wind data, translated to the height of 80 meters. A wind index translation usually incorporates a translation to the desired wind speed height, and an averaging of data to get to the desired time scale. The wind index is not the only variable that influences the contract and price. Also, a reference wind speed or power supply K and maturity T need to be defined. In the case of wind derivatives, the total time to maturity is split up into N equally sized periods. This period may be an hour, a week or a month, depending on the contract. This means that the contract is alive from $t_0 = 0$ until $t_N = T$. WS_i or WP_i will be the wind index in period i and is defined for M being the amount of data points between t_i and t_{i-1}. The size of M will thus depend on the raw data, and the type of underlying that is needed for a wind derivative contract. A visual representation of this time line is given in Figure 3.1.

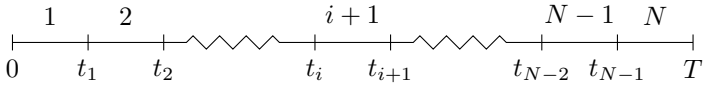

Figure 3.1: Time to maturity split up in N equally sized periods.

Within each of these N intervals, M data points are known. Using this notation, the average wind speed over i-th M points is taken to be WS_i:

$$WS_i = \sum_{j=1}^{M} \frac{S_j}{M}, \tag{3.1}$$

where M are the amount of data points in interval i, and the whole period of the contract consists of N intervals. When averaging over N data points gives the final expression for a wind speed index WS. Note here that the subscript i is dropped.

$$WS = \sum_{i=1}^{N} \frac{WS_i}{N}, \tag{3.2}$$

If, for example, we look at a wind speed index for a one week contract, which considers daily average wind speeds, and S_j is measured in hours, M will be 24. Furthermore, N is equal to the amount of days in the contract, 7. An example of a real life wind index that was used in the market (NORDIX Financial Wind Indexes) will be given in the Section 3.3.

For wind power derivatives, two different types of wind power indices can be reviewed. The underlying can be the translation (using an efficiency function) of measured wind speed to wind power electricity, but also the amount of generated electricity. In both cases, the wind power index represents an amount of MWh. The wind power index can be the translation of wind speed to the expected production in MWh through the efficiency function, but it can also simply be the cube of the wind speed multiplied with a certain constant [18]. Wind power indices can be of the following form:

$$WP_i = \sum_{j=1}^{M} \frac{f(S_j)}{M}, \quad \text{or} \tag{3.3}$$

$$WP_i = \sum_{j=1}^{M} \frac{P_j}{M}, \tag{3.4}$$

where WP_i is the i-th data point in the data set of wind power data, $f(S_j)$ is the translation of the j-th wind speed measurement to generated amount of electricity through a given efficiency function, P_j is j-th generated electricity measurement and M is again the amount of averaged data points. Possible averaging over N days gives the following expression for a wind power index WP:

$$WP = \sum_{i=1}^{N} \frac{WP_i}{N} \tag{3.5}$$

In reality, in the beginning of a wind turbine project, wind power derivatives with produced amount of electricity as underlying will be somewhat involved to price, due to a lack of power generation data, and this data will be needed if f.e. seasonality effects have to be modeled. If wind speed data are available for a longer period of time (which usually is the case since an owner of a wind farm has done research into the wind climate before the wind turbines start to produce electricity), it is possible to model generation data by first modeling wind speed data, and transforming these by using an efficiency function. Two examples of wind indices that can be useful for hedging wind risk are given below.

Example - Wind Speed Index
Certain hourly average wind speed data is available for a wind site. This wind data is measured at 10m height. An example of a Wind Speed Index can be the daily average wind speed, after the hourly data has been translated to 80m height.

Example - Wind Power Index
For another site, quarter of an hour wind speed data is available is available for 5 years, and hourly power generation data is available for 1 year. Again, this wind data is measured at 10 meters height. A first example of a Wind Power Index can be a double translation, first the translation of the wind speed to 80m height, and after that the translation using the provided efficiency function of a certain wind turbine. Any averaging can happen after both translations. Also, a multiplication can be done to represent the electricity price per kWh. A second example can be to just use the power generation data as wind power index.

The notation of (3.2) and (3.5) disguises the fact that these underlyings are path dependent. This makes payoff functions look straight forward, where in fact they are not.

3.2 Exchange-traded wind derivatives

A short review on the types of derivatives that were listed is provided in this section. Also, some recent information about possible reintroduction of wind derivatives on an exchange will be mentioned, combined with the reasoning why currently wind derivatives are not listed.

USFE

The U.S. Futures Exchange introduced electronically traded wind (speed) derivatives in August 2007 [19] [20] [21], and these products were listed until the U.S. Futures Exchanged was closed at 31th December 2008. The USFE listed seven different wind derivative products. The underlying values of these seven contracts were derived from the NORDIX Financial Wind Indexes. The NORDIX Financial Wind Indexes, created by an American company called Weather Bid LLC, were composed of deviations from 20-year historical wind speed averages compared to present daily figures. The USFE's futures contracts were based on two wind regions in New York and five wind regions in Texas, as defined by the National Oceanic and Atmospheric Administration's (NOAA) National Center for Environmental Prediction division.

CME-group

CME-Group, responsible for the world's largest derivatives exchange, headquartered in Chicago, is currently looking into introducing electronically traded wind derivatives [22]. They claim that many of their clients are interested in wind derivatives, but the problem lies finding counterparties and in the difference in wind data that is used and interpreted by their customers to price the wind derivative contracts. Parties do not necessarily have access to the same data, and also there is no general easy way to price wind derivatives accordingly. A solution to this problem may be consensus about how to price wind speed derivatives.

3.3 OTC traded wind derivatives

At the time of writing both wind speed and power derivatives are not traded at an exchange, but they are traded OTC [18]. According to the authors of [23], in 2011 the total market value for wind derivatives was $36 million. Most likely, these were all wind speed derivatives [18]. Some examples of different types of wind derivative contracts are mentioned below.

Since wind cannot be delivered, it is sensible to compare wind speed derivatives to instruments that were introduced to, for example, hedge interest rate risk or volatility risk. Also, the interest rate is not a physical object, but it can give rise to significant risk for a company. It is plausible [18] that a wind derivatives market will relate to an interest rate market or volatility market in terms of focus on OTC transactions because of the dependency of specific wind locations. Instruments that are known in the financial market to hedge interest rate risk or volatility risk are mostly cash settlement agreements or swaps, meaning that a certain amount of cash is delivered if a certain event happens. Wind speed derivatives may fall in the same category.

To determine which types of derivatives can be of interest when pricing wind power derivatives, it can be noted that wind power is a commodity, and can physically be delivered. For commodities, other types of derivatives are used to hedge risk like, for example, futures and (swing) options. In the case of commodity derivatives, the focus is more on the possibility of delivery. A possible difference of a wind power derivative with respect to well-known commodity derivatives is that the amount of electricity delivered is uncertain due to uncertainty in wind speeds. This differs from commodity futures or options on f.e. oil or cacao, where only the price is uncertain. The market so far works with plain European call and put options [18], cash settlement agreements (CSAs) [24], wind power production agreements (Wind PPAs) and wind power swaps [25]. Furthermore, it may be interesting to look at wind power derivatives for a whole wind farm [26].

3.3.1 Wind speed derivatives

We consider various wind speed derivatives here. The underlying is a wind speed index in the form of an average over a certain period (as was the case for the USFE wind futures [19]). We consider four different kinds of wind speed derivatives: futures, options, caps & floors and wind speed cash settlement agreements.

Futures

A futures contract is a contract between two parties whereby the buyer (seller) has the obligation to buy (sell) the underlying at a fixed time for a fixed price. The wind speed derivative contracts which were listed at the USFE, mentioned in Section 3.2, are examples of wind futures. For a future (or forward if the contract is traded OTC), the payoff function is as follows:

$$\mathrm{F}(WS, T) = WS - K. \tag{3.6}$$

Here $F(WS, T)$ denotes the price of a future or forward at time T, WS is the wind index, at T, and K is the reference wind speed. On exchanges, futures of a certain underlying are often traded with monthly expiration and delivery price 0. Below, an USFE wind futures example is given.

Example
From August 2007, until December 2008, the USFE listed seven different wind futures. These futures were traded with monthly expiries, and the futures trade at \$500 per index point, with a tick size of \$5. The tick size is the smallest price difference that can occur (i.e. the price is \$5 or multiple of \$5.). At the end of each month, the settling price was the sum of daily deviations of 20 year daily average wind speeds. Consider the wind speed index that models average wind speed per month. If reference wind speed, K, is taken to be the average monthly wind speed of 20 years of data, the USFE is of the form of (3.6).

Options

A second kind of wind speed derivative contracts is represented by wind speed options. Like options in the financial world, a distinction can be made between call and put options. A call (put) option gives the buyer the right to buy (sell) a certain underlying (in our case a wind speed/power index) for a certain price at a possibly fixed point in time. The seller of this call (put) option, then has the obligation to sell (buy) this underlying for the price agreed upon, at the time that the buyer executes his option, or at maturity. Clearly, options never have a negative price, nor will the buyer have to put in extra money at maturity. Options exist in all kinds of forms.

Wind options have not been listed at an exchange, but they were traded OTC [18]. When considering wind speed options and wind power options, some options are more interesting than others. Our focus will be on so-called average rate Asian options. These are options where the underlying value is an arithmetic mean of the underlying. The payoff of an average rate Asian call looks as follows [27]:

$$\max\left(\frac{1}{N}\sum_{i=1}^{N} S(t_i), 0\right), \tag{3.7}$$

where $S(t_i)$ is the value of the underlying at time t_i, and the value is measured at times t_1 up to and including maturity $t_N = T$. A wind speed index as defined in (3.2), is the monthly average, and thus an arithmetic mean of 28,29,30 or 31 data points of daily average wind speeds. By defining a wind index, the averaging is already incorporated in the underlying. The maturity of an option is a certain date at which the option expires. This means that the option has no value after maturity date.

When considering wind speed options, most interesting are options that give a payoff at maturity if the wind speed in the period the contract was either too high or too low. These are exactly the Asian type of average rate options with path dependent payoff. The payoff of such an option with fixed strike would look as follows:

$$\begin{aligned} \text{Call}(WS, T) &= \max(WS - K, 0) \\ \text{Put}(WS, T) &= \max(K - WS, 0) \end{aligned}$$

where WS is a certain wind index (so an arithmetic average of the underlying), and K represents a reference wind speed. If wind speeds are higher than the reference wind speed K, the payoff will increase. However, it is also interesting to look at Asian-style options with a fixed payoff, these are types of cash-or-nothing options of which payoffs depend on whether the average wind

speed is below or exceeds the reference wind speed. In this case the payoff will be defined as a cash-or-nothing call option:

$$\text{CON-Call}(WS, T) = \begin{cases} H & \text{if } WS \geq K, \\ 0 & \text{if } WS < K, \end{cases}$$

and the payoff for a cash-or-nothing put option will be defined as

$$\text{CON-Put}(WS, T) = \begin{cases} 0 & \text{if } WS \geq K, \\ H & \text{if } WS < K. \end{cases}$$

For both payoffs, H is the height of the payoff.

Example
Company ABC buys a wind speed cash or nothing call from company XYZ. The contract period is 1 week, and the reference speed is 5 m/s. The payoff if the average wind speed over the whole week is less than 5 m/s, will be €600,-. At the end of the week, the average wind speed was 5.1 m/s. This means that the payoff is zero. If the wind speed would have been 0.2 m/s lower, the payoff would have been €600,-.

Caps & Floors

A wind speed cap is a derivative in which the buyer receives payments at the end of each period in which the wind speed exceeded the agreed strike price (reference wind speed). The period here can be a day, a week, a month, et cetera. The wind speed cap can be seen and analyzed as a series of European call options that exist for each period the cap agreement is 'alive'. One European call option of this series is also referred to as a **caplet**. The payoff of a wind speed cap reads as follows:

$$\text{Cap}(WS, T) = \sum_{i=1}^{N} \frac{\max(WS_i - K, 0)}{N}, \tag{3.8}$$

where N represents the number of periods, WS_i the i-th set of M data points, as in (3.1), and K is the strike price or reference wind speed.

A wind speed floor is similar to a wind speed cap, except that this time a payment will be done if the average wind speed over a certain period is below the reference wind speed. A wind speed floor can be seen as a series of European put options. One European put option of this series is sometimes also called a **floorlet**. The payoff of a wind speed floor would look as follows:

$$\text{Floor}(WS, T) = \sum_{i=1}^{N} \frac{\max(K - WS_i, 0)}{N}, \tag{3.9}$$

where again M stands for the number of periods, WS_i is the i-th value of a wind index and K is the reference wind speed. If caps and call options over an equal period are considered, the difference lies in the fact that less averaging is done for the caps. For contract buyers this yields more flexibility. Since less averaging is done, also the volatility of a cap or floor will be higher.

Wind Speed Cash Settlement Agreement

Like in the case of options, the switch can be made to cash-or-nothing payoffs per caplet or floorlet. For this contract, M periods of equal length are considered. This construction yields a wind speed cash settlement agreement (WSCSA) [24]. This is a derivatives contract that gives the seller the obligation to pay a certain amount of cash per day in which the wind speed on average was above a certain fixed wind speed (reference wind speed) within a certain fixed period. This could also be a contract in which the seller has the obligation to pay a certain fixed amount of money each day that the average wind speed over a day was below a certain fixed speed. A distinction between cash settled caps (CSAcap), and cash settled floors (CSAfloor) can be made. The payoffs look like

$$\begin{aligned} \text{CSAcap}(S,T) &= \sum_{i=1}^{N} \frac{H}{N} \mathbb{1}_{K<WS_i}, \\ \text{CSAfloor}(S,T) &= \sum_{i=1}^{N} \frac{H}{N} \mathbb{1}_{K>WS_i}. \end{aligned}$$

Here $\mathbb{1}_A$ is the indicator function for the event A, and WS_i as in (3.1).

Example
Company ABC and company XYZ agree on a CSAcap for the month October 2013. Per day that the average wind speed is above 10 m/s, company ABC will pay €750,- to company XYZ. If the average wind speed is more than 10 m/s for the total of 7 days, the payoff is 7*€750 = €5250.

3.3.2 Wind power derivatives

Wind power derivatives are derivatives with a wind power index as underlying. Like well-known power derivatives, wind power derivatives can be settled both physically and with cash. The underlying wind power index can be based on delivered power, and the generated wind power can be seen as the commodity. This shows the more complicated part of this derivative when modeling mathematically, since the amount of generated wind power is uncertain. The uncertainty relates to the wind speeds, wind direction, the variation of wind speeds, the failure of the wind turbine, et cetera. All these uncertainties lead to fluctuations in power production. Since power cannot be stored (at least not in large portions, in an economical viable way), this variation of power supply from wind turbines affects energy companies which have to secure supply to energy consumers (e.g. households and industry). The payoff of a wind power derivative with as underlying generated electricity is easily calculated. This could imply that we do not need the efficiency function. The reasons why we need to make use of the efficiency function when pricing wind power derivatives is because there always is less data available on generated wind power than there is on wind speed data. This means we need the wind speed data and an efficiency function to model wind power generation.

For wind power derivatives, we also consider 4 types of derivatives. First, we consider futures and options, which look similar to the contracts for wind speed derivatives. After that we consider wind power swaps, and Wind Power Purchase Agreements.

Futures

Regarding wind power, also future contracts exist, which are futures contracts with a wind power index as underlying. The payoff for a wind power future looks like the payoff for a wind speed future:

$$\mathrm{F}(WP, T) = WP - K,$$

where WP is the wind power index and K is the reference power supply. Again K can be taken equal to zero as is done in many other future contracts. The wind power index WP will be an average of either delivered wind power or an average of translated wind speed.

Options

Wind power options are only slightly different from the wind speed options. We consider a call option and a put option, having the following payoffs:

$$\begin{aligned}\mathrm{Call}(WP, T) &= \max(WP - K, 0)\\ \mathrm{Put}(WP, T) &= \max(K - WP, 0),\end{aligned}$$

where WP is a wind power index and K is the reference wind power supply. The only difference from wind speed options is the underlying. A wind power index is also an arithmetic average, hence wind power options are also Asian average rate options.

Swaps

Another type of derivative is a swap. In the financial world, swaps are often used to hedge interest rate risk or volatility. In such a contract, f.e. an uncertain interest rate is traded for a certain interest rate or vice versa. The same can be done for wind. When considering a wind turbine, the risk lies in the uncertainty of delivered power. One way to mitigate this risk is the use of a wind power swap. A wind power swap is an instrument whereby an uncertain amount of electricity is traded for a fixed amount of electricity and a (possibly negative) amount of money. A swap can have various maturities, these maturities can differ from one day to several months or years. A wind power swap would have a wind power index based on delivered wind power or translated wind speed, and the payoff of a wind power swap looks as follows:

$$\mathrm{Swap}(S, T) \quad = \quad \sum_{i=1}^{N} WP_i - E_i B - K,$$

where WP_i is the wind power index period i as in (3.3) and (3.4), E_i is the electricity price over this period, B is the fixed amount of electricity that is sold back in the deal, and K is the strike price or reference power supply. A wind swap can be seen as the difference of a wind power future and a usual power future:

$$\begin{aligned}\mathrm{Swap}(S, T) &= \sum_{i=1}^{N} WP_i - BE_i - K\\ &= \sum_{i=1}^{N} WP_i - K_1 - (BE_i - K_2),\end{aligned}$$

so that $K = K_1 - K_2$. E_i is the electricity price in period i. For now it can be chosen to have a fixed electricity price to restrain the complexity. The payoff of a wind power swap may indicate that it is possible to partly hedge wind power derivatives with a power contract. A perfect hedge will be involved to set up, since power contracts are traded on monthly basis on six months ahead. With maturity further away, only quarterly or even yearly contracts can be traded in. Since a wind power swap can be seen as a combination of a wind power future and a power future, we will elaborate on the pricing of a wind power swap. We assume there are satisfactory models to price well-known power futures, and using this in combination with a wind power future yields a wind power swap.

Example
Company A pays €50,- and 100 kWh to Company B for the total generated amount of electricity in one day of a wind turbine which is property of Company B.

Wind Power purchase agreement

Power purchase agreements (PPA) have existed for as long as electricity has been sold. In the broadest sense, a PPA is a contract between two companies that states that one company will buy a possibly, but not necessarily fixed amount of wind generated electricity for a possibly, but again not necessarily fixed price per MWh. These contracts can become really complex, sometimes including fines for not purchasing sufficient wind generated electricity. Also, the electricity price may vary throughout the contract. Possibilities of price variation may be due to the fact that electricity is bought at different hours, with different spot prices. This derivative is similar to a wind power future with a wind power index based on the provided amount of electricity. For wind turbines, we consider a wind power purchase agreement (Wind PPA) [28]. This contract can be seen as a long-term hedging tool, but since it will have many uncertain variables and clauses it may be difficult to model it accurately.

Wind farm derivative

For companies, it may be interesting to look at a whole wind farm instead of a single wind turbine [26]. Ecofys, a former Dutch company, claimed that they could price tailor-made contracts [29]. Looking at a wind farm as a weighted sum of various wind turbines, an efficiency function for the wind farm can easily be computed. All wind power derivatives can also be priced under the assumption that the efficiency function of a wind farm is approximated by a weighted sum of efficiency functions of all wind turbines in the wind farm. This can be interpreted as a weighted sum, and not an ordinary sum of efficiency functions, since the position of one wind turbine influences the efficiency of the other, which implies that a wind farm is not as efficient as the exact sum of independent wind turbines. Splitting this contract up in smaller parts, it can be seen that this is just a sum of certain wind power futures.

3.4 Counterparties

At present, there is no exchange listed market, and wind derivative transactions are purely done OTC. The OTC market is not very liquid [22] [18], which is partly caused by a lack of counterparties for wind derivatives. Selling a risk is interesting, but buying the risk may be somewhat less interesting. Here we split up the range of contracts into short term (maturity up to one week), mid term (maturity of one week up to 3 months) and long term (maturity over 3 months). For

all categories we consider who could be on the buy and sell side of a transaction. Of course, a trading firm (like f.e. EDF trading or Danske Commodities) can be in the middle of this market, trading to both buyers and sellers.

Short term

First of all, we consider short term contracts, which are contracts with maturity up to one week. Contracts like these are interesting for speculators, who can be weather forecasters that have their own models, and find 'arbitrage' like opportunities. Also, the trading desk of an energy company can be interested in buying risk if they have in recent times sold much more mid or long term risk. A special case would be an energy company that focuses on nuclear or inflexible coal plants, as their cash flows on short term may significantly depend on wind speed, as a surplus of electricity may cause a decrease of electricity price. However, companies that focus on nuclear or inflexible coal plants cannot easily turn back their electricity production, and are thus forced to sell large amounts of electricity to the market for relatively low prices. Furthermore, rig operators can be interested to stand on the sell side of a deal, since they are affected by high wind speeds since maintenance to oil platforms, wind turbines et cetera would then be difficult. Rig operators often have performance based contracts, in which they may have to pay a fine if maintenance is not done in time. When on the sell side of a wind derivative deal, they at least get a cash reimburse if they cannot do the maintenance. The North sea could be a good example of where these deals can take place, due to the relatively high density of wind farms and oil platforms.

Mid term

Mid term contracts are contracts with maturity of one week up to 3 months. Financing parties can be specifically interested in mid term contracts. Companies that finance significant wind energy projects (large corporate banks) are also exposed to wind risk. This risk lies in the inability of the owner of a wind park to pay the interest on the borrowed money. Also, like in the case for short term contracts, energy companies that focus on inflexible conventional energy sources may be interested in mid term wind derivative contracts.

Long term

Long term contracts are contracts that have maturity of 3 months or more. From [22] we know that for long term contracts, big private equity houses or hedge funds can be interested into taking on the wind risk from an energy producing company. They will have their own models, and they see investing in these contracts as diversification of their portfolio, since weather is not correlated to stock exchanges or corporate business.

3.5 Non-derivative way of hedging wind risk

We have looked at several wind derivative contracts. However, wind derivatives are not the only way to successfully mitigate wind risk. Below, some other ways to partly manage wind risk or mitigate wind risk are mentioned.

Correlation between several wind farms

When considering two wind farms at totally different locations in the world, these farms will approximately have independent power productions. This mitigation of risk is based on that the probability of low wind speeds at two independent farms is smaller than the probability of low

wind speeds at one farm. For locations not to have correlations in wind speed, the distances have to be relatively large. When considering the North Sea near England and the North Sea near Denmark, it would be possible to have the electricity transported to the same grid, however in practice this probably will hardly happen. This means that only financial risk is mitigated, as cash flows coming from a sum of wind farms should be more stable than for a single wind turbine, by the same reasoning that the probability of two farms generating a lot or no electricity is smaller than just considering one wind farm.

Hedging at client contracts

Another way of hedging risk is by mitigating it to the client side. In this case, clients can be energy suppliers, but also normal and big households or companies. In such contracts, a wind speed clause can be built in. This mitigating can only be done by companies who actually have a supplier side. Contracts with variable prices for electricity are examples of this.

Example

Eneco, a Dutch energy producer and supplier introduced a client side product called *HollandseWind and gas* focused on the consumer. The higher the average wind speed, the higher a certain discount to the consumers' power price is. The company advertises with a possible discount of €108 per three years. On average, a customer with such a contract will most likely pay a bit more in the beginning, and get back some money when the average wind speed is above a certain level over a certain period of time.

This is an example for households, but similar ways of mitigating risk can also be thought of for contracts with companies or energy suppliers.

Correlation wind speed and electricity or gas price

In recent years it has shown that the electricity market is getting increasingly dependent on wind. Since more and more wind turbines are being built, this dependency will increase over the next couple of years [25]. This opens a window of opportunity to hedge wind speed and power derivatives by setting up a portfolio of a wind derivative and well-known power derivatives. These thoughts are strengthened by the authors in [30] and [31], who suggest the use of a well-known power, gas or coal contracts to party hedge for temperature risk. Similar thoughts are applicable for wind risk hedging. Since electricity prices are established by supply and demand, if there is wind, electricity is produced, which may cause an electricity surplus, that causes prices to drop. This would indicate a negative correlation between wind speed and electricity price. It may be possible to hedge wind risk with electricity contracts. If f.e. wind speeds in the Netherlands and Germany are low, the price may increase, so electricity will be worth more. When a company owns a gas fired power plant and a wind farm, if the gas-electricity ratio is favorable, more profit may be made by a company. Similar reasoning may trigger one to think that wind and gas prices may also be negatively correlated. With respect to gas contract, we also know from section 2.3.1 that temperature and wind are slightly negatively correlated. Since low temperature yields a higher gas price by supply and demand and vice versa, this correlation could be increased.

Chapter 4

Modeling wind

After the discussions about wind, how it has behaved over the last years and how electricity can generated from it, we set up a model for wind. To price wind derivatives, the underlying driver, wind, should be understood and be modeled. Our goal in this chapter is to set up a model for wind with the ability to reproduce the statistical properties of wind speed as accurate as possible, using the available wind speed data. Several ways to model wind speed can be found in literature, both discrete [32][33] (f.e. GARCH models) and continuous models, using seasonality effects [3], and without using seasonality effects [34]. In this thesis we will suggest two ways to model wind: one with incorporating seasonal effects and one without. We have seen that wind speeds show seasonal dependence, so we will prefer a method of modeling wind using this knowledge. If however, insufficient data is available to extract a good estimate of the seasonal effects, wind can be modeled without the incorporation of seasonal effects. We first consider three distributions that are considered good fits for wind speed distribution over a long period of time without taking into account seasonality effects. After that, we discuss the incorporation of seasonal effects and suggest a continuous time model to reproduce wind speeds more accurately. Literature about incorporating seasonal effects in continuous time models exist [35][3]. We will suggest a new method of removal and incorporation of seasonality which will result in a better approximation of the wind speed distribution.

4.1 Long-term distribution of wind speeds

When there is insufficient data available to extract seasonal effects, a long-term distribution without seasonality can be used to price wind derivatives. There are several distributions that may be a satisfactory fit for long-term wind data. In this section, we will test a Weibull, a Rayleigh and a lognormal distribution to see how well these distributions fit the KNMI data. To see how the distributions match with the data, the two-sample Kolmogorov-Smirnov test (K-S test) [36] is used. In this test, the hypothesis that two samples come from the same distribution is tested. For the Weibull, the Rayleigh and the lognormal distribution we fit the parameters using the MATLAB command `fitdist`, which uses the maximum-likelihood estimators for the parameters of the distributions. We produce 100.000 random numbers of the distribution and compare the samples of original wind speed data and generated random numbers in the K-S test. If the p-value of this test is below 0.05, with 95% certainty we may confirm the hypothesis. Wind behaves differently at different wind sites. Therefore, we compute the average of the p-values per location for each of the distributions. The results of this analysis are presented in Table 4.1.

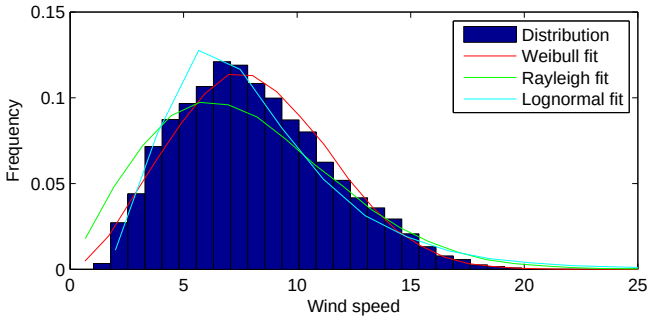

Wind site	Mean p-value
Weibull	0.0356
Rayleigh	0.0914
Lognormal	0.0487

Table 4.1: p-values per wind site and per distribution

Figure 4.1: Fitted Weibull, Rayleigh and Lognormal distributions for wind speed distribution.

From Table 4.1, we conclude that the Weibull distribution is the best distribution for model daily average wind speeds in our case, and we use it to model wind speed distributions over a long period of time. The Rayleigh distribution, which was suggested in [37] and [13] is not a satisfactory distribution for the wind sites we considered. The lognormal distribution can also be a satisfactory distribution to model wind speed distributions. This distribution is often used in financial engineering, which may be advantageous. On the basis of the p-values as computed by the K-S tests considering various wind sites, we suggest to use the Weibull distribution to model the long term distribution of wind speeds if insufficient wind speed data is available to extract the seasonal effects. Later on we will discuss how one can estimate whether sufficient data is available to extract a seasonality function. Figure 4.1 shows for one wind site how the fitted distributions match the wind speed data.

4.1.1 The Weibull and Rayleigh distributions

To get familiar with the Weibull distribution, we present some of its properties. The Weibull and Rayleigh distributions closely related and are often used in survival analysis and reliability engineering. However, the Weibull and Rayleigh distributions can also be used to describe the distribution of wind speeds over a longer period of time [37]. The Weibull distribution is defined [38] as follows:

$$f(x,k,\lambda) = \begin{cases} \frac{k}{\lambda}(\frac{x}{\lambda})^{k-1} \exp\left(-(\frac{x}{\lambda})^k\right) & \text{if } x \geq 0 \\ 0 & \text{if } x < 0, \end{cases} \tag{4.1}$$

where, $k > 0$ is the shape parameter and $\lambda > 0$ is the scale parameter.

The Rayleigh distribution is a simplification of the Weibull distribution. If for the Weibull distribution $k = 2$ and $\lambda = \sqrt{2}\theta$ are taken, then we have the Rayleigh distribution with one free parameter, θ, mathematically [39] we find:

$$f(x,\theta) = \begin{cases} \frac{x}{\theta^2} \exp\left(-\frac{1}{2}\frac{x^2}{\theta^2}\right) & \text{if } x \geq 0 \\ 0 & \text{if } x < 0. \end{cases}$$

The influence of the parameters of Weibull and Rayleigh variables on the distribution is displayed in Figure 4.2. In the upper plot of this figure variation of the parameter k is shown, and in the

lower plot the effect of variation of the parameters λ is shown. Since k was chosen to be equal to 2 in the lower plot, this is also a variant of the Rayleigh distribution, where $\theta = \frac{\lambda}{\sqrt{2}}$.

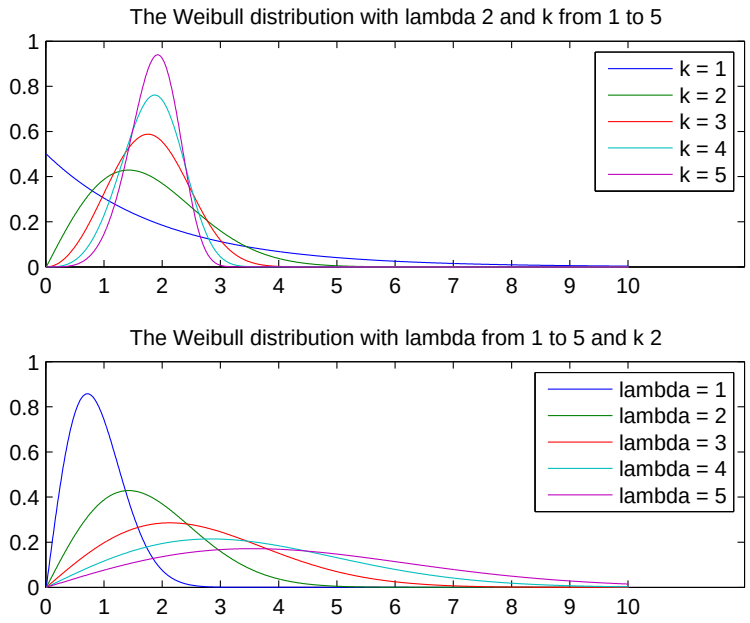

Figure 4.2: Weibull (and Rayleigh) distribution with different values for scale and shape parameters.

4.2 Incorporating seasonality

In this section we start another tranche of modeling in which we aim to incorporate seasonality within the model for wind. When looking at the wind speed time series, at first it looks like a random process. This can be seen in Figure 4.2. However, in Chapter 2, we have discussed that wind shows two clear seasonal patterns: a yearly and a daily seasonal pattern. We will choose one of the following ways to decompose wind data into a seasonal component, $g(t)$ and a random component, $X(t)$:

$$\begin{aligned} S(t) &= g(t) + X(t), \\ S(t) &= g(t)X(t), \end{aligned}$$

where $S(t)$ is the wind speed at time t, $g(t)$ is a continuous seasonality function at time t, and $X(t)$ is a random process at time t. This means that we must determine a function $g(t)$ such that after the removal of this function preferably only random noise remains. When seasonality is removed using subtraction $X(t)$ (unit m/s) can be seen as the difference in speed between the seasonal average and the measured wind speed. If division is used to remove the seasonality, $X(t)$ (unit -/- or %) can be the wind speed percentage with respect to the seasonal average.

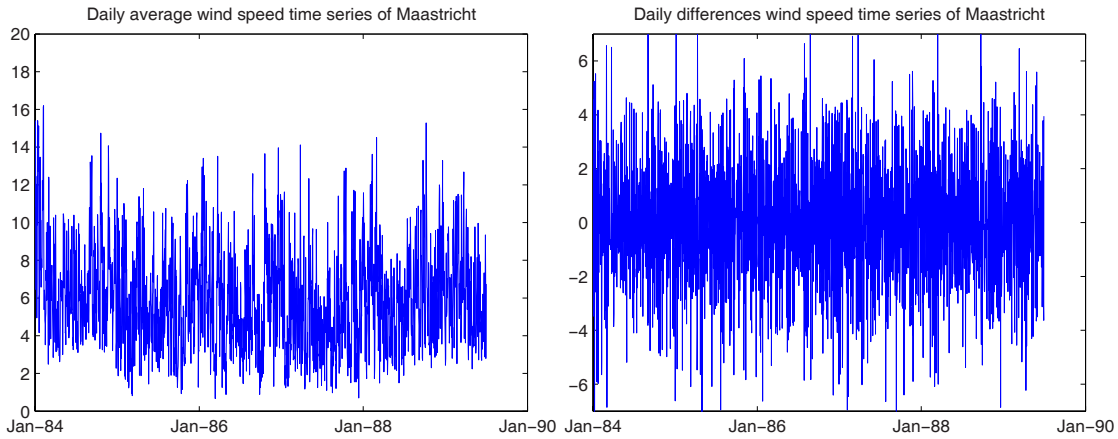

Figure 4.3: Daily average wind speed time series for Maastricht.

The modeling of wind speed data can now be split into two parts. First of all, there is the modeling of the seasonality component: from the original wind data the seasonality component (a continuous time function) is extracted. This seasonality component is removed from the original wind data, and the result of this removal is a remaining random process. After this, the remaining random process is modeled. There are various ways to model the seasonality and extract it and various ways to model the remaining process. We suggest one approach to model the seasonality, and two approaches to remove it in Section 4.3. After that we consider one approach to model the remaining process in Section 4.4, and incorporate the seasonality again.

Furthermore, we will distinguish two different kinds of wind speeds that are to be modeled: daily average wind speeds and hourly average wind speeds. Current literature only addresses the modeling of daily average wind speed. This is probably due to the fact that the wind derivatives that were listed at the USFE were based on daily average wind speeds. However, if we eventually wish to price wind power derivatives, the average of wind speed per day is not representative for the generated amount of electricity the same day [40]. To model the electricity production, quarter hourly or hourly wind data have to be modeled. This due to the fact that the power production is related to the cube of the wind speed. Therefore, small differences in wind speed may result in significant differences in power production. So, to model wind power derivatives, we have to model the hourly average wind speed, rather than the daily average wind speed. The concepts to model daily or hourly average wind speeds are the same, however, the actual models and model parameters can be different, and also different input data is used. First, the concept is explained in Sections 4.3, 4.4 and 4.5. Later on, in Section 4.6.2 we look into the differences between daily and hourly average wind speed modeling.

4.3 Removing seasonality

In this thesis we consider two approaches to model the seasonality, the yearly average regression approach and the so-called consecutive regressions approach. Since the yearly average regression approach exhibits better results, and similar approaches are used in literature [19], we only elaborate on the yearly average approach. The consecutive approach is, explained in Appendix B.1.1 for completeness, and the results for this approach are shown in Appendix B.3.4. The idea

behind the yearly average regression approach is based on the rotation of the Earth around the sun. Since the orbit of the Earth around the sun is the considered same every year, we assume the same seasonal effect every year. This seasonal effect can be computed by looking at the average wind speed per day of the year. The computation of this method is done as follows:

1. Take the average wind speed of all January 1sts in the data set, then the average of all January 2nds,... etc.
2. Use nonlinear regression on the computed function to determine with an approximation of the yearly seasonal effect.

Using the `fit` function in MATLAB, the data can be fitted to a sum of sine functions. For this MATLAB function, a sum up to nine sine functions can be chosen. Since the underlying technique is to model a seasonal effect due to the rotation of the Earth around to Sun, one sine function would suffice. To improve the extracted seasonality, a higher number of sine functions can be used. After the seasonality function has been computed, the data can be corrected for this seasonality. Since there is a yearly seasonality function, each data point can be corrected by either subtraction or division. What remains is a random process, $X(t)$, which exhibits mean reversion. In Figure 4.4, an example of the seasonality function is shown using one sine function. The (non-linear) regression line through the data is the approximation for the yearly seasonality that will be used.

Deseasonalizing by the yearly average regression method can be used directly on raw wind data, as well as on the logarithm of the raw wind data. The procedure is exactly the same, but the results will prove to be slightly different.

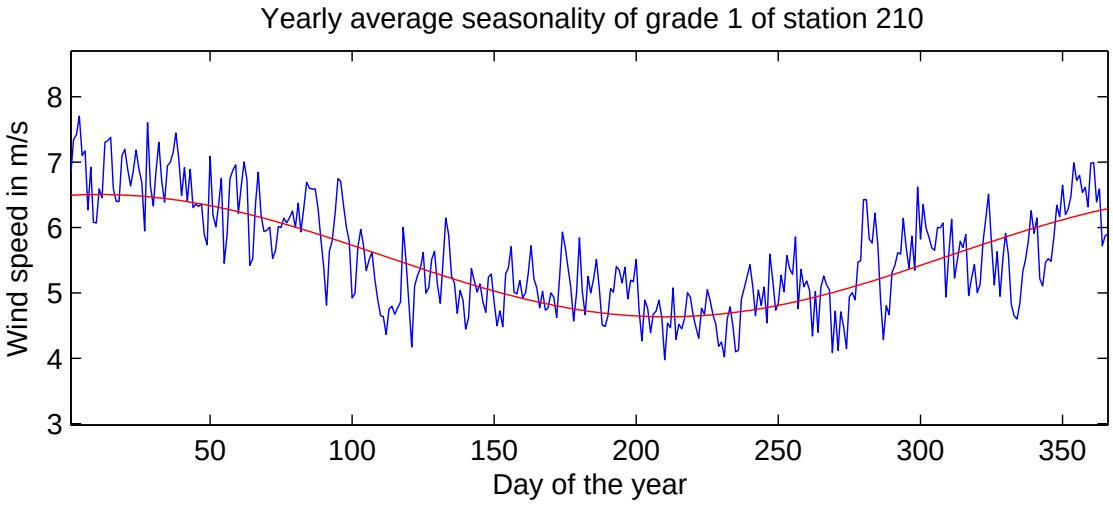

Figure 4.4: The yearly average wind speed function and regression.

As was said, we prefer reconstructing wind speed data with seasonality incorporated in it, but whether or not we can extract a satisfying seasonality function depends on the quality and the amount of data. To look into how many years of data will be needed, we look at the limiting behavior of the seasonality function. To this extent, using the fit function in MATLAB, after each year, a nonlinear regression is performed to calibrate the parameters of one sine function. An iterative process of yearly updated seasonality functions is given in Figure 4.5. The behavior of

four parameters, of $g(t)$, the seasonality function y, A, ω and ϕ are plotted. These are the four parameters that define the following sine function:

$$g(t) = y + A\sin(\omega t + \phi) \tag{4.2}$$

The parameters of (4.2) are updated per year. The thick black line represents the seasonality in the last available full year in the data set.

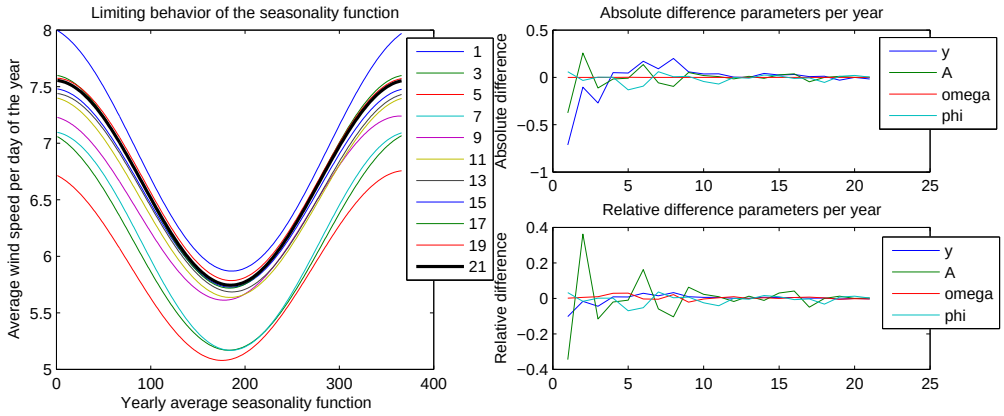

Figure 4.5: Limiting behavior of the seasonality function.

In the right part of Figure 4.5 can be seen that the absolute and relative differences per iteration decrease. We conclude that A is the most variable parameter. One way to judge whether or not the seasonality function has sufficiently converged to its 'true' values, a tolerance level can be chosen, and whenever either the absolute or the relative iteration difference is below this tolerance, sufficient data is available.

4.4 Analyzing the remaining process

After the seasonality has been removed, the assumption is that deseasonalized wind speeds can be modeled by a random process. This can be random process with a mean of 1 or 0, depending on whether division or subtraction was used to remove the seasonality. Therefore, we assume that this remaining process will be mean reverting, around 0 or 1. Intuition behind the fact that this process should be mean reverting is that wind comes from pressure differences. Wind speed will decrease at a certain point where wind is piling up until a temporary high pressure equilibrium is attained. Then air will move to a low pressure area, causing wind speeds to increase again, and slow down as moving towards a temporary low pressure equilibrium. These pressures constantly vary by amongst others the rotation of the Earth around its axis, hence a total equilibrium is never obtained. Since we work with a mean reverting process, several well-known processes from literature can be used to model the remaining process. The easiest choice will be to model the remaining process by an Ornstein-Uhlenbeck process (OU-process) [41]. In literature on temperature derivatives this is also suggested ([42]). An OU-process is defined as follows [43]:

$$\mathrm{d}X(t) = \lambda(\mu - X(t))\mathrm{d}t + \sigma\mathrm{d}W(t), \tag{4.3}$$

where $W(t) : t \geq 0$ is a Wiener process. In our case, μ will be equal to either 0 (when using subtraction to remove seasonality) or 1 (when using division to remove seasonality). To reconstruct wind data using an OU-process, the differences of wind data should be normally distributed. Figure 4.6 shows both the mean reverting behavior of the random process, and the normally distributed differences. The distribution of the daily differences seems normally distributed. When computing a weekly rolling window, using 2 years of data, the Jarque-Bera test for normality [44] rejects the hypothesis (of the daily differences coming from a normal distribution with certain mean and standard deviation) 25% of the time. The Jarque-Bera test returns 1 if the hypothesis of normality is rejected. Figure 4.7 displays a graph for the observed wind speed data, and the deseasonalized wind data after using subtraction and division respectively. We take 25% to be a sufficient rolling window score to assume normality of the daily differences.

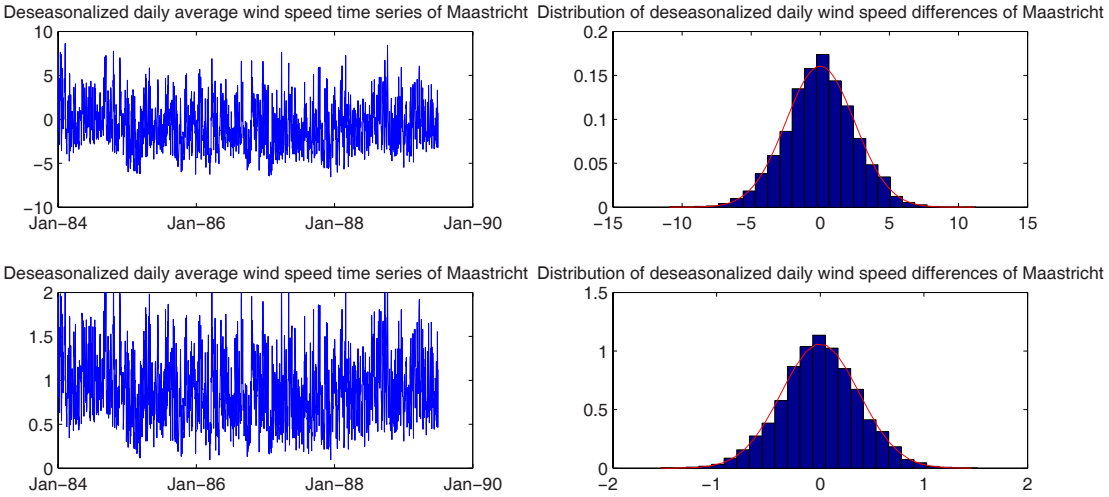

Figure 4.6: Deseasonalized daily average wind speeds and daily differences after using subtraction (upper) and division (lower) to remove seasonality.

Furthermore, for an OU-process, autocorrelation for the wind speeds should decrease exponentially over time, and the daily differences need to be independent and non-correlated. Also, since we use a fixed value σ to model volatility of the remaining process, the autocorrelation of the squared wind speeds should decrease exponentially. Figure 4.8 shows the autocorrelation for the remaining process. We see in the upper part of Figure 4.8 that after subtracting the seasonality function, there still is a seasonality pattern in the autocorrelation remaining, whereas this is not the case when dividing by the seasonality function, which is shown in the lower part of Figure 4.8. This implies that an OU-process would be a better fit for the division-deseasonalized data than for the subtraction-deseasonalized data. At this moment, literature only address subtraction as a method to deseasonalize weather data. The seasonality in the squared autocorrelation is coped with by multiplying σ in 4.6 by another sum of sine functions. In the next section, we will see that this extra continuous function is not needed when deseasonalizing the data using division. Figure 4.9 shows that daily differences can be assumed to be uncorrelated after deseasonalizing by subtraction and by division, since both the daily differences and the squared daily differences have low autocorrelation. From this, we conclude that the OU-process is an appropriate choice to model the remaining process.

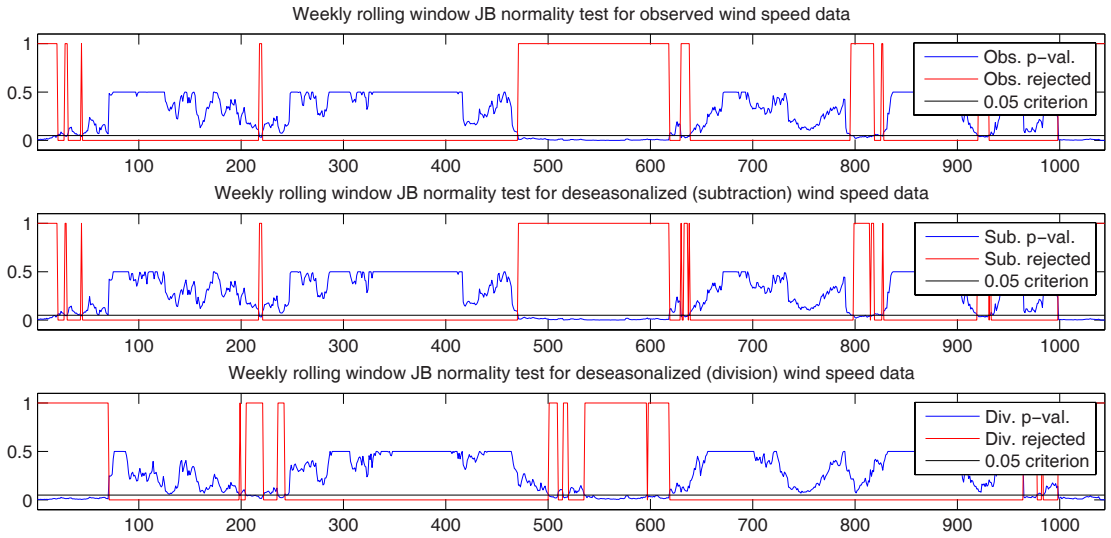

Figure 4.7: Rolling window JB normality tests for deseasonalized wind data, with 0.05 criterion, hypothesis rejected if p-value smaller than 0.05.

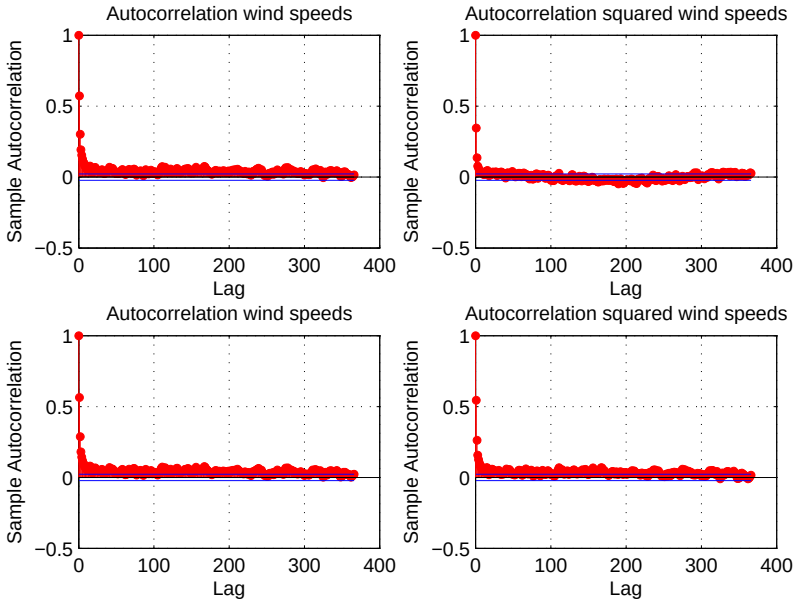

Figure 4.8: Autocorrelation for deseasonalized daily average wind speeds after using subtraction (upper) and division (lower) to remove seasonality.

4.5 Substituting back the seasonality function

As was denoted earlier, we consider wind speeds as a combination of a random process $X(t)$ and a continuous time function $g(t)$. The seasonality component and the random component

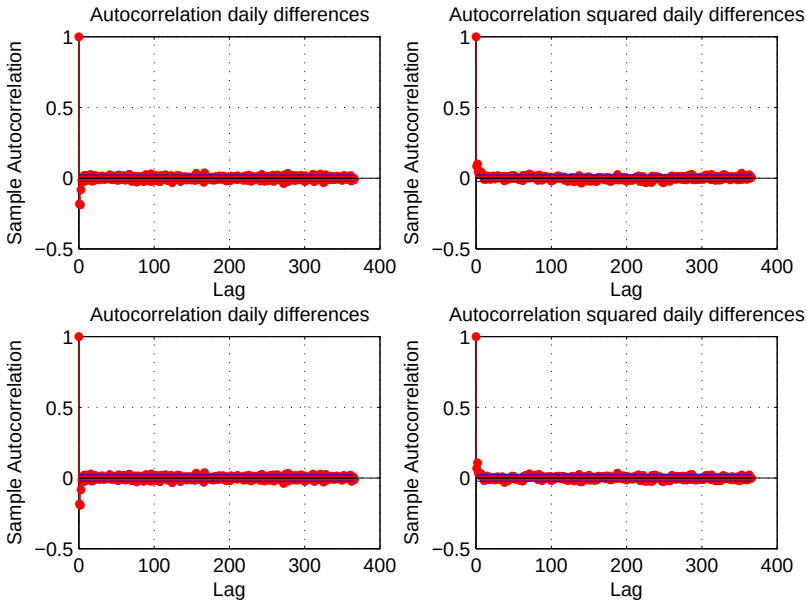

Figure 4.9: Autocorrelation for deseasonalized daily differences of average wind speeds after using subtraction (upper) and division (lower) to remove seasonality.

can be combined by either summation, $S(t) = X(t) + g(t)$, or multiplication, $S(t) = X(t)g(t)$. Furthermore, the normal wind speed data or the natural logarithms of the wind speed data can be taken as the governing processes. Combinations give rise to four random processes:

$$\begin{aligned}
S_1(t) = \exp(X_1(t) + g_1(t)) \quad &\Leftrightarrow \quad X_1(t) = \log(S_1(t)) - g_1(t), \text{ or} \\
S_2(t) = \exp(X_2(t)g_2(t)) \quad &\Leftrightarrow \quad X_2(t) = \frac{\log(S_2(t))}{g_2(t)}, \text{ or} \\
S_3(t) = X_3(t) + g_3(t) \quad &\Leftrightarrow \quad X_3(t) = S_3(t) - g_3(t), \text{ or} \\
S_4(t) = X_4(t)g_4(t) \quad &\Leftrightarrow \quad X_4(t) = \frac{S_4(t)}{g_4(t)}.
\end{aligned}$$

Itô's lemma [43] can be used to analyze how the seasonality is incorporated when $X(t)$ is modeled by an OU-process. All four models will yield slightly different stochastic differential equations. The derivations of the models below are presented in Appendix B.2. After applying Itô's lemma, we find:

$$\begin{aligned}
\mathrm{d}R_1(t) &= \lambda_1 \left[g_1(t) + \frac{1}{\lambda_1} g_1'(t) - R_1(t) \right] \mathrm{d}t + \sigma_1 \mathrm{d}W(t); \\
\mathrm{d}R_2(t) &= \lambda_2 \left[g_2(t) - \left(\frac{\lambda_2 g_2(t) - g_2'(t)}{\lambda_2 g_2(t)} \right) R_2(t) \right] \mathrm{d}t + \sigma_2 g_2(t) \mathrm{d}W(t); \\
\mathrm{d}S_3(t) &= \lambda_3 \left[g_3(t) + \frac{1}{\lambda_3} g_3'(t) - S_3(t) \right] \mathrm{d}t + \sigma_3 \mathrm{d}W(t); \\
\mathrm{d}S_4(t) &= \lambda_4 \left[g_4(t) - \left(\frac{\lambda g_4(t) - g_4'(t)}{\lambda g_4(t)} \right) S_4(t) \right] \mathrm{d}t + \sigma_4 g_4(t) \mathrm{d}W(t).
\end{aligned} \tag{4.4}$$

In the derivations of the first two equations transformations $\exp(R_1(t)) = S_1(t)$ and $\exp(R_2(t)) = S_2(t)$ are used. These four models are all satisfactory models, and are compared in Section 4.6 regarding their capability to reconstruct wind speeds as accurately as possible. All of the models include parameters λ_i and σ_i which have to be calibrated. Methods to do so will be discussed in the next section.

4.5.1 Calibrating the stochastic process

Since an OU-process as in (4.3) remains, there are two parameters to be approximated: λ and σ. These are the parameters denoted by λ_i and σ_i in (4.4). Although we deal with a continuous time model, the parameters cannot be determined analytically, and therefore they are approximated by calibration on the available data. A discretization of our models has to be made, and this discretization can be done in two ways. We can solve the OU-process directly, or we can use the Euler discretization scheme [45].

There are various techniques to determine the values of these parameters, for example by ordinary least squares (OLS) regression or by maximum likelihood estimation (MLE). In our case, these parameters can be calibrated using the (deseasonalized) data or the raw data over the total time scale. We considered the calibration of the remaining OU-process and not of the raw data, as this was more natural. With respect to the methods of calibration, OLS can be used on both the Euler and the exact type of discretization. These discretizations are closely related, the Euler discretization is a Taylor approximation of the exact discretization. More on this can be found in Appendix B.3.1. Three calibration methods will be considered in this thesis: exact OLS, Euler OLS and MLE. All of these methods will yield stable parameters, for both deseasonalizing methods, division and subtraction, as can be seen in Figure 4.10. The choice of what calibration method to use, will be based on what reconstructed distribution is the best fit for observed wind data.

To draw a conclusion on which approach works most optimally, several Kolmogorov-Smirnov tests (K-S tests) are performed. Although we calibrate an OU-process, our goal will be to reconstruct wind speeds. Therefore, the choice of the eventual model is based p-values coming from a comparison of reconstructed wind data and the original wind speed. For nine wind sites, the reconstructed wind speed data is compared with the raw wind data using the K-S test. To this extent, for all nine wind sites, a p-value is computed. The average of the p-values per wind site is taken to be the final p-value. We wish to model both hourly and daily wind speeds. In Section 4.6, the results will be discussed and conclusions on which model performs best will be drawn.

4.6 Comparing the constructed processes

In this section, the results of the K-S tests and corresponding best distributions are provided. Four models as described in (4.4) are compared, using exact OLS, Euler OLS and MLE as parameter calibration techniques. As a statement of why adding seasonality is useful, also a mean reverting process with constant mean is tested and compared. First daily average wind speeds are considered, after that hourly average wind speeds are considered.

4.6.1 Optimal model choice for daily average wind speeds

We compare all models for modeling the daily average wind speed. The four models in (4.4) are tested using K-S tests over nine wind sites. MLE, exact OLS and Euler OLS are used to calibrate

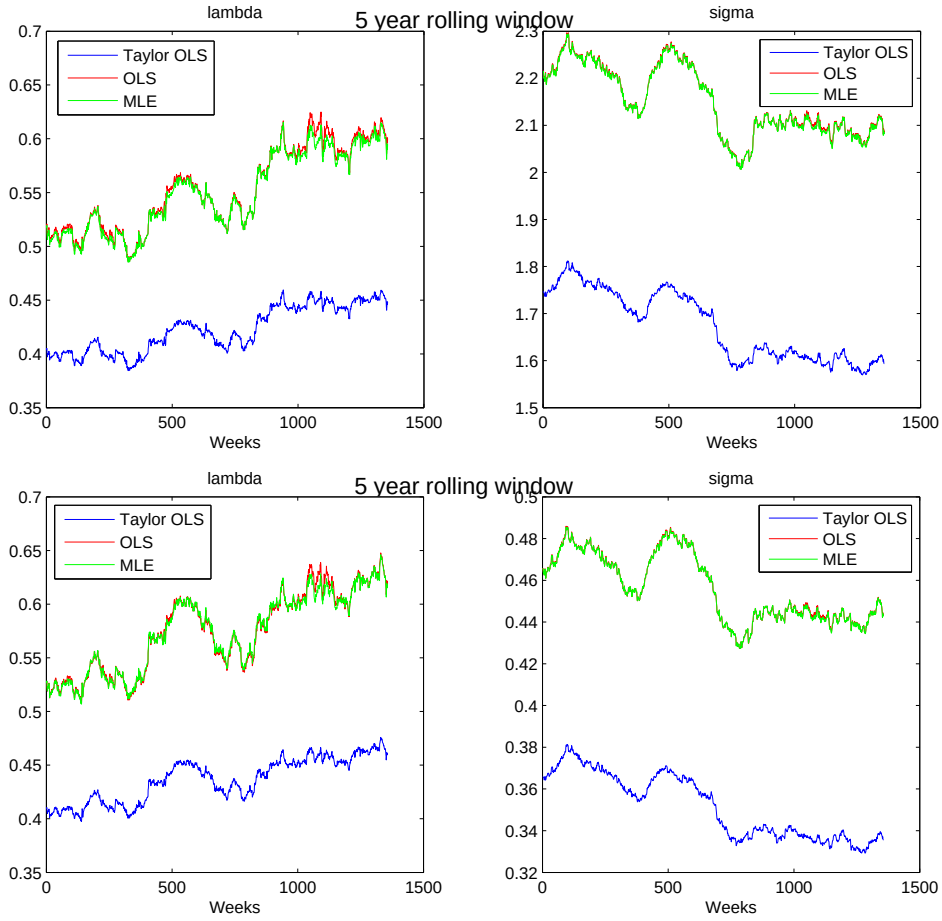

Figure 4.10: A 5 year rolling window for the parameters, as found by several calibration methods, of the OU-process after seasonality removal by subtraction (upper) and division (lower).

the parameters of the deseasonalized OU-process. The results are shown in Table 4.2.

Data type	**Seasonality Removal**	**Wind speed distribution**			**Daily differences distribution**		
		Euler OLS	Exact OLS	MLE	Euler OLS	Exact OLS	MLE
logarithm	subtraction	0.0573	0.0787	0.0787	0.0425	0.0794	0.0795
logarithm	division	0.0629	0.0828	0.0827	0.0444	0.0802	0.0809
normal	subtraction	0.0597	0.0744	0.0749	0.0203	0.0606	0.0610
normal	division	0.0485	0.0691	0.0699	0.0154	0.0580	0.0581
normal	none	0.0587	0.0737	0.0719	0.0271	0.0655	0.0647

Table 4.2: p-values for the four models for daily wind speed, and a mean reverting model as reference.

We conclude that to optimally reconstruct daily average wind data, we may divide by a yearly seasonality function that is found by using non-linear regression with one sine function on raw wind data, then calibrate our parameters using Euler OLS, and put back in our seasonality func-

tion as proposed in (4.4), Model 4. Doing so, returns the lowest p-value over nine wind sites, using the two sample K-S test. However, the other models perform well too. The main difference between the log-wind speeds in the distribution can be seen in Figure 4.11. When looking at this figure, that using log-wind speeds yields a stronger skew in the reconstructed distribution. However, its tail towards high wind speeds is too fat, which makes the K-S test appoint it with a higher p-value. Also, the daily differences are modeled well by any of the four proposed models.

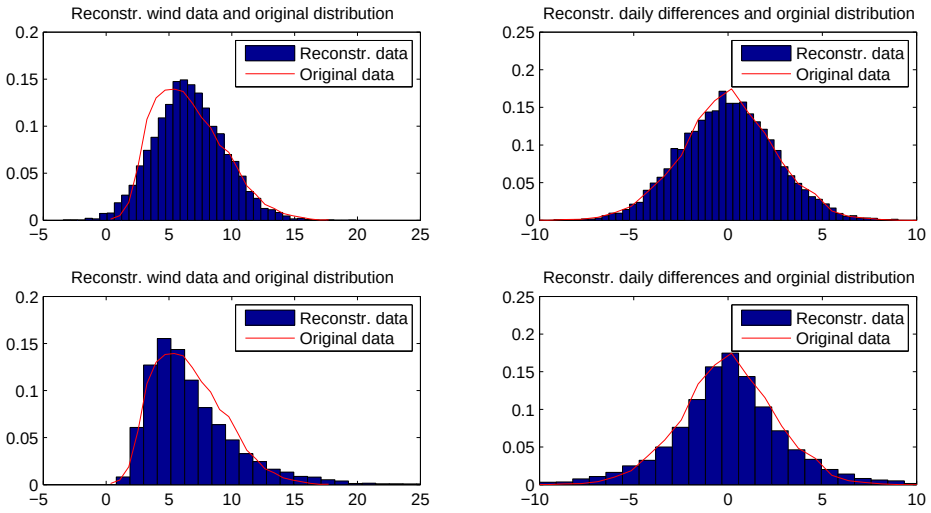

Figure 4.11: Reconstructed distributions of wind speeds and daily differences of Models 1 and 4.

4.6.2 Optimal model choice for hourly average wind speeds

As was mentioned, to model wind power generation, hourly average wind speed data have to be modeled. To test which of the proposed models is a satisfactory model for the modeling of hourly wind speeds, we set up a similar table to Table 4.3. In this case, the seasonality will look differently. The seasonality function is modeled by 366 (days) times 24 (hours) data points, and an example is shown in Figure 4.12. To get a highly satisfactory fit, again a sum of sine functions is used, however now the sum will contain 9 sine functions. It can be seen that the seasonality function jumps up and down very quick. This is to capture the effects of the diurnal cycle as accurately as possible.
First of all, we conclude that models that use log-wind speeds are no satisfactory fit to model hourly average wind speeds. These models exhibit too fat tails for high wind speed values, therefore the K-S computes a high p-value. Secondly we denote that for hourly data, the technique of calibrating the parameters does not matter, as the p-values do not differ much. As in the case of daily average wind speeds, to compute hourly average wind speeds Model 4 appears most accurate. None of the models reconstruct the hourly differences very well, which may be due to the quality of the data. As was showed before, in Figure 2.7, this distribution is not smooth. It causes the K-S test to find large p-values when comparing with the smoother reconstructed hourly differences. In Figure 4.13, reconstructed wind data by using Models 1 and 4 can be seen. We again note the fat tails for Model 1, and the significant difference between the hourly differences of wind speeds and the reconstructed wind speeds.

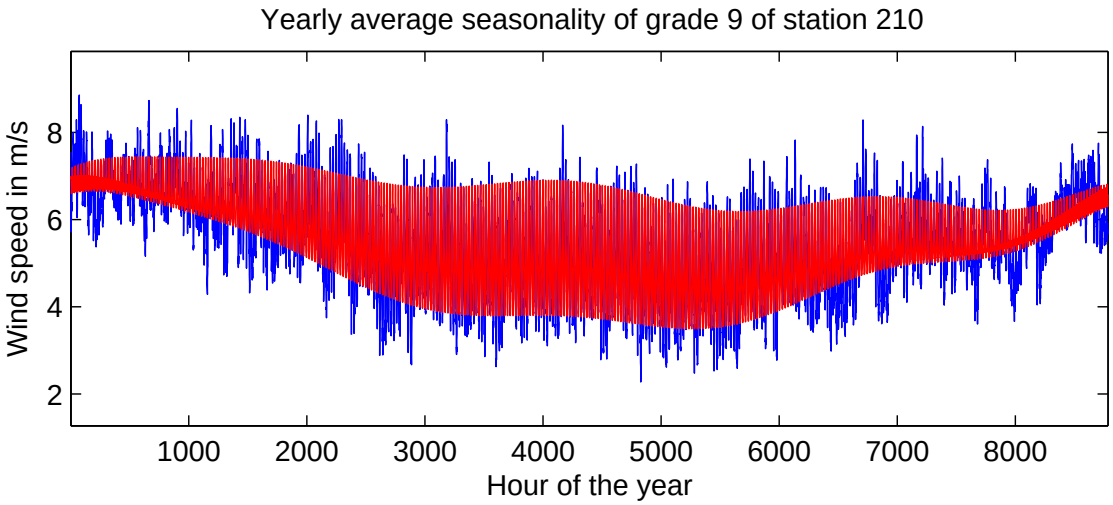

Figure 4.12: The yearly average wind speed function and regression.

Data type	**Seasonality Removal**	**Wind speed distribution**			**Daily differences distribution**		
		Euler OLS	Exact OLS	MLE	Euler OLS	Exact OLS	MLE
logarithm	subtraction	0.1207	0.1218	0.1238	0.2293	0.2404	0.2399
logarithm	division	0.1324	0.1359	0.1376	0.2334	0.2448	0.2445
normal	subtraction	0.0663	0.0662	0.0709	0.1654	0.1656	0.1647
normal	division	0.0543	0.0521	0.0531	0.1657	0.1652	0.1654
normal	none	0.0687	0.0656	0.0645	0.1651	0.1655	0.1651

Table 4.3: p-values for the four models for hourly wind speed, and a mean reverting model as reference.

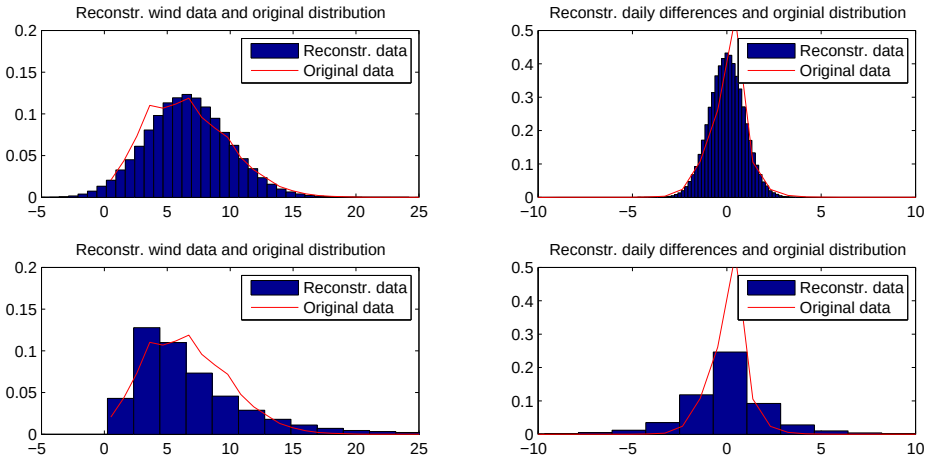

Figure 4.13: Reconstructed distributions of wind speeds and hourly differences.

The results of the full comparison, including yet another method to remove the seasonality from wind data are shown in Appendix B.3.4 and B.3.4. Overall we conclude that whether we wish to reproduce hourly or daily average wind speeds, Model 4 appears to be the optimally performing model. This model again tests best when using the K-S test for nine wind sites. Model 4 may be the optimal model because the reconstructed OU-process is the best fit for our noise when deseasonalizing by division. This can be seen in Figure 4.8. Furthermore, we conclude it is better to work directly with the raw wind data than with log-wind data.

Chapter 5

Pricing wind derivatives

In this chapter we will consider various derivative pricing methods. The Monte Carlo method, numerical methods, analytical solutions and the COS-method will all revue. Note again, that our focus lies with pricing of long term contracts, which can priced by modeling of the historical statistical behavior of the underlying.

5.1 Arbitrage-free pricing

Since wind is not storable nor tradable, futures and option contracts cannot be hedged in a standard way, which implies the incompleteness [46] of a wind derivatives market. Another issue is that the wind derivatives market is quite illiquid. This is probably because of the great dependence of location. Since wind cannot be traded on financial markets, well-known pricing methods like discounted payoff cannot immediately be used. Since there is no active trading in the underlyings of wind derivatives, it is not straight-forward to hedge these derivatives. Assets that show strong correlation with wind speeds may be used to partly hedge a wind derivative. The authors in [30] suggest the use of a normal power contract to party hedge for temperature risk, whereas the authors in [31] claim it is more appropriate to use gas prices. However, an exact replication of a portfolio of tradable asset and cash can not be attained. Since exact hedging is not possible, the market price of risk for wind derivatives contract will most likely be high. It is this market price of risk that implies that expected discounted payoff will not yield a fair wind derivative price. Literature exist on risk-neutral pricing of weather derivatives [47][48][46][49]. Unfortunately no consensus has emerged about the valuation of weather derivatives [49].

Whereas in financial options and futures, the underlying asset, $S(t)$, and a money savings account, $B(t)$, combined can yield a hedge portfolio of an option in the Black-Scholes world, this will not be the case for wind derivatives. We have a mean reverting process as basis for the model for $S(t)$. Theoretically a risk-neutral distribution can be extracted from the market using quoted prices, however since there is no liquid market and no quoted prices this is impossible in practice at this stage. To still have a workable framework, we will base our pricing on [48]. This means that we will transfer from a true statistical measure $\mathbb{P}$ to a risk-neutral measure $\mathbb{Q}$ by incorporating the market price of risk. Since the market for wind derivatives is incomplete, no unique measure for $\mathbb{Q}$ can be found.
The authors in [48] use Girsanov's theorem [50] to transfer to a risk-neutral measure. Let $\theta(t)$ be a real-valued measurable and bounded function that denotes the market price of risk at time t, and let $W(t)$ be a Brownian motion. We define $Z(t)$ and $\tilde{W}(t)$ as:

$$Z(t) = \exp\left(-\int_0^t \theta(u)\mathrm{d}W(u) - \frac{1}{2}\int_0^t \theta^2(u)\mathrm{d}u\right) \tag{5.1}$$

$$\tilde{W}(t) = W(t) - \int_0^t \theta(u)\mathrm{d}u, \tag{5.2}$$

and we assume that

$$\mathbb{E}\int_0^T \theta^2(u)Z^2(u)\mathrm{d}u < \infty.$$

Then, $\mathbb{E}[Z] = 1$, and under $\mathbb{Q}$, $\tilde{W}(t)$ is a Brownian motion. We assume we can switch to a risk-neutral measure by incorporating the market risk. Under measure $\mathbb{Q}$ the stochastic differential equations as noted in (4.4) will change slightly. (5.3) shows the models with market price of risk included, where the adjusted parts are stated bold.

$$\begin{aligned}
\mathrm{d}R_1(t) &= \lambda_1\left[g_1(t) + \frac{1}{\lambda_1}(g_1'(t) + \boldsymbol{\sigma_1\theta}(\mathbf{t})) - P(t)\right]\mathrm{d}t + \sigma_1\mathrm{d}\tilde{W}(t);\\
\mathrm{d}R_2(t) &= \lambda_2\left[g_2(t) + \boldsymbol{\sigma_2\theta}(\mathbf{t}) - \left(\frac{\lambda_2 g_2(t) - g_2'(t)}{\lambda_2 g_2(t)}\right)P_2(t)\right]\mathrm{d}t + \sigma_2 g_2(t)\mathrm{d}\tilde{W}(t);\\
\mathrm{d}S_3(t) &= \lambda_3\left[g_3(t) + \frac{1}{\lambda_3}(g_3'(t) + \boldsymbol{\sigma_3\theta}(\mathbf{t})) - S_3(t)\right]\mathrm{d}t + \sigma_3\mathrm{d}\tilde{W}(t);\\
\mathrm{d}S_4(t) &= \lambda_4\left[g_4(t) + \boldsymbol{\sigma_4\theta}(\mathbf{t}) - \left(\frac{\lambda g_4(t) - g_4'(t)}{\lambda g_4(t)}\right)S_4(t)\right]\mathrm{d}t + \sigma_4 g_4(t)\mathrm{d}\tilde{W}(t).
\end{aligned} \tag{5.3}$$

In the next sections, we will not go into detail about the market price of risk, and will assume this to be equal to zero. Industry parties have their own models for calculating the market price of risk or risk premiums [18], incorporating, amongst, others seasonality effects, the size of the contract, historical variability of the wind site, et cetera [18]. The methodology for pricing explained here is rather general, and sophisticated models for the market price of risk can be included loss of generality.

5.2 Wind derivative pricing methods

In Chapter 4 we proposed a model in the form of a stochastic differential equation, to model both daily and hourly average wind speeds. Also, we know that when insufficient data is available to extract a seasonality function, the Weibull distributed describes the wind speed distribution best. In this chapter, we combine these models with the wind indices as proposed in Chapter 3. With these wind indices as underlying, wind speed or power derivatives can be priced. In this section, various pricing methods are discussed, and pros and cons per method will be stated. We consider the Monte Carlo method, closed form solutions, numerical methods and the COS-method. Note that the preferred pricing method may differ per wind derivative contract. Moreover, we consider wind to be modeled with and without seasonality effects.

Note that we do not know anything about the distribution of generated electricity. We therefore cannot model this underlying, or price options with this underlying. However, we have distributions for wind speeds with and without seasonality effects. Using a polynomial function to approximate the efficiency function opens the door to pricing by the Monte Carlo method, numerical methods and the COS-method.

5.2.1 the Monte Carlo method

The first method to price wind derivative contracts we consider is the Monte Carlo method. The Monte Carlo method relies on repeated random sampling. In the case of wind speeds, N paths of daily or hourly average wind speeds are constructed of the wind speeds are computed through the models of (4.4). This way a distribution of wind data can be simulated, and the payoff for these reconstructed data can be composed. For all of the realizations, a mean and standard deviation can be computed. The discounted average of f.e. 10.000 of these reconstructed payoffs is taken to be the option price via the discounted expected value of the payoff approach and the law of large numbers. A positive aspect about pricing wind derivatives with the Monte Carlo method is that the payoff function may be very complex. A disadvantage of the Monte Carlo method is that the pricing is relatively slow, and possibly inaccurate. Variance reduction techniques exist to reduce the number of simulations.

The Monte Carlo method can be applied to the models with and without the incorporation of seasonality. Furthermore, simulated wind speeds can easily be translated to generated amount of electricity if desired. So, any derivative that was mentioned in Chapter 3 can be priced using the Monte Carlo method. The Monte Carlo method is preferred when pricing complex contracts. This means that the Monte Carlo method is the preferred choice for pricing wind power purchase agreements and for Asian average rate types of options and futures. For caps, floors, and futures and options with underlying being only one specific day in the future, faster and more accurate pricing methods are available.

Pricing Asian average rate options

Literature exists on the fast pricing of Asian style European options [51], but for now, we will only price the Asian average rate options using the Monte Carlo method. Recapitulating, using (3.1) and (3.2), the payoff of an example wind speed option is:

$$\begin{aligned} \text{Call}(WS, T) &= \max(\sum_{i=1}^{N} \frac{WS_i}{N} - K, 0) \\ &= \max(WS - K, 0), \end{aligned}$$

which clearly shows the arithmetic mean of daily or hourly average wind speeds as underlying. The model with or without seasonality incorporated is chosen, and used to simulate n paths of wind speeds. In Figure 5.1, the straight lines are 7 examples of reconstructed daily average wind speeds, and the dashed lines are their respective monthly means. For each of the dashed lines, the payoff is calculated. In the end, the discounted average of all payoffs is taken to be the option value.

Contracts of any length can be priced, but the longer the lifetime of the contract, the longer it will take to calculate. As was stated, the discounted mean of n computations can be seen as an approximation of the price of a contract. The accuracy of this mean will depend on the standard deviation of underlying data. If this standard deviation is small, the mean can be an accurate representation of the fair derivative price. The standard deviation can be reduced by increasing the number of simulations, n. Especially when seasonality has to be extracted from the raw data, and new data has to be reconstructed this may be time-consuming. However, increasing n is not the only technique to reduce the standard deviation. In the next section we will discuss a well-known variance reduction technique.

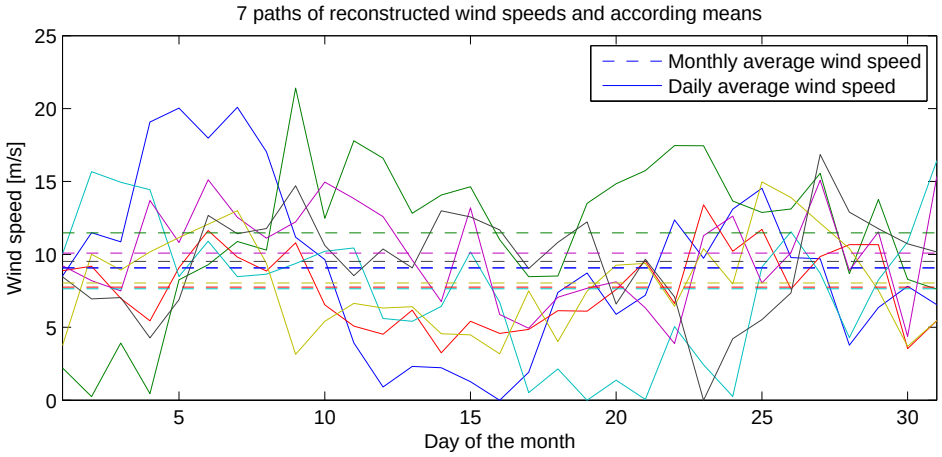

Figure 5.1: 7 reconstructed wind speed paths (solid) using the Monte Carlo method with their according means (dashed).

Variance reduction by antithetic sampling

To decrease the standard deviation of the underlying data, increasing the amount of simulations is not the only choice. We will discuss a well-known variance reduction technique. All variance reduction techniques aim to bring down the variance (and thus standard deviation) of the Monte Carlo simulations, without increasing the amount of simulations. The variance can, amongst others, be reduced by the use of antithetic variates, control variables, or importance sampling.

We consider reducing the variance by means of antithetic variates. Suppose we want to estimate $\theta = \mathbb{E}[Y]$, where $Y = h(\mathbf{X})$ and wish to reduce $\mathrm{Var}(Y)$. In our case, $\mathbf{X}$ are simulations of wind speeds, and Y can be the payoff of a wind derivative. If we have generated two samples of Y, i.e. Y_1 and Y_2, then an unbiased estimate, $\hat{\theta}$, and the variance of this estimate are given by:

$$\begin{aligned} \hat{\theta} &= \frac{Y_1 + Y_2}{2}, \quad \text{and} \\ \mathrm{Var}(\hat{\theta}) &= \frac{\mathrm{Var}(Y_1) + \mathrm{Var}(Y_2) + 2\mathrm{Cov}(Y_1, Y_2)}{4}. \end{aligned}$$

The variance can be reduced if $\mathrm{Cov}(Y_1, Y_2) < 0$. In our case, we apply the Monte Carlo method by simulating many standard normal distributed numbers. If Y_1 would be a standard normal variables, so would $Y_2 = -Y_1$ be, by symmetry. Also, we would have:

$$\begin{aligned} \mathrm{Cov}(Y_1, Y_2) &= \mathrm{Cov}(Y_1, -Y_1) \\ &= -\mathrm{Var}(Y_1) = -1. \end{aligned}$$

We conclude that in our case, we can reduce our variance by antithetic sampling in a straight forward way.

5.2.2 Closed-form solutions

We are able to express certain wind speed derivatives in closed-form. This means that the calculation of these wind derivative prices can happen fast and accurately. Moreover, the Greeks can be

computed, which means that sensitivity analysis can be performed per input variable. Also, the closed-form solutions can be used for calibration purposes. We are able to compute closed form option and future prices for wind speed derivatives with daily average wind speed index that consider only one day in the future, both with seasonality and without seasonality effects. Also, the caplets and floorlets can be priced, and summing these, cap and floors or cash-settlement-agreements can be priced.

Weibull distribution

Closed-form solutions are for example available for financial options and futures [52]. This means that when daily average wind speed is well modeled by a Weibull distribution, and an option or future is considered on one day in the future, this closed-form solution can be used to price this kind of wind derivative. The closed-form solution from [52] is rewritten, and the expression for the Weibull put option is derived in Appendix C.6.1. We find the following closed-form expressions for European call (v^C) and put (v^P) options, with strike price or reference wind speed K, and with an underlying following a Weibull(k,λ) distribution at maturity, T:

$$\begin{aligned} v^C(t_0,x) &= e^{-rT}\lambda\Gamma\left(1+\frac{1}{k},\left(\frac{K}{\lambda}\right)^k\right) - e^{-rT}K\exp(-\left(\frac{K}{\lambda}\right)^k), \quad \text{and} \\ v^P(t_0,x) &= e^{-rT}K\left(1-\exp\left(-\left(\frac{K}{\lambda}\right)^k\right)\right) - e^{-rT}\lambda\gamma\left(1+\frac{1}{k},\left(\frac{K}{\lambda}\right)^k\right), \end{aligned} \tag{5.4}$$

where, r is the risk-free interest rate and $\Gamma(a,b)$ and $\gamma(a,b)$ are the incomplete Gamma functions from b up to infinite and from 0 up to b, respectively. Having closed-form solutions for these options, means fast and accurate pricing. However, since we're not pricing under a risk-neutral measure, the market price of risk is not incorporated. If there would be quoted prices to wind speed options, these closed-form solutions may be helpful for calibration purposes. The closed-form solutions as attained in 5.4 can be used to price caps, floor, and futures and options that only consider one day in the future and have Weibull distributed underlying.

Incorporation of seasonality effects

For the models of (4.4) where seasonality is removed by subtraction, we can derive an exact solution. To find this exact solution, we have to find the probability density function of $S(t)$. This probability density function can be found by solving our model for $S(t)$. For the models where seasonality is removed by division the derivation is non-trivial, and are not treated here. We start from the model:

$$\begin{aligned} \mathrm{d}S(t) &= \lambda\left(g(t)+\frac{1}{\lambda}g'(t)-S(t)\right)\mathrm{d}t+\sigma\mathrm{d}W(t) \\ &= (\theta(t)-\lambda S(t))\mathrm{d}t+\sigma\mathrm{d}W(t), \end{aligned}$$

where $\theta(t)=\lambda g(t)+g'(t)$. Using Itô's lemma on $e^{\lambda t}S(t)$, we get the following derivation:

$$\begin{aligned} \mathrm{d}(e^{\lambda t}S(t)) &= e^{\lambda t}\mathrm{d}S(t) + \lambda e^{\lambda t}S(t)\mathrm{d}t \\ &= e^{\lambda t}(\theta(t) - \lambda S(t))\mathrm{d}t + e^{\lambda t}\sigma \mathrm{d}W(t) + \lambda e^{\lambda t}S(t)\mathrm{d}t \\ &= e^{\lambda t}\theta(t) + e^{\lambda t}\sigma \mathrm{d}W(t). \end{aligned} \tag{5.5}$$

Taking the integral from 0 up to t for Equation (5.5), will give the following:

$$e^{\lambda t}S(t) = S(0) + \int_0^t e^{\lambda s}\theta(s)\mathrm{d}s + \sigma \int_0^t e^{\lambda s}\mathrm{d}W(s),$$

which by multiplication by $e^{\lambda t}$ on both sides is equal to:

$$S(t) = e^{-\lambda t}S(0) + \int_0^t e^{\lambda(s-t)}\theta(s)\mathrm{d}s + \sigma \int_0^t e^{\lambda(s-t)}\mathrm{d}W(s).$$

Since we consider $\theta(t) = \lambda g(t) + g'(t)$, and $g(t)$ is a sum of sine functions, we have the following expression for $\theta(t)$:

$$\begin{aligned} \theta(t) &= \lambda g(t) + g'(t) \\ &= \lambda \sum_{i=1}^{M} \alpha_i \sin(\beta_i t + \gamma_i) + \sum_{i=1}^{M} \alpha_i \beta_i \cos(\beta_i t + \gamma_i). \end{aligned}$$

Using this expression for $\theta(t)$, we do the following derivation:

$$\begin{aligned} S(t) &= e^{-\lambda t}S(0) + e^{-\lambda t}\int_0^t e^{\lambda s}\left(\lambda \sum_{i=1}^{M} \alpha_i \sin(\beta_i s + \gamma_i) + \sum_{i=1}^{M} \alpha_i \beta_i \cos(\beta_i s + \gamma_i)\right)\mathrm{d}s \\ &\quad + \sigma \int_0^t e^{\lambda(s-t)}\mathrm{d}W(s) \\ &= e^{-\lambda t}S(0) + e^{-\lambda t}\sum_{i=1}^{M} \lambda\alpha_i \int_0^t e^{\lambda s}\sin(\beta_i s + \gamma_i)\mathrm{d}s + e^{-\lambda t}\sum_{i=1}^{M} \alpha_i\beta_i \int_0^t e^{\lambda s}\cos(\beta_i s + \gamma_i)\mathrm{d}s \\ &\quad + \sigma \int_0^t e^{\lambda(s-t)}\mathrm{d}W(s), \end{aligned}$$

where we use the fact that the integral of the product of an exponential function $e^{\lambda t}$ and a sine function can be solved by integration by parts [53]:

$$
\begin{aligned}
\int_s^t e^{\lambda x}\sin(\beta_i x+\gamma_i)\mathrm{d}x &= \frac{e^{\lambda x}}{\lambda^2+\beta_i^2}\left(\lambda\sin(\beta_i x+\gamma_i)-\beta_i\cos(\beta_i x+\gamma_i)\right)\Big|_s^t \\
&= \frac{1}{\lambda^2+\beta_i^2}\left[e^{\lambda t}(\lambda\sin(\beta_i t+\gamma_i)-\beta_i\cos(\beta_i t+\gamma_i))\right. \\
&\quad \left.-e^{\lambda s}(\lambda\sin(\beta_i s+\gamma_i)-\beta_i\cos(\beta_i s+\gamma_i))\right] \\
\int_s^t e^{\lambda x}\cos(\beta_i x+\gamma_i)\mathrm{d}x &= \frac{e^{\lambda x}}{\lambda^2+\beta_i^2}\left(\lambda\cos(\beta_i x+\gamma_i)+\beta_i\sin(\beta_i x+\gamma_i)\right)\Big|_s^t \\
&= \frac{1}{\lambda^2+\beta_i^2}\left[e^{\lambda t}\left(\lambda\cos(\beta_i t+\gamma_i)+\beta_i\sin(\beta_i t+\gamma_i)\right)\right. \\
&\quad \left.-e^{\lambda s}\left(\lambda\cos(\beta_i s+\gamma_i)+\beta_i\sin(\beta_i s+\gamma_i)\right)\right].
\end{aligned}
$$

This means that we get:

$$
\begin{aligned}
S(t) &= e^{-\lambda t}S(0)+e^{-\lambda t}\sum_{i=1}^{M}\frac{\lambda\alpha_i}{\lambda^2+\beta_i^2}\left[e^{\lambda t}(\lambda\sin(\beta_i t+\gamma_i)-\beta_i\cos(\beta_i t+\gamma_i))-(\lambda\sin(\gamma_i)-\beta_i\cos(\gamma_i))\right] \\
&\quad +e^{-\lambda t}\sum_{i=1}^{M}\frac{\alpha_i\beta_i}{\lambda^2+\beta_i^2}\left[e^{\lambda t}\left(\lambda\cos(\beta_i t+\gamma_i)+\beta_i\sin(\beta_i t+\gamma_i)\right)-e^{\lambda s}\left(\lambda\cos(\beta_i s+\gamma_i)+\beta_i\sin(\beta_i s+\gamma_i)\right)\right] \\
&\quad +\sigma\int_0^t e^{\lambda(s-t)}\mathrm{d}W(s) \\
&= e^{-\lambda t}S(0)+\sum_{i=1}^{M}\frac{\alpha_i}{\lambda^2+\beta_i^2}\left[\lambda^2\sin(\beta_i t+\gamma_i)+\beta_i^2\sin(\beta_i t+\gamma_i)\right] \\
&\quad +\sum_{i=1}^{M}\frac{\alpha_i}{\lambda^2+\beta_i^2}\left[-\beta_i\lambda\cos(\beta_i t+\gamma_i)+\beta_i\lambda\cos(\beta_i t+\gamma_i)\right]+e^{-\lambda t}\sum_{i=1}^{M}\frac{\alpha_i}{\lambda^2+\beta_i^2}\left[-\lambda^2\sin(+\gamma_i)-\beta_i^2\sin(\gamma_i)\right] \\
&\quad +e^{-\lambda t}\sum_{i=1}^{M}\frac{\alpha_i}{\lambda^2+\beta_i^2}\left[\beta_i\lambda\cos(\gamma_i)-\beta_i\lambda\cos(\gamma_i)\right]+\sigma\int_0^t e^{\lambda(s-t)}\mathrm{d}W(s) \\
&= e^{-\lambda t}S(0)+\sum_{i=1}^{M}\alpha_i\left[\sin(\beta_i t+\gamma_i)-e^{-\lambda t}\sin(\gamma_i)\right]+\sigma\int_0^t e^{\lambda(s-t)}\mathrm{d}W(s)
\end{aligned}
$$

We conclude that the cosine terms cancel out. Analyzing this process we find the following expressions for the expectation and variance:

$$
\begin{aligned}
\mathbb{E}[S(t)] &= \mathbb{E}[e^{-\lambda t}S(0)+\sum_{i=1}^{M}\alpha_i\left[\sin(\beta_i t+\gamma_i)-e^{-\lambda t}\sin(\gamma_i)\right]+\sigma\int_0^t e^{\lambda(s-t)}\mathrm{d}W(s)] \quad (5.6) \\
&= e^{-\lambda t}S(0)+\sum_{i=1}^{M}\alpha_i\left[\sin(\beta_i t+\gamma_i)-e^{-\lambda t}\sin(\gamma_i)\right]+\mathbb{E}[\sigma\int_0^t e^{\lambda(s-t)}\mathrm{d}W(s)] \\
&= e^{-\lambda t}S(0)+\sum_{i=1}^{M}\alpha_i\left[\sin(\beta_i t+\gamma_i)-e^{-\lambda t}\sin(\gamma_i)\right]
\end{aligned}
$$

$$
\begin{aligned}
\mathbb{V}ar[S(t)] &= \mathbb{E}[S(t)^2] - \mathbb{E}[S(t)]^2 \qquad (5.7)\\
&= (e^{-\lambda t}S(0) + \sum_{i=1}^{M} \alpha_i \left[\sin(\beta_i t + \gamma_i) - e^{-\lambda t}\sin(\gamma_i)\right])^2 + \sigma^2 \int_0^t e^{2\lambda(s-t)}\mathrm{d}t - \mathbb{E}[S(t)]^2\\
&= \sigma^2 \int_0^t e^{2\lambda(s-t)}\mathrm{d}s\\
&= \frac{\sigma^2}{2\lambda}(1 - e^{-2\lambda t})
\end{aligned}
$$

We conclude that $S(t)$ is normally distributed with mean $S(0)+\sum_{i=1}^{M} \alpha_i \left[\sin(\beta_i t + \gamma_i) - e^{-\lambda t}\sin(\gamma_i)\right]$ and standard deviation $\sigma\sqrt{\frac{1-e^{-2\lambda t}}{2\lambda}}$. We have:

$$
S(t) \sim \mathcal{N}\left(S(0) + g(t) - e^{-\lambda t}g(0), \sigma^2\frac{1-e^{-2\lambda t}}{2\lambda}\right).
$$

Since we have expressed $S(t)$ as a normally distributed variable with certain mean and standard deviation, we can use the probability density function of $S(t)$ to find exact solutions for options with $S(t)$ as underlying, but we can also use the probability density function to price derivatives using numerical methods. We can thus calculate the price of a call and put option. For notational convenience, we write:

$$
\begin{aligned}
\mu &= S(0) + g(t) - e^{-\lambda t}g(0), \text{ and}\\
\hat{\sigma}^2 &= \sigma^2\frac{1-e^{-2\lambda t}}{2\lambda}.
\end{aligned}
$$

Note that μ is a function of t, λ, and $\hat{\sigma}$ is a function of λ and σ. We define $y = S(T)$, the wind speed at maturity, T. Then $f_{Y|S}(y|S(t))$ is equal to the probability density function of a normally distributed random variable with mean μ and standard deviation $\hat{\sigma}$. We find the following derivation for the price of a wind call with reference speed K:

$$
v^C(0, S(0)) = e^{-rT}\int_{-\infty}^{\infty}(y-K)^+\frac{1}{\sqrt{2\pi}\hat{\sigma}}e^{-\frac{(y-\mu)^2}{2\hat{\sigma}^2}}\mathrm{d}y.
$$

We substitute $\frac{y-\mu}{\hat{\sigma}} = z$

$$
\begin{aligned}
v^C(0, S(0)) &= \int_{\frac{K-\mu}{\hat{\sigma}}}^{\infty}\frac{z\hat{\sigma}+\mu-K}{\sqrt{2\pi}}\exp(-\frac{1}{2}z^2)\mathrm{d}z\\
&= \frac{\hat{\sigma}}{\sqrt{2\pi}}\int_{\frac{1}{2}\left(\frac{K-\mu}{\hat{\sigma}}\right)^2}^{\infty}\exp(-w)\mathrm{d}w + \frac{\mu-K}{\sqrt{2\pi}}\int_{\frac{K-\mu}{\hat{\sigma}}}^{\infty}\exp(-\frac{1}{2}z^2)\mathrm{d}z\\
&= \frac{\hat{\sigma}}{\sqrt{2\pi}}\exp\left(-\frac{1}{2}\left(\frac{K-\mu}{\hat{\sigma}}\right)^2\right) + (\mu-K)\left[1 - N\left(\frac{K-\mu}{\hat{\sigma}}\right)\right]. \qquad (5.8)
\end{aligned}
$$

In step 2 we used $\frac{z^2}{2} = w$, and $zdz = \mathrm{d}w$. Furthermore, $N(x)$ is the cumulative standard normal distribution. Similarly, for the a wind put option we find:

$$
\begin{aligned}
v^P(0, S(0)) &= e^{-rT} \int_{-\infty}^{\infty} (K-y)^+ \frac{1}{\sqrt{2\pi}\hat{\sigma}} e^{-\frac{(y-\mu)^2}{2\hat{\sigma}^2}} \mathrm{d}y \\
&= e^{-rT} \int_{-\infty}^{K} (K-y) \frac{1}{\sqrt{2\pi}\hat{\sigma}} e^{-\frac{(y-\mu)^2}{2\hat{\sigma}^2}} \mathrm{d}y \\
&= \frac{K-\mu}{\sqrt{2\pi}} \int_{-\infty}^{\frac{K-\mu}{\hat{\sigma}}} \exp(-\frac{1}{2}z^2)\mathrm{d}z - \frac{\hat{\sigma}}{\sqrt{2\pi}} \int_{\frac{1}{2}\left(\frac{K-\mu}{\hat{\sigma}}\right)^2}^{\infty} \exp(-w)\mathrm{d}w,
\end{aligned}
$$

where in (5.9) we again used substitution of $\frac{1}{2}z^2 = w$, and the property $I(-x) = -I(x)$ for the second integral. We thus write:

$$
v^P(t0, S(0)) = (K-\mu)N\left(\frac{K-\mu}{\hat{\sigma}}\right) - \frac{\hat{\sigma}}{\sqrt{2\pi}} \exp\left(-\frac{1}{2}\left(\frac{K-\mu}{\hat{\sigma}}\right)^2\right) \tag{5.9}
$$

So, we found closed-form solutions to the OU-process with seasonal mean. Here, the seasonality is modeled by a sum of sine functions. Besides the fact that we derived a closed-form solution for a certain type of wind derivatives, this conclusion may have application in the pricing of option and future contracts of seasonality-sensitive commodities, as well as calibration for these types of derivatives.

We can use this closed-form solution to price caplets or floorlets as defined in (3.8) and (3.9) and sum them to find prices to caps, floor, and cash settlement agreements with an OU-process with seasonal mean as underlying. Also, the fact that we found a closed-form solution for the OU-process with seasonality mean implies better calibration of the parameters of models in (4.4) where the seasonality is removed by subtraction. Instead of calibrating the underlying OU-process, now the wind speed model can be calibrated. This may yield better fitting parameters λ and σ under assumption of a fixed seasonality function $g(t)$, which will result in a better statistical reconstruction of the distribution of wind speeds.

5.2.3 Numerical methods

Now, numerical methods will be discussed. Since we have probability density functions of the Weibull distribution and an OU-process with seasonal mean, numerical methods can be used calculate option prices considering one day in the future. The price of an option under the risk-neutral measure, is the discounted expected payoff. If the probability density function of the underlying is known, this is an integral that looks like:

$$
v(t_0, x) = e^{-r\Delta t}\mathbb{E}^{\mathbb{Q}}[v(T, y)] = e^{-r\Delta t} \int_{-\infty}^{\infty} v(T, y) f_{Y|X}(y|x)\mathrm{d}y, \tag{5.10}
$$

where $v(t_0, x)$ is the price of the option at time t_0, and underlying has value x at time t_0. y is the value of the underlying at maturity, T. $v(T, y)$ is the payoff functions, and $f_{Y|X}(y|x)$ is the probability density function of y, given the price of x at t_0. There is a wide range of numerical methods to approximate (5.10). We will discuss the trapezoidal rule and Simpson's rule, as these methods will give sufficiently accurate solutions.

Trapezoidal rule

The integral in (5.10) can be solved using the trapezoidal rule [45] when $f_{Y|X}(y|x)$ is known in closed form. The trapezoidal rule is defined as:

$$\begin{aligned}\int_a^b g(x)\mathrm{d}x &\approx \frac{h}{2}\sum_{k=1}^{N}(g(x_{k+1})+g(x_k)) \\ &= \frac{b-a}{2N}(g(x_1)+2g(x_2)+2g(x_3)+\cdots+2g(x_N)+g(x_{N+1})).\end{aligned}$$

If we divide our interval in N equal parts, with points on the x-axis having equal distances $h = x_{i+1} - x_i$, the integral (5.10) can be solved numerically by choosing appropriate a and b for integration interval $[a, b]$. Small enough distances for h will yield a satisfying approximation. If faster or more accurate numerical methods are desired, one may use Simpson's rule to approximate the integral in (5.10).

Simpson's rule

The integral (5.10) can also be solved using the Simpson's rule [45]. Simpson's rule reads:

$$\begin{aligned}\int_a^b g(x)\mathrm{d}x &\approx \frac{h}{6}\sum_{k=1}^{N}(g(x_{k+1})+4g(x_k)+g(x_{k-1})) \\ &= \frac{b-a}{6N}(g(x_1)+5g(x_2)+5g(x_3)+\cdots+5g(x_N)+g(x_{N+1})).\end{aligned}$$

We again have N intervals of the same size h, and a and b as lower and upper bound for the integration interval $[a, b]$. Often the integral in (5.10) cannot be solved analytically, and numerical methods have to be used. In the case of wind derivatives, we may encounter derivatives that can be priced by numerical methods, but not analytically. When derivatives can be priced using numerical methods, these values will be satisfactory reference prices to confirm the implementation of analytically computed prices. We can confirm our analytically attained prices by using the trapezoidal rule to solve (5.10).

Since we have the probability density function of a model with seasonality and a model without seasonality, both wind speed and wind power derivatives can be priced considering one day in the future. The wind speed index is then the daily average wind speed at maturity, and a wind power index can be a translation of this wind speed to generated amount of electricity. This translation will be an approximation of the efficiency function, f.e. a function $l(x)$ that is a polynomial of grade n, and should work as long as $l(x)$ is bounded on $[0, \infty)$.

5.2.4 COS-method

The last method we consider is the COS-method, as developed by Oosterlee et. al [54]. Research on option pricing by the COS-method has amongst others been done for European options [54], OU-processes [55], and for Asian options under Lévy processes [51]. In [55] the ability of the COS-method to price options with OU-process underlying is shown. Moreover, in [51] it is shown that the COS-method can price Asian options under Lévy processes. Since an OU-process is driven by a Brownian motion, it is a Lévy process. This indicates that also Asian average rate options with an OU-process with seasonal mean can be priced using the COS-method. When insufficient data

is available to model seasonality, the daily wind speed distribution is best described by a Weibull distribution. In this section we will look into the pricing of European and Asian style wind speed derivatives with Weibull distributed underlying.

COS for Weibull & Rayleigh

Options and futures with the underlying being Weibull or Rayleigh distributed at maturity can be priced using an exact solution [52]. To attain faster pricing and calibration of Asian average rate options with Weibull distributed underlying (possible wind derivatives), we suggest the COS-method. By showing that it is possible to price options that are Weibull distributed at maturity, we conclude from existing framework [51], in combination with properties of the Weibull and log-Weibull distribution that it is also possible to price Asian options with Weibull underlying using the COS-method.

The steps we take to approximate the Weibull distribution and calculate the European option prices are similar to the steps taken in [54]. First, we approximate the probability density function of the Weibull distribution using a Fourier-cosine series expansion, and after that, we look into European options (which can only be executed at maturity) with the underlying being Weibull distributed at maturity. Finally, we compute the errors for the COS-method for Weibull.

Approximating the Weibull distribution using the COS-method

We wish to place option pricing with a Weibull distribution into a well-known framework of Fourier option pricing techniques. These techniques may be well-suited for calibration purposes. For the COS-method, the characteristic functions of either the Weibull distribution or log-Weibull distribution are used. Since the characteristic function of the log-Weibull distribution is a stable function for all values of the parameters of the Weibull distribution, this will yield the most accurate results. The characteristic function of the Weibull distribution can be used, but the computational time increases and accuracy decreases as of compared to the log-Weibull distribution. Therefore, we discuss the COS-method using the characteristic function of the log-Weibull distribution in this section. There are ways around the instability of the Weibull characteristic function to price European options. This approach and these results, using the characteristic function of the usual Weibull distribution, are discussed in Appendix C.1.

We start with the approximation of the Weibull distribution by using a Fourier-cosine series expansion and using the characteristic function of the log-Weibull distribution. We expect exponential convergence of the weighted sum of cosine function, because the probability density function of the log-Weibull distribution, being a combination of entire functions, is also an entire function. Exponential convergence is a fundamental property for pricing based on Fourier-cosine expansion. Now let Y be a Weibull distributed random variable, then $Z = \log(Y)$ is a log-Weibull distributed variable. Since Y is a Weibull distributed random variable, it does not depend on a starting point (x), however to maintain uniform notation, we still express the probability density function as $f_{Y|X}(y|x)$. Using a Fourier-cosine expansion we find:

$$f_{Y|X}(y|x) = \sum_{k=1}^{\infty}{}' A_k \cdot \cos(ky), \text{ with } A_k = \frac{2}{\pi}\int_0^{\pi} f(\theta)\cdot\cos(k\theta)\mathrm{d}\theta, \tag{5.11}$$

where $\sum'$ indicates that the first term in the summation is weighed by one-half. We find[39], by the change of variables $z = \log(y)$, that:

$$f_{Y|X}(y|x) = \frac{1}{y} f_Z(\log(y)), \tag{5.12}$$

hence we can approximate the log-Weibull distribution on a general interval $[a, b]$ by the following transformation of the parameters in (5.11):

$$\theta = \frac{z-a}{b-a}\pi \quad \Leftrightarrow \quad z = \frac{b-a}{\pi}\theta + a.$$

This transformation yields the following notation for $f_Z(z)$, using the Fourier-cosine series expansion:

$$f_Z(z) = {\sum_{k=0}^{\infty}}' A_k \cos\left(k\pi \frac{z-a}{b-a}\right), \text{ with } A_k = \frac{2}{b-a}\int_a^b f_Z(z) \cdot \cos\left(k\pi \frac{z-a}{b-a}\right) \mathrm{d}z.$$

We consider the characteristic function of the log-Weibull distribution with parameters k and λ:

$$\phi_Z(\omega) \quad = \quad \lambda^{i\omega}\Gamma\left(1 + \frac{i\omega}{k}\right).$$

The derivation of this characteristic function can be found in Appendix C.4. Choosing appropriate values for interval boundaries a and b will result in an approximation of the integral defining the characteristic function:

$$\phi_Z(\omega) = \int_{\mathbb{R}} e^{i\omega z} f_Z(z) \mathrm{d}z \approx \int_a^b e^{i\omega z} f_Z(z) \mathrm{d}z = \phi_Z^*(\omega), \tag{5.13}$$

where a and b are set as -10σ and 10σ, as proposed in [54], and σ is the standard deviation of the considered log-Weibull distribution. With these values for $[a, b]$ the integral is well approximated. Using this characteristic function, we can rewrite A_k as follows:

$$A_k \quad = \quad \frac{2}{b-a}\mathrm{Re}\left\{\phi_Z^*\left(\frac{k\pi}{b-a}\right)\exp\left(-i\frac{ka\pi}{b-a}\right)\right\}.$$

With (5.13) A_k can be approximated by F_k, defined as:

$$F_k \quad = \quad \frac{2}{b-a}\mathrm{Re}\left\{\phi_Z\left(\frac{k\pi}{b-a}\right)\exp\left(-i\frac{ka\pi}{b-a}\right)\right\}.$$

Looking at $f_Z(z)$ and using (5.13) we replace A_k by F_k and write the following as an approximation of the log-Weibull probability density function:

$$f_Z^*(z) \approx {\sum_{k=0}^{\infty}}' F_k \cos\left(k\pi \frac{z-a}{b-a}\right),$$

and as F_k is decreasing exponentially as k increases, we may expect exponential convergence in k. Small values for k will yield accurate approximations, so we may truncate the sum to attain:

$$f_Z^{**}(z) = \sum_{k=0}^{N-1}{}' F_k \cos\left(k\pi\frac{z-a}{b-a}\right),$$

for a certain N. Using a change of variables, as proposed in (5.12), we find for the approximation for $f_{Y|X}(y|x)$:

$$f_{Y|X}^{**}(y|x) = \frac{1}{y}\sum_{k=0}^{N-1}{}' F_k \cos\left(k\pi\frac{\log(y)-a}{b-a}\right).$$

With this approximation for the probability density function of the Weibull distribution we are able to accurately approximate the Weibull distribution. If $\lambda = 9$ and $k = 2.25$ for example, and we choose $[a, b] = [-5, 5]$, we measure the maximum error between the Fourier-cosine approximation of the probability density function and the Weibull probability density function at points $\{1, 2, ..., 19, 20\}$. The maximum errors per value of N are displayed in Table 5.1.

N	4	8	16	32	64	128
error	1.47e-01	7.43e-02	1.47e-02	6.47e-04	7.44e-07	3.45e-12
cpu time (sec.)	0.0002	0.0002	0.0002	0.0003	0.0003	0.0005

Table 5.1: Maximum error when recovering $f_{Y|X}(y|x)$ from $\phi_Z(\omega)$ by Fourier-cosine expansion.

Table 5.1 indicates accurate results for the approximation of $f_{Y|X}(y|x)$ for small N in very little cpu time. This is promising when pricing derivatives under a Weibull distribution. It furthermore confirms the exponentially converging sum of weighted cosine functions.

European options

Since we have accurate approximations for the probability density function for small values of N, options with Weibull distributed underlying can be priced using the COS-method. In context of wind derivatives we will focus on European options, which can only be exercised at maturity. Within the range of European options we will look at plain vanilla options and cash-or-nothing options, as these are both being traded OTC [18]. We start with the discounted expected payoff:

$$v(t_0, x) \quad = \quad e^{-r\Delta t}\int_{-\infty}^{\infty} v(T, z) f_Z(z)\mathrm{d}z.$$

Here, $v(T, z)$ is the value of the payoff at maturity, T, when the wind has speed e^z, and $v(t_0, x)$ is the option price at time t_0. In this case the value of a European option is the expected payoff under the risk-neutral measure. Again, it is questionable whether or not we can work with the discounted expected payoff, however a fairer approach is not available at this time. Note that we are again working in the log-domain, so $z = \log(y|x)$. If we truncate this integral to a specific interval $[a, b]$, we find the following:

$$
\begin{aligned}
v_1(t_0,x) &= e^{-r\Delta t}\int_a^b v(T,y)f_Z(z)\mathrm{d}z \\
&= e^{-r\Delta t}\int_a^b v(T,z)\sum_{k=0}^{\infty}{}'A_k\cos\left(k\pi\frac{z-a}{b-a}\right)\mathrm{d}z \\
&= e^{-r\Delta t}\sum_{k=0}^{\infty}{}'A_kV_k \text{ with } V_k=\int_a^b v(T,z)\cos\left(k\pi\frac{z-a}{b-a}\right)\mathrm{d}z.
\end{aligned}
$$

Fubini's theorem was used in step 3 to interchange the summation and integration signs. If we truncate the sum, we find:

$$
v_2(t_0,x) = e^{-r\Delta t}\sum_{k=0}^{N-1}{}'A_kV_k.
$$

The last step to efficiently pricing options is to use (5.13) again to replace A_k by F_k. We find that option prices may be expressed as

$$
\begin{aligned}
v_3(t_0,x) &= e^{-r\Delta t}\sum_{k=0}^{N-1}{}'F_kV_k \\
&= e^{-r\Delta t}\sum_{k=0}^{N-1}{}'\mathrm{Re}\left\{\phi_Z\left(\frac{k\pi}{b-a}\right)\exp\left(-i\frac{k\pi a}{b-a}\right)\right\}V_k.
\end{aligned}
\tag{5.14}
$$

Pricing plain vanilla options or cash-or-nothing options will yield different expressions for $v(T,z)$ and thus for V_k. These will be considered in the following two subsections. For various approximations, an error analysis can be found in [54].

Coefficients V_k for plain vanilla options

To consider the expressions of V_k for plain vanilla options, we look at the payoff of these options. The payoff for a plain vanilla option is given by:

$$
v(T,z)=[\alpha(z-K)]^+, \text{with } \alpha=\begin{cases} 1 & \text{for a plain vanilla call option} \\ -1 & \text{for a plain vanilla put option.}\end{cases}
$$

As in [54] we now define $\chi_(c,d)$ and $\psi(c,d)$, with $c,d\in[a,b]$ and $c<d$ to be

$$
\begin{aligned}
\chi_k(c,d) &= \int_c^d e^y\cos\left(k\pi\frac{d-a}{b-a}\right)\mathrm{d}y, \\
\psi_k(c,d) &= \int_c^d \cos\left(k\pi\frac{d-a}{b-a}\right)\mathrm{d}y.
\end{aligned}
$$

These integrals can both be solved analytically having the following exact answers:

$$
\begin{aligned}
\chi_k(c,d) &= \frac{1}{1+\left(\frac{k\pi}{b-a}\right)^2}\left[\cos\left(k\pi\frac{d-a}{b-a}\right)e^d - \cos\left(k\pi\frac{c-a}{b-a}\right)e^c\right. \\
&\quad \left. + \frac{k\pi}{b-a}\sin\left(k\pi\frac{d-a}{b-a}e^d - \frac{k\pi}{b-a}\sin\left(k\pi\frac{c-a}{b-a}\right)e^c\right)\right] \\
\psi_k(c,d) &= \begin{cases} \left[\sin\left(k\pi\frac{d-a}{b-a}\right) - \sin\left(k\pi\frac{c-a}{b-a}\right)\right]\frac{b-a}{k\pi} & k \neq 0 \\ d-c & k = 0. \end{cases}
\end{aligned}
$$

These integrals yield the following expressions for V_k for a plain vanilla call we have $\alpha = 1$, and thus $v(T,z) = [e^z - K]^+$:

$$
\begin{aligned}
V_k^{\text{call}} &= \int_a^b v(T,z)\cos\left(k\pi\frac{z-a}{b-a}\right)\mathrm{d}z \\
&= \int_a^b [e^z - K]^+\cos\left(k\pi\frac{z-a}{b-a}\right)\mathrm{d}z \\
&= \int_{\log(K)}^b (e^z - K)\cos\left(k\pi\frac{z-a}{b-a}\right)\mathrm{d}z \\
&= \chi_k(\log(K), b) - K\psi_k(\log(K), b).
\end{aligned}
$$

A similar derivation yields the expression for V_k^{put}:

$$
V_k^{\text{put}} = K\psi_k(a, \log(K)) - \chi_k(a, \log(K)).
$$

These expressions for V_k^{call} and V_k^{put} can be used in (5.14) to compute plain vanilla put and call option prices.

Coefficients V_k for cash-or-nothing options

The computations for the coefficients V_k for cash-or-nothing options are done in a similar matter. Consider a cash-or-nothing call that pays B if $e^y > K$ and 0 otherwise. The payoff function then is defined by

$$
v(T,z) = B\mathbb{1}_{(\alpha e^z > \alpha K)}, \text{with } \alpha = \begin{cases} 1 & \text{for a call,} \\ -1 & \text{for a put.} \end{cases}
$$

This means that also an analytic expression for the coefficients V_k for cash-or-nothing options can be found. We find the following expressions for a cash-or-nothing call (conc) and cash-or-nothing put (conp):

$$
\begin{aligned}
V_k^{\text{conc}} &= B\psi(\log(K), b) \\
V_k^{\text{conp}} &= B\psi(a, \log(K)).
\end{aligned}
$$

These expressions for V_k^{conc} and V_k^{conp} can be substituted in (5.14) to compute cash-or-nothing call and put option prices.

Collars

An often used strategy within finance is the use of a collar. From conversation with [18] it was noted that collars are also used for wind derivatives. A collar is a combination of two options with the same underlying and maturity, but with different strike prices. The idea of a collar is to buy a call (put) option with a certain strike K and maturity T, and sell another call (put) with the same maturity, but a slightly higher (lower) strike price. This way, the possibility to make a significant profit on the option position is traded for an overall lower portfolio price. The COS-method is an excellent method to quickly price collars of plain vanilla options and cash-or-nothing options, as the only terms that has to be adjusted for a call (put) collar is the upper (lower) bound of the integral in the V_k term, and the V_k coefficient.

Plain vanilla option prices

The probability density function of the Weibull distribution can well be approximated by Fourier-cosine series expansion. As we have exponentially converging terms F_k, we expect fast and accurate results for option prices with Weibull distributed underlying at maturity. In this section we compute prices for these options. We look at option prices for plain vanilla options, and for cash-or-nothing options. We will discuss on the prices as computed by the Monte Carlo method, numerical methods (using the trapezoidal rule) and by the COS-method, together with the according cpu times. We start with the pricing of plain vanilla call and put options. The input parameters we work with are:

$$N = 64, \quad r = 0.02, \quad T = 1, \quad \lambda = 9 \quad \text{and} \quad k = 2.25.$$

The option prices that were found are displayed in Table 5.2.

	K	1	6	11	16	21	26
Call	Analytic	6.8357	2.5806	0.5065	0.0441	0.0015	0.0000
	COS	6.8357	2.5806	0.5065	0.0441	0.0015	0.0000
Put	Analytic	0.0021	0.6481	3.4749	7.9136	12.7720	17.6715
	COS	0.0021	0.6481	3.4749	7.9136	12.7720	17.6715

Table 5.2: Prices of plain vanilla options having different strike prices as calculated analytically and with the COS-method

We see that the prices of plain vanilla call and put options are the same. Since we have an exact solution, this is taken as a reference for the errors of the COS-method. To look at sensitivity of the value N, in Table 5.3 the maximum errors per value of N are presented for the call and put options. We conclude that $N = 64$ indeed gives us satisfying small errors.

N	4	8	16	32	64
max. error Call	2.94e-0	7.12e-1	1.08e-1	-9.24e-4	1.04e-6
max. error Put	7.45-1	1.14e-1	2.61e-2	3.65e-4	9.63e-7

Table 5.3: Maximum errors per value of N for European options with strikes 1, 6, 11, 16, 21, 27.

We compared the cpu times of the analytical method, Monte Carlo method, the numerical method and the COS-method, and these are displayed in Table 5.7. We conclude that the COS-method is about ten times slower than the analytical method, however 5 milliseconds cpu time is still a positive perspective when we wish to price Asian type of options with Weibull underlying.

Method		Ana	MC	Num	COS
cpu. time	Call	0.4157	56110	31.5743	5.0289
(msec.)	Put	0.4516	53464	31.5742	4.1001

Table 5.4: Computation times using different methods to compute prices of plain vanilla options in milliseconds.

Cash-or-nothing option prices

We can compute closed-form solution prices for cash-or-nothing options with Weibull underlying, as can be seen in Appendix C.6.2. It is also interesting to look at the computation of cash-or-nothing options with Weibull underlying at maturity , since this would indicate that using the COS-method, also the Asian variant of cash-or-nothing options can be priced. The prices of cash-or-nothing options with Weibull underlying at maturity are computed using the input variables

$$N = 64, \quad r = 0.02, \quad T = 1, \quad \lambda = 9, \quad k = 2.25 \quad \text{and} \quad B = 11.$$

We find the following table for cash-or-nothing option prices:

	K	1	6	11	16	21	26
Call	Analytic	10.7064	7.2175	2.238	0.2811	0.0133	0.0002
	COS	10.7056	7.216	2.2417	0.2804	0.0129	0.0002
Put	Analytic	0.0739	3.5623	8.5396	10.5029	10.7691	10.782
	COS	0.0766	3.5662	8.5405	10.5018	10.7693	10.782

Table 5.5: Prices of cash-or-nothing options having different strike prices as calculated analytically and with the COS-method.

Again we use the analytical solutions as reference values for the COS-method prices. The errors of these computations are again satisfactory for small values of N, as can be seen in Table 5.6.

N	4	8	16	32	64
max. error Call	1.89e-0	5.56e-1	3.49e-2	2.43e-3	5.36e-5
max. error Put	1.68e-0	5.91e-1	8.07e-2	2.42e-3	5.50e-5

Table 5.6: Maximum errors per value of N for cash-or-nothing options with strikes 1, 6, 11, 16, 21, 27.

The computation times for the cash-or-nothing options using the COS-method are also satisfactory, taking only 4 milliseconds to compute the cash-or-nothing option prices.

Method		Anal	MC	Num	COS
cpu. time	Call	0.0307	62418	4307.1	4.012
(msec)	Put	0.0308	60892	4146.8	4.2745

Table 5.7: Computation times using different methods to compute prices of cash-or-nothing options.

Altogether, we conclude that the COS-method is a fast and accurate method to price plain vanilla and cash-or-nothing options with Weibull distributed underlying at maturity. Since the Rayleigh

distribution is a simplification of the Weibull distribution, we may draw the same conclusion for plain vanilla and cash-or-nothing options that have Rayleigh underlying at maturity. Since the computation times are fast, this gives a satisfactory perspective for our wish to price Asian average rate options with Weibull underlying using the COS-method.

Pricing Asian average rate options with Weibull underlying

A framework for Asian options under Lévy processes for this is provided in [51]. Moreover, the author of [56] states that any distribution that is infinitely divisible, is a Levy process. We used the log-Weibull distribution when pricing with the COS-method, so, if the log-Weibull distribution is infinitely divisible, then it is a Levy process. To prove that the log-Weibull distribution is in fact infinitely divisible, we use the Gumbel distribution, which is infinitely divisible [57]. The probability density function of a Gumbel distribution with parameters μ and β is written as:

$$\begin{aligned} f(x) &= \frac{1}{\beta}\exp\left(-\left(\frac{x-\mu}{\beta}\right)+\exp\left(-\frac{x-\mu}{\beta}\right)\right) \\ &= \frac{1}{\beta}\exp\left(-\left(\frac{x-\mu}{\beta}\right)\right)\exp\left(\exp\left(-\frac{x-\mu}{\beta}\right)\right). \end{aligned}$$

Now take use transformations $\mu = \log(\lambda)$ and $\beta = -\frac{1}{k}$, we find:

$$f(x) = \frac{k}{\lambda}\left(\frac{e^x}{\lambda}\right)^{k-1}\exp\left(-\left(\frac{e^x}{\lambda}\right)^k\right).$$

Since the Gumbel distribution is infinitely divisible, and the log-Weibull is a translation of the Gumbel distribution, so is the log-Weibull distribution. A log-Weibull random variable is therefore a Lévy process, and so it may be possible to price Asian average rate options with Weibull underlying using the framework as proposed in [51].

Pricing wind power options with the COS-method

We considered pricing of wind speed options with the COS-method, however wind power options with underlying being a transformed wind speed. If wind power options are considered, we should find expressions for V_k^{powerc} and V_k^{powerp}. Let again $l(x)$ be the transformation that is done on the wind speeds. $l(x)$ should be a function such that:

$$V_k^{powerc} = \int_a^b [l(z)-K]^+ \cos\left(k\pi\frac{z-a}{b-a}\right)\mathrm{d}z,$$

can analytically be solved. This is the case when $l(x)$ is a polynomial, so we may be able to price wind power options using the COS-method, using similar methodology as when pricing wind speed derivatives. The same should be true for V_k^{powerp}.

Chapter 6

Conclusion and outlook

6.1 Conclusion & summary

The goal of this thesis was to design (when necessary and not yet existent) and price financial derivative products such that wind risk can be hedged. We made a distinction between wind speed derivatives, based on average wind speed in m/s over a defined interval, and wind power derivatives, based on generated power in MWh over a defined interval.

To price wind speed or power derivatives, the behavior of the underlying was analyzed. In Chapter 2 we looked into the behavior of wind over the last twenty to fifty years in the Netherlands. We concluded that there are two types of seasonal patterns in wind speed data: daily seasonality caused by the rotation of the Earth, and yearly seasonality, caused by the rotation of the Earth around the sun. Furthermore, we concluded that wind is not (strongly) correlated to other weather components such as temperature, overcast or rainfall. With respect to the transfer to wind energy, we concluded that transforming wind speed to power generation can be done using an efficiency function. This way, the behavior of the underlying of wind power derivatives, generated power, can be analyzed and simulated.

In Chapter 3 we introduced wind speed and wind power indices, which are translations from observed wind speed data. Several wind derivatives, as known in the market at this moment, were discussed and the payoffs were given. At this moment, wind derivatives are only traded OTC, however wind derivatives were exchanged listed before, and an industry party is interested into reintroducing wind derivatives at an exchange. Moreover, we concluded that one of the problems of the wind derivatives market is the dependence on location, which makes it hard to find a counterparty for a contract. Another possible issue is the difficulty to hedge wind speed options, as no trading can be done in the underlying. This can be different for wind power options, as its underlying, power, can be traded in. We saw that an energy company can also mitigate wind risk by using wind speed clauses in consumer contracts, or by looking at the correlation of two different wind farms.

The modeling of wind speed was discussed in Chapter 4. We looked at two methods to model wind: with incorporating seasonal effects and without. The latter method can be used if not sufficient data is available to extract a seasonality function from. Without seasonality, the distribution of hourly and daily average wind speeds can be modeled by a Weibull distribution. If, however, sufficient data is available to extract a satisfying estimate of the seasonality function, incorporat-

ing this seasonality is the preferred method. When seasonality is incorporated, the wind speed process is set to be a combination of a seasonality function and a random process. This random process can well be modeled by an OU-process. A benefit of incorporating seasonality is that it may be possible to price shorter term derivatives. The Weibull distribution can only be applied for contract over long periods of time. The seasonality can best be extracted by fitting a sum of sine functions to the yearly average function. We proposed deseasonalizing the data by dividing the observed data by the seasonality function, whereas in literature mostly subtraction of this seasonality function is used. The result of this approach is an OU-process without autocorrelation in its returns or squared returns. Using 2-sample Kolmogorov-Smirnov tests, we conclude that modeling wind speed by multiplication of an OU-process and the estimated seasonality function is the optimal model choice to model both hourly and daily average wind speeds.

In Chapter 5 we concluded that the wind derivatives market is not a complete market, due to the inability to trade in the underlying and the level of illiquidity. The incompleteness of the wind derivatives market complicates the use of the discounted expected payoff as a pricing method. When using Girsanov's theorem, the transformation to a risk-neutral measure can be done by accounting for the market price of risk. Since there are no quotes, it will however be hard to find a fair risk-neutral measure. Because of the illiquidity, this may lead to the request of significant risk premiums by the seller of a wind derivative. Under the assumption of the existence of a risk-neutral measure, pricing of derivatives can however be done by calculating the discounted expected payoff. Options and futures on a wind index that is averaged over more than one day can be seen as Asian average rate types of derivatives. These can be priced by the Monte Carlo method, possibly using variance reduction techniques to enhance the Monte Carlo simulations and presumably by the COS-method. We derived closed-form solutions for plain vanilla options with an underlying that incorporates seasonality considering one day in the future. This may also yield an exact solution to wind speed caps and floors. Furthermore, we concluded that options with Weibull underlying at maturity can be priced by the COS-method and we argued that is may be possible to price Asian style options with Weibull underlying by the COS-method. Both the analytical and the COS-method results can be used for fast and accurate calibration purposes.

6.2 Outlook

Many questions that can give a more realistic view on wind derivatives are still unanswered. Moreover, new questions appeared while doing the research, not necessarily in the field of wind derivatives, but also in related fields. In this section we will shortly discuss on some questions that have emerged, and could be worth answering in future research.

Further advancements in the COS-method for Weibull

At the end of Section 5.2.4 we shortly discussed that presumably the COS-method can also be used to price Asian average rate options with Weibull underlying. Also, we state that wind power derivatives can be priced by using a translation function to translate wind speed to amount of generated power. It would not be much work to write out pricing functions in MATLAB to confirm whether this is true or not. This could mean that all Asian type of wind derivatives can be priced in a fast and accurate way. Also, it would be interesting to look at the calibration of parameters λ and σ in the model that incorporates seasonality, using either the COS-method or analytical solutions. This may give better estimates for these parameters, and for the total reconstructed wind speed distribution.

Incorporating daily seasonality to model hourly average wind speeds

One flaw in the modeling of hourly wind speeds was that the diurnal cycle was not accounted for. Our seasonality function $g(t)$ was the yearly average seasonality. Another seasonality function could be added to $g(t)$, the daily average seasonality function, for example $h(t)$. The combination of these two could serve as the total seasonality function to model quarter of an hour or hourly average wind speeds more accurately.

Solar or photo voltaic derivatives

Like wind energy, solar energy is a rising source of energy. During the project, we noticed the relation between radiation coming from the sun, and wind. Radiation, coming from the sun is the main driver for solar (or photo voltaic or PV) energy. Radiation is exposed to the same kinds of seasonality effects, and therefore similar modeling could be used as was used for wind. To price solar (or PV) derivatives, the radiation should be analyzed in a similar way that we analyzed wind. This means that the time series has to be analyzed for seasonality effects and noise, correlations can be computed et cetera. We tend to think that radiation will be harder to model, since it will be a lot more volatile. For example clouds can appear and disappear in seconds from a solar plant's point of view. Solar energy production may also be hard to price. Complications like snow lying on the solar panels, or the strong correlation of the efficiency of a solar panel to temperature are hard to model.

Not only the underlying is different, but also the market for solar derivatives will be different. Solar energy is generated at many different spots within a country (decentralized), whereas wind farms are installed at specific spots. This means that every solar energy producer, will be exposed to smaller risk, since little energy is generated. In total, this may not make the solar derivatives market an interesting market. On the other hand, also crops are exposed to influence of radiation. More parties will benefit or suffer from a lack or surplus of radiation. This could make the market more interesting than the wind derivatives market, as counterparties are found easier.

Ideal height of a wind turbine

One question that emerged while doing this research was the question what the ideal height of a wind turbine is from an economic point of view. To answer this questions, the total costs and total benefits must be specified and identified. Our idea was to use basic economics to calculate the Net Present Value of a wind turbine as a function of the height. Taking the derivative and setting it equal to zero should then do the trick. The NPV is nothing but a summation of discounted yearly cash flows. These cash flows will hold some uncertainty, which will make it hard to draw a conclusion on the ideal height. Industry terminology to define investment costs and operational costs are CAPEX (Capital Expenditure) and OPEX (Operational Expenditure). CAPEX can be defined to be the costs that are needed until a wind turbine is delivered, the OPEX the costs that are made after delivery to keep the wind turbine running. Revenues from a wind turbine come from generated electricity, and possibly the scrap value of the wind turbine at the end of its lifetime.

To give an accurate picture of the economics, we noticed that detailed information will be needed from developers (usually energy companies), suppliers (Vestas, Siemens et cetera) and an EPC (Engineering Procurement and Construction) party. Bringing all this information together and building an appropriate model was beyond the scope of this thesis, but could be interesting as future research for the wind energy community.

Correlations wind speed and electricity price

As was mentioned in this report, wind speed and electricity price are assumed [18] to become more closely correlated than a couple of years ago, due to the increasing installed capacity of wind turbines. If the desired data is available, a simple rolling window of direct and lagged correlation of wind speeds and electricity spot market prices could give more insight in this assumption. If indeed a strong correlation is found, this will open a window of opportunity to hedge wind speed or power derivatives by trading in power.

Storing energy for higher profit

Another economic issue of a wind turbine is that the electricity has to be sold to the grid immediately, since it cannot be stored. Wind turbine owners are therefore fully dependent on the electricity spot price market. If a loss in power would be accepted by for example using all the electricity to pump water in a reservoir, it would be possible for the owner of the reservoir to decide when to generate electricity by letting the water come down again. Whether 'storing' the electricity in a reservoir is economically viable could be calculated by calculating the loss of energy by pumping up the water, and the possible increase in electricity price when letting it down.

Modeling of weekly or monthly average wind speed

Weekly and monthly average wind speed seem lognormal distributed instead of Weibull distributed, as can be seen in Figure **??**. This could be interesting to look in to when pricing wind speed contracts with average wind speed per week or month as underlying. Unfortunately, wind power derivatives will be impossible to price with this model.

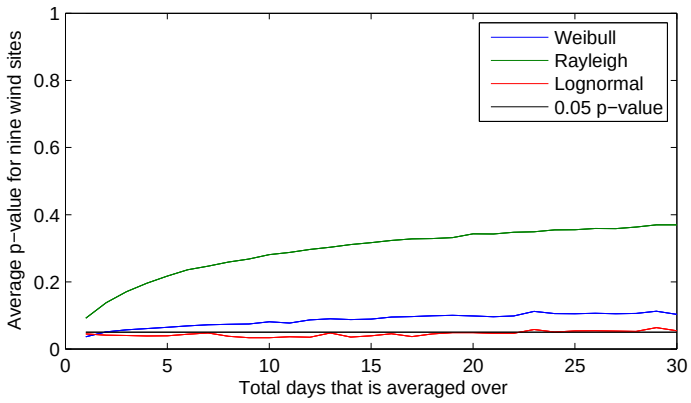

Figure 6.1: p-values per distribution when modeling an n day average wind speed

Appendix A

Wind & wind energy

A.1 Betz' limit

To find the maximum value of C_p as in (2.6), we take the derivative of C_p with respect to $\frac{v_0}{v}$, and set it equal to zero:

$$\begin{aligned}
\frac{\partial C_p}{\partial \frac{v_0}{v}} &= \frac{\partial}{\partial \frac{v_0}{v}} \left(\frac{\left(1+\frac{v_0}{v}\right)\left(1-\left(\frac{v_0}{v}\right)^2\right)}{2} \right) \\
&= \frac{1}{2}\left[\left((1-\left(\frac{v_0}{v}\right)^2 \right) - \left(1+\frac{v_0}{v}\right) 2\frac{v_0}{v} \right] \\
&= -\frac{3}{2}\left(\frac{v_0}{v}\right)^2 - \frac{v_0}{v} + \frac{1}{2} \\
&= 0.
\end{aligned}$$

We find $\frac{v_0}{v}$ is either equal to -1 or to $\frac{1}{3}$. Since both $v \geq 0$ and $v_0 \geq 0$, the only answer is $\frac{v_0}{v} = \frac{1}{3}$. This indicates that the maximum power from the wind is extracted at speed ratio 1:3, meaning that the downstream wind is one-third of the upstream wind speed. Filling in $\frac{v_0}{v} = \frac{1}{3}$ for C_p yields $C_p = \frac{16}{27} \approx 0.59$.

A.2 Weather & wind correlations

Using KNMI data, average wind speed over one hour and over a day can be tested for correlation against the hourly or daily average of other weather components. We have tested wind direction (in degrees), wind speed (in m/s), temperature (in degrees Celsius), radiation (in J/cm^2), pressure (in hPa), horizontal sight (0 means less than 100m, 1=100-200m, 2=200-300m,..., 49=4900-5000m, 50=5-6km, 56=6-7km, 57=7-8km, ..., 79=29-30km, 80=30-35km, 81=35-40km,..., 89=more than 70km), overcast (scale 0-9, where 9 means upper air is not visible), humidity (percentage). To look into correlations we have tested both real data vectors, as well as the hourly or daily differences vectors for correlation. The testing is based on computing the correlation for the measured data, and daily or hourly differences of the measured data in MATLAB.

The correlation of the absolute and differentiated hourly and daily averages of these weather components are set out in correlation matrices. A correlation matrix is a symmetric matrix by

definition. To see any (longer term) influence, we also checked the lagged correlations until 7 data points away (7 hours/days later). A visual representation of the correlation matrices can be found in Figure A.1 up to Figure A.4, which are displayed below. In these images, a visual representation of a correlation matrix is given. When there is no correlation, a square is given no color, when there is large negative correlation, a square is given a red color, and when there is large positive correlation, a square is given a green color. The depth of the color green or red represents the level of correlation. Since we are interested in the correlation of wind with other weather segments, we look at the second row or second column (these are the same by symmetry).

Correlation ($\rho(\mathbf{x}, \mathbf{y})$ of two samples $\mathbf{x} = [x_1, ..., x_n]$ and $\mathbf{y} = [y_1, ..., y_n]$ is defined as:

$$\rho(\mathbf{x}, \mathbf{y}) = \frac{\sum_{i=1}^{n}(x_i - \bar{x})(y_i - \bar{y})}{\sqrt{\sum_{i=1}^{n}(x_i - \bar{x})^2 \sum_{i=1}^{n}(y_i - \bar{y})^2}}.$$

If we consider j lags in the correlation, then the correlation changes slightly to:

$$\rho_j(\mathbf{x}, \mathbf{y}) = \frac{\sum_{i=1}^{n-j}(x_i - \bar{x})(y_i - \bar{y})}{\sqrt{\sum_{i=1}^{n-j}(x_i - \bar{x})^2 \sum_{i=1+j}^{n}(y_i - \bar{y})^2}}.$$

When we look at the differences of a series, we define the difference as:

$$\text{diff}(\mathbf{x}) = [x_1 - x_2, x_2 - x_3, ..., x_{n-1} - x_n],$$

which shows that a vector of differences of a vector of n components has length $n - 1$.

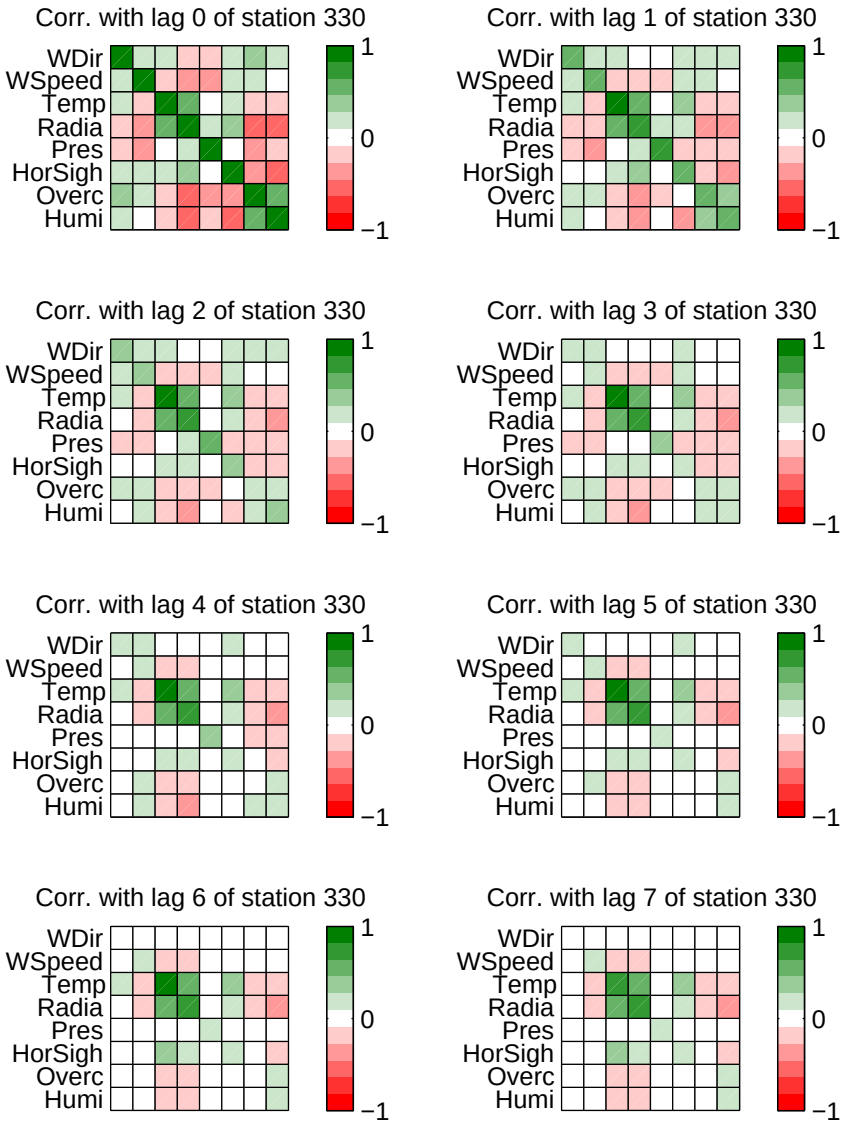

Figure A.1: Daily average correlation matrices of several weather components, with 0 up to 7 lags.

Figure A.1 gives a visual display of the correlation matrix of raw data, using lags 0 up to 7. When no lags are used, the correlation of for example wind with wind, is one, as can be seen from the figure.

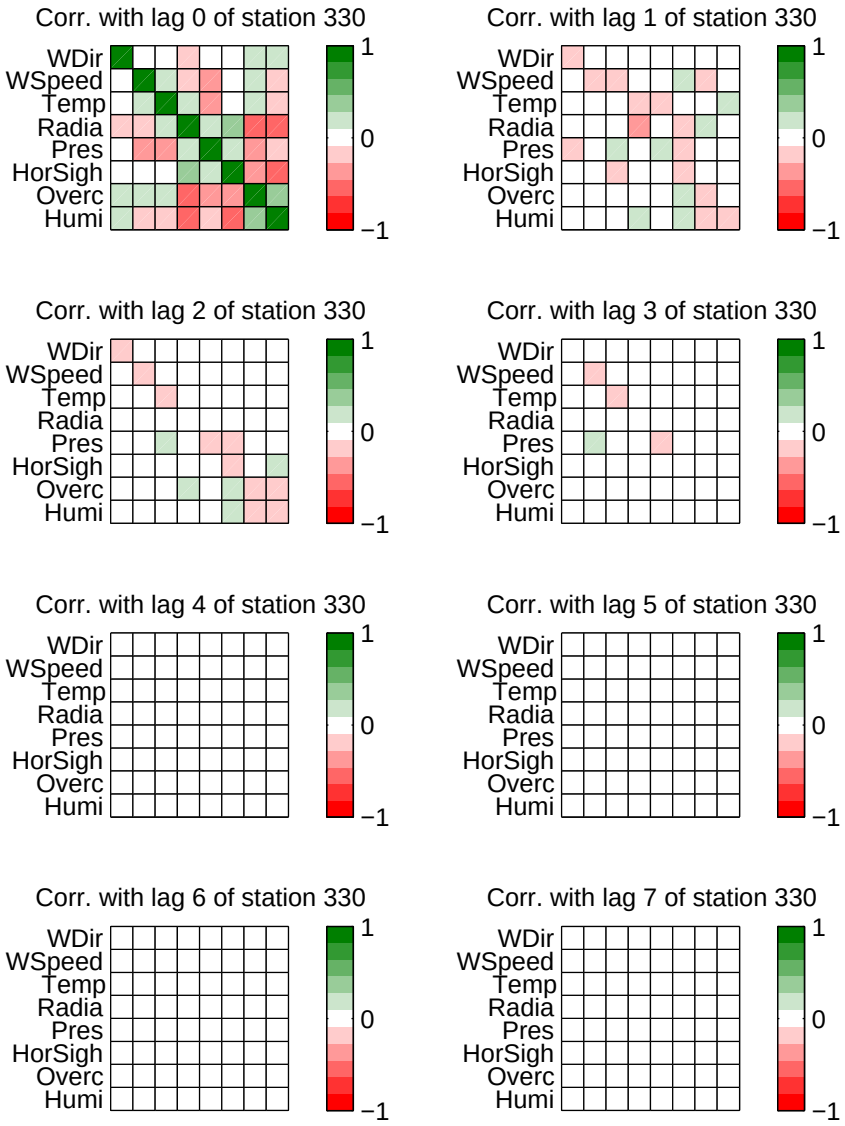

Figure A.2: Differences of daily average correlation matrices of several weather components, with 0 up to 7 lags.

From Figure A.2 we conclude that the differences of daily average wind speeds show no significant correlation with other weather components.

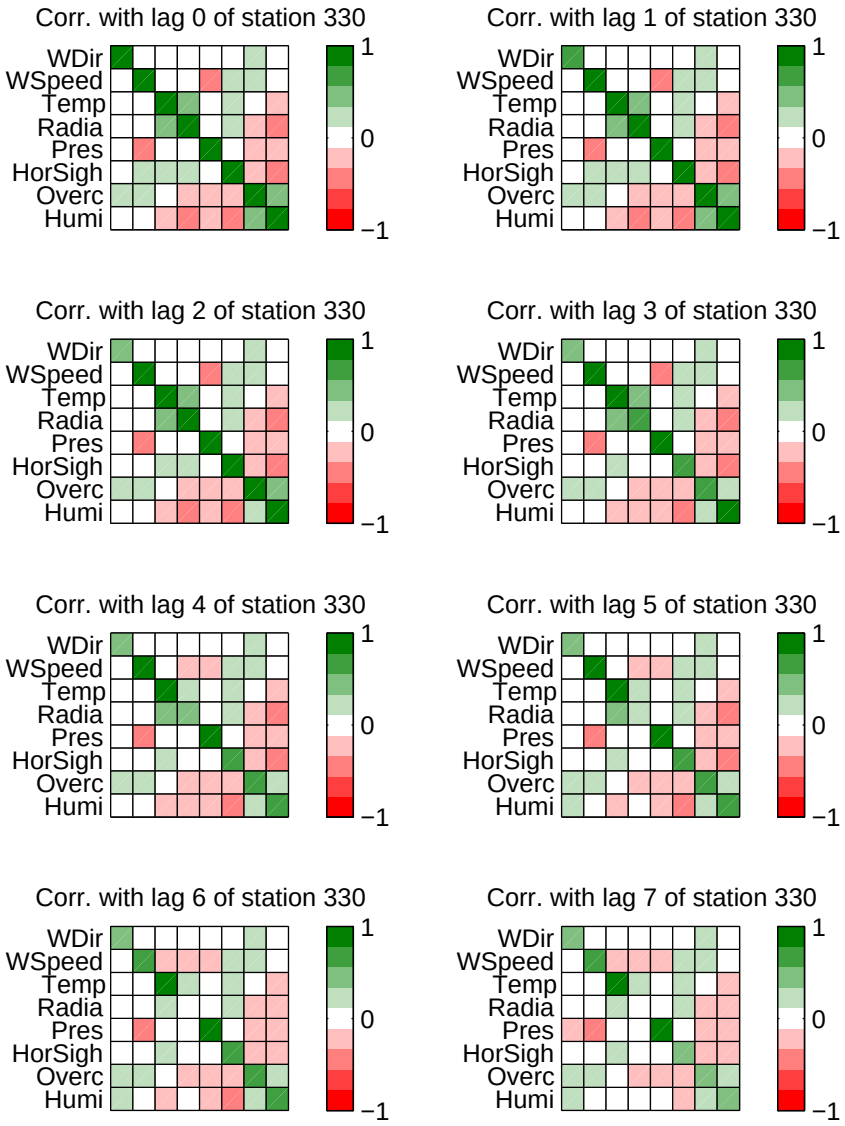

Figure A.3: Hourly average correlation matrices of several weather components, with 0 up to 7 lags.

Here, we conclude that daily hourly average wind speeds are slightly negatively correlated with hourly average pressure.

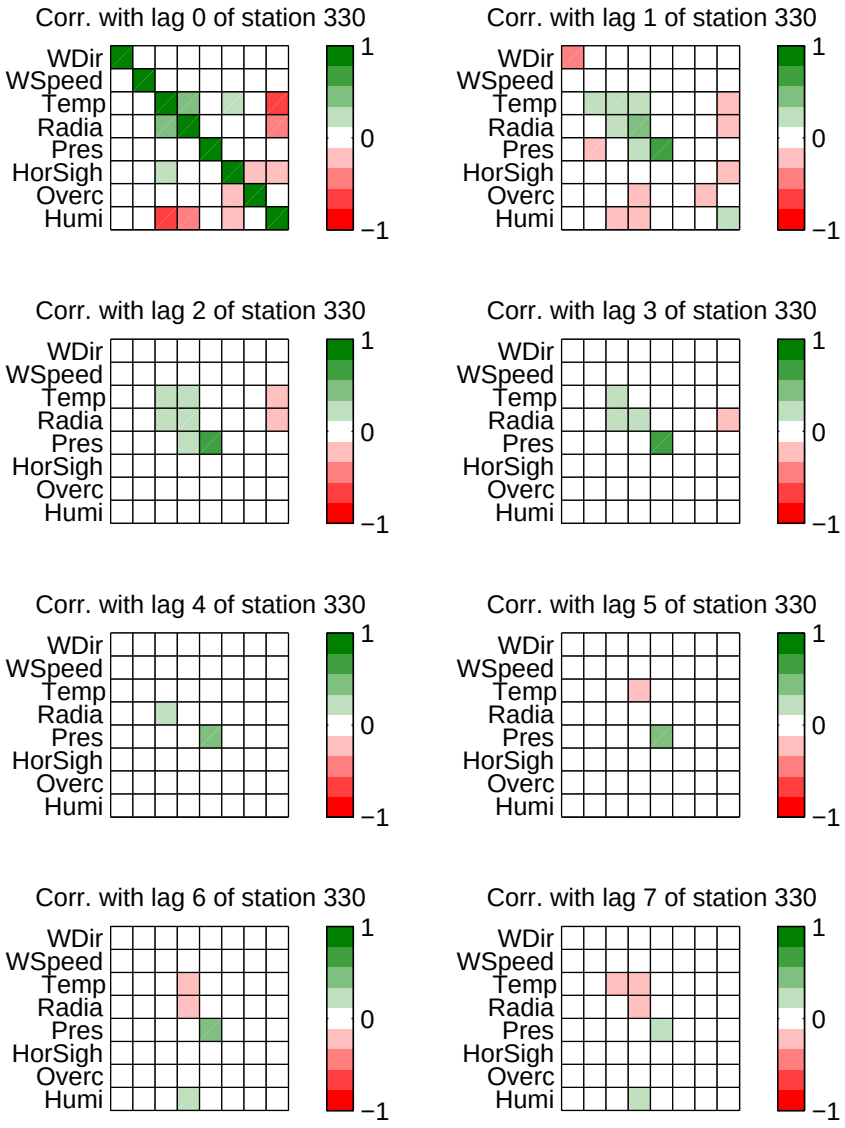

Figure A.4: Differences of hourly average correlation matrices of several weather components, with 0 up to 7 lags.

From Figure A.4 we conclude that also hourly differences of wind speeds are not correlated with hourly differences of other weather components.

A.3 Wind speed visualization tool

While doing this thesis, in cooperation with 3 students from the Hogeschool van Amsterdam (HvA), we designed a software tool which displays the characteristics of wind per wind site. Each

of the displayed KNMI weather stations can be loaded, by dragging the point on to the load button. When a station is loaded, the point will turn red. It will take a second or two to load, and then wind data is visualized by displaying the diurnal cycle per month of the year, a wind rose, weekly, monthly and quarterly seasonality and the distribution of wind speeds. In the timeline the input data of the station can be chosen, such that smaller time intervals can also be analyzed. Two more screen shots of the software and a little explanation can be found in Figure A.5 and A.6

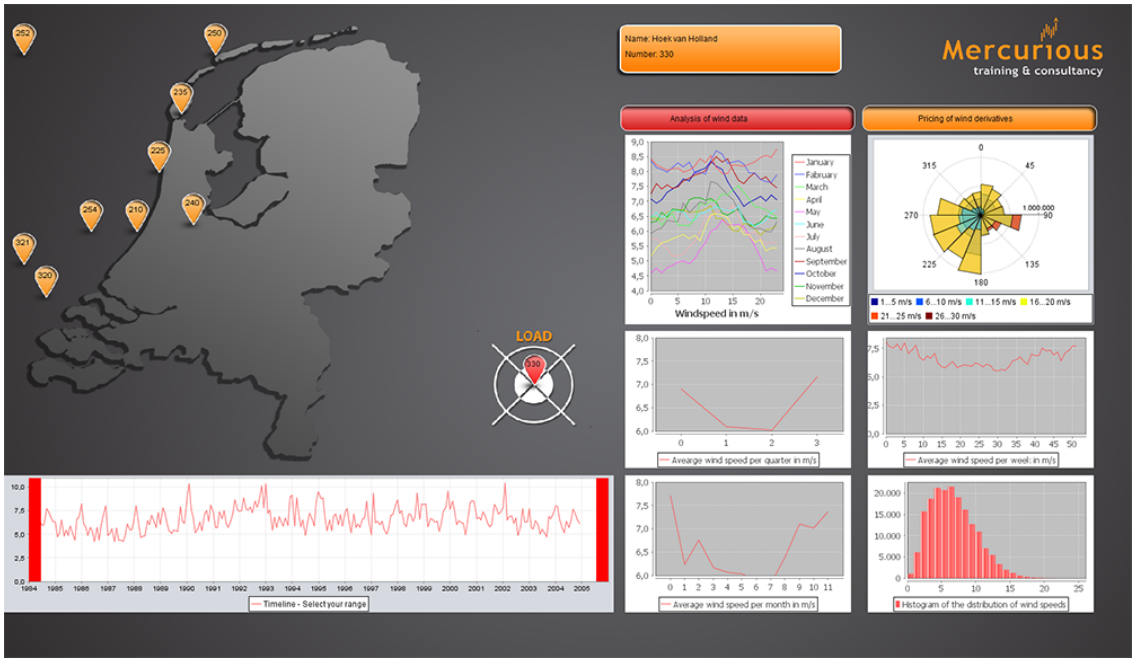

Figure A.5: A wind station can be loaded by dragging the logo on the load button, provided by Mercurious.

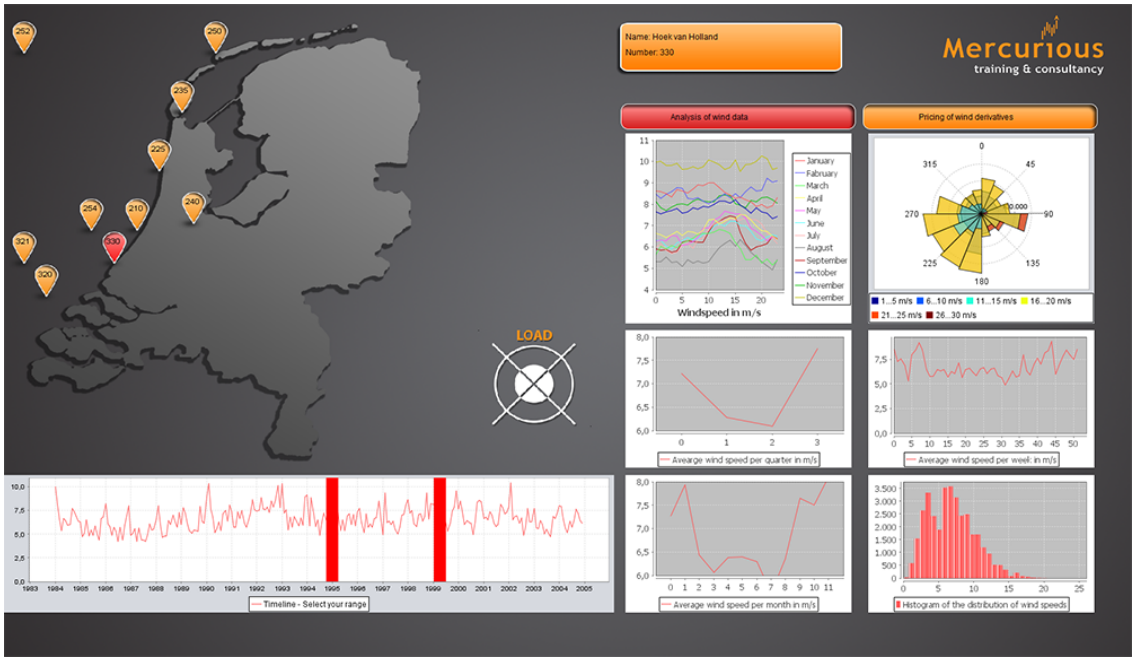

Figure A.6: By adjusting the timeline, the input data can be chosen, provided by Mercurious.

Appendix B

Modeling wind

B.1 Removing seasonality

During the research for this thesis, we considered two methods to compute the seasonality, the yearly average approach and the consecutive regressions approach. The yearly average approach seems to be more accurate, therefore the focus on this approach in the main text. The consecutive regressions approach may prove to be a better approach when there is a clear indication that wind speeds have been changing over the last couple of years, since this approach incorporates yearly trend, whereas the yearly average method assumes a stable (wind) climate. In this appendix, the methodology behind the consecutive regressions approach is discussed.

B.1.1 Consecutive regressions approach

The idea behind the consecutive regressions approach is to remove the seasonality at several time scales (yearly/quarterly/monthly/daily/hourly) of the whole original time series. Computation of the seasonality function (and thus the remaining stochastic process) will be done as follows:

1. Take all wind speed observations $(x_1, x_2, x_3....)$
2. For every year calculate the yearly average wind speed, $(y_1, Ay_1), (y_2, Ay_2), ...(y_N, Ay_N)$ where y_i means the i-th year and Ay_i stands for average from a given year. Based on this, we build a regression line (linear regression), $f_y(t)$ which in essence determines a trend of 'yearly' wind changes. This may give an indication for the long term wind speed development, and it can give an indication of possible climate effects.
3. Subtract this yearly trend from all observations.
4. Then consider quarterly, monthly or weekly averages, and calculate the average wind speeds for these periods. For example the monthly effects, $(m_1, Am_1), (m_2, Am_2), ...(m_{12N}, Am_{12N})$ are calculated the same way as the yearly effects. Using a regression (non linear regression, since most likely there is a seasonal effect) on this function gives us a monthly seasonality function, $f_m(t)$.
5. After performing the same procedure for a combination of yearly, quarterly, monthly, weekly and/or hourly trends, we only observe the random noise. This noise can be described by a stochastic process.

6. The full trend line or seasonality function would be $g(t) = f_y(t) + f_{q|y}(t) + f_{m|y,q}(t)$, the cumulated effects of yearly, quarterly and monthly seasonality.

The full model, incorporating yearly, quarterly and monthly trends would then be of the form: $X(t)+f_y(t)+f_{q|y}(t)+f_{m|y,q}(t)$, with $X(t)$ a stochastic process. $X(t)$ is described by an OU-process.

The key of this approach is to make the wind data insensitive to several periodic wind changes. This method is fairly intuitive, and thus easily understandable, however the amount of nonlinear regressions that have to be done may make the method a slow method. Figure B.1 shows the wind speeds, corrected per time scale, and the consecutive regressions that are done. What remains is a process that is mean reverting around zero.

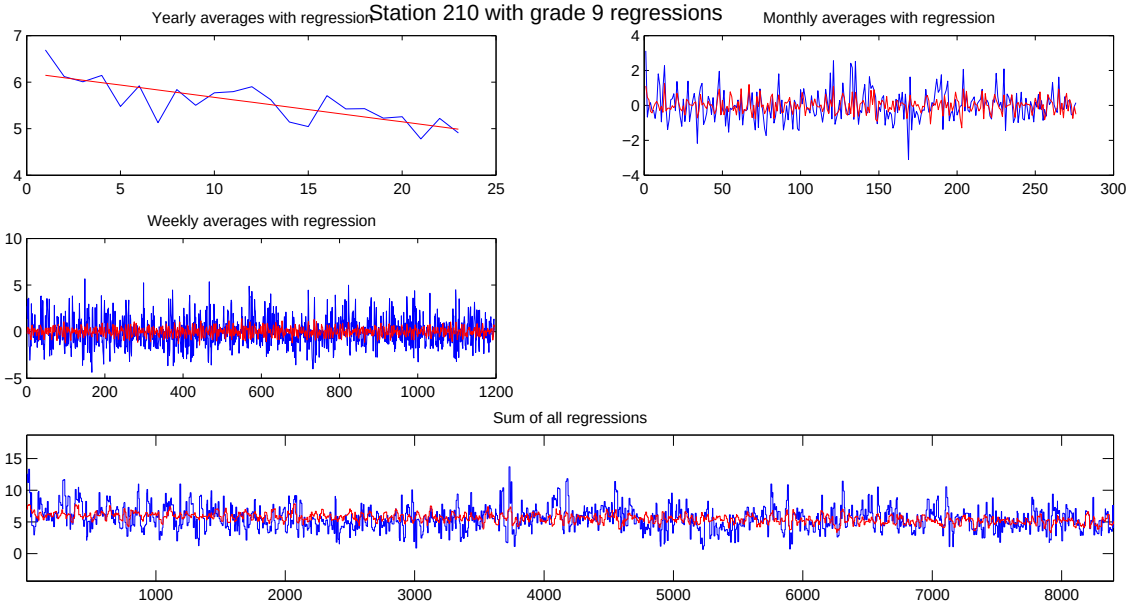

Figure B.1: The consecutive regressions for yearly, monthly and weekly trends, and the associated remaining process.

For each timescale the choice can be made whether to correct for the timescale or not. This implies that when taking yearly, quarterly, monthly, weekly, daily and hourly regressions into account, there are $2^6 = 64$ possible models. If the daily averages are modeled, the hourly regressions will not have to be taken into account, so in that case $2^5 = 32$ possibilities for a model exist. We refer to a specific model by abbreviation. In this naming, y stands for year, q for quarter, m for month, w for week, d of day and h for hour. For example, the model that takes yearly, monthly and weekly seasonality into account is referred to as 'ymw'.

Differences consecutive regressions and yearly average approach

The main differences between these approaches is that in the consecutive regressions approach, the whole time series is reviewed, and the seasonality for the whole sequences is removed. The yearly average approach extracts a yearly average seasonality. The consecutive regressions approach may lack accuracy because it is exposed to too much noise, however, the yearly average approach may not take other seasonal effects than yearly seasonal effects in consideration.

B.2 Derivations different SDE models

In Section 4.5 four models for reconstruction of wind data are discussed. The derivations for these models are done in this appendix.

B.2.1 Itô for seasonal processes derivations

Incorporating a seasonal component into the model of wind gives a slightly different process. To look at the new characteristics, Itô's formula is used to look the changes. This is done similar to [35] and [55].

Wind speeds are nonnegative, and exhibit clear seasonality. Seasonality can be removed by subtracting a seasonal function, or dividing by a seasonal function. Furthermore, heuristically it may make sense to look at a process of which the log-differences are normally distributed. This yields a transformation of the wind data of the following kinds:

$$\begin{aligned}
S_1(t) = \exp(X_1(t) + g_1(t)) \quad &\Leftrightarrow \quad X_1(t) = \log(S_1(t)) - g_1(t), \text{ or} \\
S_2(t) = \exp(X_2(t))g_2(t) \quad &\Leftrightarrow \quad X_2(t) = \log\left(\frac{S_2(t)}{g_2(t)}\right), \text{ or} \\
S_3(t) = \exp(X_3(t)g_3(t)) \quad &\Leftrightarrow \quad X_3(t) = \frac{\log(S_3(t))}{g_3(t)}, \text{ or} \\
S_4(t) = X_4(t) + g_4(t) \quad &\Leftrightarrow \quad X_4(t) = S_4(t) - g_4(t), \text{ or} \\
S_5(t) = X_5(t)g_5(t) \quad &\Leftrightarrow \quad X_5(t) = \frac{S_5(t)}{g_5(t)},
\end{aligned} \tag{B.1}$$

where $S_1(t)...S_5(t)$ are processes for wind speeds, $g_1(t)...g_5(t)$ are seasonal functions, and $X_1(t)...X_5(t)$ are new processes. We've chosen this different notation to emphasize the fact that we're working with different models. It will be concluded that models $S_2(t)$ and $S_5(t)$ are essentially the same models, after Itô's lemma has been applied. We now shortly discuss all five models in (B.1).

1. $S_1(t) = \exp(X_1(t) + g_1(t))$

In the first case, the daily differences of wind speeds are approximately normally distributed, and all seasonality is assumed to be removed by the function $g_1(t)$. $X_1(t)$ may therefore be a process, reverting to a mean of 0. This yields the following model for $X_1(t)$:

$$\mathrm{d}X_1(t) = -\lambda_1 X_1(t)\mathrm{d}t + \sigma_1 \mathrm{d}W(t).$$

Using Itô's lemma, we find the characteristics of $S_1(t) = \exp(X_1(t) + g_1(t))$. Let $\phi(t, X_1(t))$ be equal to $S_1(t)$. Then, since $S_1(t) = \exp(X_1(t) + g_1(t))$, we find from Itô's lemma that

$$
\begin{aligned}
\mathrm{d}S_1(t) &= \left[\phi_t + \phi_x \cdot -\lambda_1 X_(t) + \frac{1}{2}\phi_{xx}\sigma_1^2\right]\mathrm{d}t + \phi_x \cdot \sigma_1 \mathrm{d}W(t) \\
&= \left[g_1'(t) - \lambda_1 X_1(t) + \frac{1}{2}\sigma_1^2\right] S_1(t)\mathrm{d}t + \sigma_1 S_1(t)\mathrm{d}W(t) \\
&= \left[g_1'(t) - \log(S_1(t)) + \lambda_1 g_1(t) + \frac{1}{2}\sigma_1^2\right] S_1(t)\mathrm{d}t + \sigma_1 S_1(t)\mathrm{d}W(t) \\
&= \lambda_1 \left[\theta_1(t) - \log(S_1(t))\right] S_1(t)\mathrm{d}t + \sigma_1 S(t)_1 \mathrm{d}W(t),
\end{aligned}
$$

where $\theta_1(t) = \frac{1}{\lambda_1}\left(g_1'(t) + \frac{1}{2}\sigma_1^2 + \lambda_1 g_1(t)\right)$. Using Itô's lemma again, based on the transformation $P(t) = \log(S_1(t))$, we find

$$
\mathrm{d}P(t) = \lambda_1 \left(\tilde{\theta_1}(t) - P(t)\right) dt + \sigma_1 \mathrm{d}W(t),
$$

and $\tilde{\theta_1}(t) = \theta_1(t) - \frac{\sigma_1^2}{2\lambda_1}$. So for $P(t) = \log(S_1(t))$ we have:

$$
\mathrm{d}P(t) = \lambda_1 \left(g_1(t) + \frac{1}{\lambda_1} g_1'(t) - P(t)\right) dt + \sigma_1 \mathrm{d}W(t),
$$

2. $S_2(t) = \exp(X_2(t))g_2(t)$

A slightly modified version leads to an intuitive understanding of the method above. In this case, we look at dividing by a seasonal function, and looking at the log differences. Heuristically the following is assumed:

$$
\log\left(\frac{S_{i+1}}{g_{i+1}}\right) - \log\left(\frac{S_i}{g_i}\right) \sim N(0, \sigma)
$$

Taking the exponent, we find the second model $S_2(t) = \exp(X_2(t))g_2(t)$. We first take $Y(t) = \exp(X_2(t))$, and we expect $Y(t)$ to be mean reverting around 1, because $X_2(t)$ should be mean reverting around 0. This yields the following SDE for Y(t):

$$
dY(t) = \lambda_2(1 - Y(t))\mathrm{d}t + \sigma_2 \mathrm{d}W(t)
$$

Using Itô's lemma for the transformation $X_2(t) = \log(Y(t))$, gives us:

$$
\begin{aligned}
\mathrm{d}X_2(t) &= \left[\phi_t + \phi_x \cdot \lambda_2(1 - Y(t)) + \frac{1}{2}\phi_{xx}\sigma_2^2\right]\mathrm{d}t + \phi_x \cdot \sigma_2 \mathrm{d}W(t) \\
&= \left[\frac{\lambda_2(1 - \exp(X(t)))}{\exp(X(t))} - \frac{1}{2}\frac{\sigma_2^2}{\exp(X(t))^2}\right]\mathrm{d}t + \frac{\sigma_2}{\exp(X(t))}\mathrm{d}W(t)
\end{aligned}
$$

We use Itô's lemma for the function $S_2(t) = \exp(X_2(t))g_2(t)$, let $\phi(t, X_2(t))$ be equal to $S_2(t)$. Then we have the following:

$$
\begin{aligned}
\mathrm{d}S_2(t) &= \left[\phi_t + \phi_x \cdot \left(\frac{\lambda_2(1-\exp(X(t)))}{\exp(X(t))} - \frac{1}{2}\frac{\sigma_2^2}{\exp(X(t))^2}\right) + \frac{1}{2}\phi_{xx}\frac{\sigma_2}{\exp(X_2(t))}^2\right]\mathrm{d}t \\
&\quad +\phi_x \cdot \frac{\sigma_2}{\exp(X_2(t))}\mathrm{d}W(t) \\
&= \left[\exp(X_2(t))g_2'(t) + \exp(X_2(t))g_2(t) \cdot \left(\frac{\lambda_2(1-\exp(X(t)))}{\exp(X(t))} - \frac{1}{2}\frac{\sigma_2^2}{\exp(X(t))^2}\right)\right. \\
&\quad \left. +\frac{1}{2}\exp(X_2(t))g_2(t)\frac{\sigma_2}{\exp(X_2(t))}^2\right]\mathrm{d}t + \exp(X_2(t))g_2(t) \cdot \frac{\sigma_2}{\exp(X_2(t))}\mathrm{d}W(t) \\
&= \left[\frac{S_2(t)}{g_2(t)}g_2'(t) + S_2(t) \cdot \left(\frac{\lambda_2(1-\frac{S_2(t)}{g_2(t)})}{\frac{S_2(t)}{g_2(t)}} - \frac{1}{2}\frac{\sigma_2^2}{\frac{S_2(t)}{g_2(t)}^2}\right) + \frac{1}{2}S_2(t)\frac{\sigma_2}{\frac{S_2(t)}{g(t)}}^2\right]\mathrm{d}t \\
&\quad +S_2(t) \cdot \frac{\sigma_2}{\frac{S_2(t)}{g_2(t)}}\mathrm{d}W(t) \\
&= \left[\frac{g_2'(t)}{g_2(t)} + \lambda_2\left(1 - \frac{S_2(t)}{g_2(t)}\right)\frac{g_2(t)}{S_2(t)}\right]S_2(t)\mathrm{d}t + g_2(t)\sigma\mathrm{d}W(t) \\
&= \left[\lambda_2\left(g_2(t) - \left(\frac{\lambda g_2(t) - g_2'(t)}{\lambda g_2(t)}\right)S_2(t)\right)\right]\mathrm{d}t + \sigma_2 g_2(t)\mathrm{d}W(t)
\end{aligned}
$$

3. $S_3(t) = \exp(X_3(t)g_3(t))$

This model is based on the log-wind speeds, and division is used to remove the seasonality. Since division is used, the process $X_3(t)$ can be expected to exhibit mean reversion around 1. Using Itô's lemma we derive:

$$
\begin{aligned}
\mathrm{d}S_3(t) &= \left[\phi_t + \phi_x \cdot \lambda_3(1 - X_3(t)) + \frac{1}{2}\phi_{xx}\sigma_3^2\right]\mathrm{d}t + \phi_x \cdot \sigma_3\mathrm{d}W(t) \\
&= \left[S_3(t)X_3(t)g_3'(t) + S_3(t)g_3(t)\lambda_3(1 - X_3(t)) + \frac{1}{2}S_3(t)g_3^2(t)\sigma_3^2\right]\mathrm{d}t + S_3(t)g_3 \cdot \sigma_3\mathrm{d}W(t) \\
&= \left[\log(S_3(t))\frac{g_3'(t)}{g_3(t)} + g_3(t)\lambda_3(1 - \frac{\log(S_3(t))}{g_3(t)}) + \frac{1}{2}g_3^2(t)\sigma_3^2\right]S_3(t)\mathrm{d}t + S_3(t)g_3\sigma_3\mathrm{d}W(t) \\
&= \left[\lambda_3 g_3(t) + \frac{1}{2}g_3^2(t)\sigma_3^2 + \log(S_3)\left(\frac{g_3'(t)}{g_3(t)} - \lambda_3\right)\right]S_3(t)\mathrm{d}t + S_3(t)g_3(t)\sigma_3\mathrm{d}W(t)
\end{aligned}
$$

By the transformation $P_3(t) = \log(S_3(t))$ and Itô's lemma we then have:

$$
\begin{aligned}
\mathrm{d}P_3(t) &= \left(\phi_t + \phi_x\left[\lambda_3 g_3(t) + \frac{1}{2}g_3^2(t)\sigma_3^2 + \log(S_3)\left(\frac{g_3'(t)}{g_3(t)} - \lambda_3\right)\right]S_3(t) + \frac{1}{2}\phi_{xx}(S_3(t)g_3(t)\sigma_3)^2\right)\mathrm{d}t \\
&\quad +\phi_x \cdot S_3(t)g_3(t)\sigma_3\mathrm{d}W(t) \\
&= \lambda_3\left[g_3(t) - \left(1 - \frac{g_3'(t)}{\lambda_3 g_3(t)}\right)P_3(t)\right]\mathrm{d}t + g_3(t)\sigma_3\mathrm{d}W(t) \\
&= \lambda_3\left[g_3(t) - \left(\frac{\lambda_3 g_3(t) - g_3'(t)}{\lambda_3 g_3(t)}\right)P_3(t)\right]\mathrm{d}t + g_3(t)\sigma_3\mathrm{d}W(t)
\end{aligned}
$$

We thus conclude that Models 2 and 3 are exactly the same, except that Model 3 models the logarithm of wind speeds.

4. $S_4(t) = X_4(t) + g_4(t)$

This model is the model as was used in [35] [55]. Since subtraction is used to remove the seasonality, the process $X_4(t)$ exhibits mean reversion around 0.

$$\begin{aligned} \mathrm{d}S_4(t) &= \left[\phi_t + \phi_x \cdot -\lambda_4 X_4(t) + \frac{1}{2}\phi_{xx}\sigma_4^2\right]\mathrm{d}t + \phi_x \cdot \sigma_4 \mathrm{d}W(t) \\ &= \left[g_4'(t) - \lambda_4 X_4(t)\right]\mathrm{d}t + \sigma_4 \mathrm{d}W(t) \\ &= \lambda_4\left[\frac{1}{\lambda_4}g_4'(t) + g_4(t) - S_4(t)\right]\mathrm{d}t + \sigma_4 \mathrm{d}W(t) \end{aligned}$$

This model is similar to the model using $S_1(t) = \exp(X_1(t) + g_1(t))$, except that in the first model the log prices were constructed.

5. $S_5(t) = X_5(t)g_5(t)$

In this case, since seasonality is assumed to be removed by dividing by a seasonal function, $X_5(t)$ will be mean reverting around 1. This yields:

$$\mathrm{d}X_5(t) = \lambda_5(1 - X_5(t))\mathrm{d}t + \sigma_5 \mathrm{d}W(t).$$

Using Itô's lemma, we find the characteristics of $S_5(t) = X_5(t)g_5(t)$. Let $\phi(t, X_5(t))$ be equal to $S_5(t)$. Then, since $S_5(t) = X_5(t)g_5(t)$, we find from Itô's lemma that:

$$\begin{aligned} \mathrm{d}S_5(t) &= \left[\phi_t + \phi_x \cdot \lambda(1 - X_5(t)) + \frac{1}{2}\phi_{xx}\sigma_2^2\right]\mathrm{d}t + \phi_x \cdot \sigma_2 \mathrm{d}W(t) \\ &= \left[S_5(t)\frac{g_5'(t)}{g_5(t)} + \lambda_5(g_5(t) - S_5(t))\right]\mathrm{d}t + \sigma_5 g_5(t)\mathrm{d}W(t) \\ &= \left[\lambda_5\left(g_5(t) - \left(\frac{\lambda g_5(t) - g_5'(t)}{\lambda g_5(t)}\right)S_5(t)\right)\right]\mathrm{d}t + \sigma_5 g_5(t)\mathrm{d}W(t) \end{aligned}$$

Note that this is exactly the same model as Model 2.

B.3 Calibrating the remaining process

In this thesis, three methods for calibrating the parameters of an OU-process are used: two versions of Ordinary Least Squares (OLS), Euler OLS and exact OLS and one version of MLE. In this appendix we will show that Euler OLS and exact OLS are closely related, when Taylor expansion of e^t around 0 is used for the exponential powers in exact OLS, Euler OLS is the result. We will prove this in Section B.3.1. After that we will derive the OLS estimates of the parameters λ and σ, as in (4.3).

B.3.1 Two models for OLS regression

OLS is a method that is often used in the field of Econometrics [58], and is based on minimizing the square of error terms. We consider two discretizations, Euler discretization and discretization by solving the stochastic differential equation (4.3). We start with solving (4.3). To this extent, we use Itô's lemma on $e^{\lambda t}X(t)$ to find the following:

$$\begin{aligned} \mathrm{d}(e^{\lambda t}X(t)) &= (\lambda e^{\lambda t}X(t) + e^{\lambda t}\lambda(\mu - X(t)))\mathrm{d}t + e^{\lambda t}\sigma \mathrm{d}W(t) \\ &= \lambda\mu e^{\lambda t}\mathrm{d}t + e^{\lambda t}\sigma \mathrm{d}W(t). \end{aligned} \tag{B.2}$$

Now, (B.2) implies that when we take the integral from t_{i-1} to t_i, we find:

$$\begin{aligned} X(t_i) &= e^{-\lambda(t_i - t_{i-1})}X(t_{i-1}) + \lambda\mu\int_{t_{i-1}}^{t_i} e^{\lambda(s-t_i)}\mathrm{d}s + \sigma\int_{t_{i-1}}^{t_i} e^{\lambda(s-t_i)}\mathrm{d}W(s) \\ &= e^{-\lambda(t_i - t_{i-1})}X(t_{i-1}) + \mu(1 - e^{\lambda(t_i - t_{i-1})})) + \sigma\int_{t_{i-1}}^{t_i} e^{\lambda(s-t_i)}\mathrm{d}W(s). \end{aligned}$$

Let $\delta t = t_i - t_{i-1}$ be the time step and ϵ_t be a standard normal random variable, then the discretization can be written as follows:

$$X_t = e^{-\lambda\delta t}X_{t-1} + \mu(1 - e^{-\lambda\delta t}) + \sigma\sqrt{\frac{1 - e^{-2\lambda\delta t}}{2\lambda}}\epsilon_t$$

This stochastic term can be rewritten because $\mathrm{Var}(X_t) = \sqrt{\frac{1-e^{-2\lambda\delta t}}{2\lambda}}$, as was shown in (5.7). The steps for performing an OLS regression on this discretization are explained in Appendix B.3. Alternatively, we can use a straightforward Euler discretization of (4.3). This gives us the following:

$$X_t = \lambda\mu\delta t + (1 - \lambda)\delta t X_{t-1} + \sigma\sqrt{\delta t}\epsilon_t,$$

where again δt is the time step, and ϵ_t is a standard normal random variable. The relation between these two discretizations is a Taylor expansion of e^t around 0. This can be seen by comparing the discretizations, and assuming they should be the same for our model. We find:

$$e^{-\lambda\delta t}X_{t-1} = (1 - \lambda)\delta t X_{t-1} \tag{B.3}$$

$$\mu(1 - e^{-\lambda\delta t}) = \lambda\mu\delta t \tag{B.4}$$

$$\sigma\sqrt{\frac{1 - e^{-2\lambda\delta t}}{2\lambda}}\epsilon_t = \sigma\epsilon_t\sqrt{\delta t} \tag{B.5}$$

These statements are true if:

$$\begin{aligned} e^{-\lambda\delta t} &= (1 - \lambda)\delta t \\ 1 - e^{-\lambda\delta t} &= \lambda\delta t \\ \sqrt{\frac{1 - e^{-2\lambda\delta t}}{2\lambda}} &= \sqrt{\delta t}. \end{aligned}$$

Taylor expansion of $e^{\lambda t}$ around 0 gives:

$$e^{\lambda \delta t} \approx 1 + \lambda \cdot 1 \cdot (\delta t - 0) = 1 + \lambda \delta t.$$

Using this Taylor expansion, we conclude that (B.4), (B.5) and (B.5) are valid equations. We compared both OLS approaches using the KS-test again, and concluded the best calibration is done when using OLS with Taylor expansion of e^t around 0. Apparently, when using Euler discretization less noise terms are taken into account, and we obtain a better approximation of the underlying.

B.3.2 Calibrating λ and σ through OLS

Computing an OLS regression on a model is done by minimizing the squared errors of a certain discretization. Our discretizations have the following form:

$$X_t = a + bX_{t-1} + \sigma\epsilon_t. \tag{B.6}$$

As the idea behind OLS is to minimize the squared errors, this minimum for a is attained when:

$$\frac{\partial}{\partial a} \sum_{t=1}^{T} \epsilon_t^2 = 0.$$

Filling in for (B.6), we find that for a we have

$$\begin{aligned} 0 &= \frac{\partial}{\partial a} \sum_{t=1}^{T} \left(\frac{X_t - a - bX_{t-1}}{\sigma} \right)^2 \\ &= \frac{1}{\sigma^2} \sum_{t=1}^{T} 2(X_t - a - bX_{t-1}) \cdot -1 \\ &\Leftrightarrow \\ a &= \frac{\sum_{t=1}^{T} (X_t - bX_{t-1})}{T}. \end{aligned}$$

A similar approach for finding the optimal value for b is done:

$$
\begin{aligned}
0 &= \frac{\partial}{\partial b}\sum_{t=1}^{T}\left(\frac{X_t - a - bX_{t-1}}{\sigma}\right)^2 \\
&= \frac{1}{\sigma^2}\sum_{t=1}^{T} 2(X_t - a - bX_{t-1})\cdot -X_{t-1} \\
&\Leftrightarrow \\
b &= \frac{\sum_{t=1}^{T}(X_tX_{t-1} - aX_{t-1})}{\sum_{t=1}^{T} X_{t-1}^2} \\
&= \frac{\sum_{t=1}^{T} X_tX_{t-1}}{\sum_{t=1}^{T} X_{t-1}^2} - \frac{\sum_{t=1}^{T}(X_t - bX_{t-1})X_{t-1}}{T\sum_{t=1}^{T} X_{t-1}^2} \\
&= \frac{T\sum_{t=1}^{T} X_tX_{t-1}}{T\sum_{t=1}^{T} X_{t-1}^2} - \frac{\sum_{t=1}^{T} X_tX_{t-1} - bX_{t-1}^2}{T\sum_{t=1}^{T} X_{t-1}^2} \\
&= \frac{(T-1)\sum_{t=1}^{T} X_tX_{t-1}}{T\sum_{t=1}^{T} X_{t-1}^2} \Big/ \frac{T\sum_{t=1}^{T} X_{t-1}^2 - X_{t-1}^2}{T\sum_{t=1}^{T} X_{t-1}^2} \\
&= \frac{\sum_{t=1}^{T} X_tX_{t-1}}{\sum_{t=1}^{T} X_{t-1}^2}.
\end{aligned}
$$

Here, a and b are actually functions of λ and μ. Simple transformations will yield expressions for λ. σ is just the standard deviation of the errors after using the just derived regression.

B.3.3 Computing λ, κ, and σ through MLE

Another way to estimate the parameters is by using the MLEs of σ and λ. These cannot be solved analytically, but a numerical approximation that is just as good can be computed. The steps to be taken are:

1. Compute the likelihood function, on basis of the observations
2. Take the natural logarithm of this likelihood function
3. Compute the derivatives with respect to λ and σ and put the equations equal to zero
4. Compute λ and σ analytically if possible, and approximate numerically otherwise

To find a probability density function, we look at the discretization that shows after solving (4.3). Similar derivations as in (5.6) and (5.7) yield that we have a normally distributed random variable:

$$
\mathcal{N}\left(e^{-\lambda\delta t}X_{t-1} + \mu(1 - e^{-\lambda\delta t}), \sigma^2\frac{1 - e^{-2\lambda\delta t}}{2\lambda}\right) \tag{B.7}
$$

For notational sake, we define $\hat{\sigma}^2 = \sigma^2\frac{1-e^{-2\lambda\delta t}}{2\lambda}$We know the probability density function to be:

$$
\begin{aligned}
f_{Y|X}(X_t|X_{t-1}) &= \frac{1}{\sqrt{2\pi}\hat{\sigma}}\exp\left\{-\frac{(X_t - (e^{-\lambda\delta t}X_{t-1} + \mu(1 - e^{-\lambda\delta t})))^2}{2\hat{\sigma}^2}\right\} && \text{(B.8)} \\
&= \frac{1}{\sqrt{2\pi}\hat{\sigma}}\exp\left\{-\frac{(X_t - e^{-\lambda\delta t}X_{t-1} - \mu(1 - e^{-\lambda\delta t}))^2}{2\hat{\sigma}^2}\right\} && \text{(B.9)}
\end{aligned}
$$

Multiplying this probability density function per observation, and taking the natural logarithm gives the following:

$$\mathcal{L}(\mathbf{x}) = \sum_{i=1}^{n} \log(f_{Y|X}(X_t|X_{t-1})). \tag{B.10}$$

Where $\mathbf{x}$ are the observations. Setting $\mu = 0$ or $\mu = 1$ and taking the derivatives of $\mathcal{L}(\mathbf{x})$ with respect to λ and σ and putting these equations equal to zero gives the desired parameter optimization.

For an OU-process, the approximations of λ and σ are not of closed form. However, using MATLAB, good values for these approximations can be found. The approximations for the parameters using these two methods differ, and they are both subjected to a fair amount of bias ([59]). To choose whether to approximate the parameters of the OU-process using Euler OLS, exact OLS or MLE, we compare these two methods. The results of this comparison is given in Section B.3.4. We conclude that using Euler OLS results into the best fitting parameters.

B.3.4 Comparing the constructed processes

In this thesis for the reconstruction of daily average wind speeds we tested 4 yearly average models, 31 consecutive regressions models, and one benchmark model for the daily average wind speeds. Furthermore, we tested test 4 yearly average models, 63 consecutive regressions models and one benchmark model for the hourly average wind speeds. In total, we test 36 models for the daily average wind speed, and we test 67 models for the hourly average wind speed. All of these models will be tested using Euler OLS and MLE to compute the desired parameters. The results are presented in Table B.1. Table B.1 is filled with averages of p-values. The first columns and rows show what models and what parameter calibration methods were used. For the consecutive regressions method, we denote the deseasonality method by the characters of timescales at which seasonality was removed. So, if wind speed data were corrected for yearly and weekly timescales, the notation of the method of deseasonalizing is 'YW'. If the monthly and daily trends are removed, we denote 'MD', et cetera.

Parameter comp.	MLE		Euler OLS	
Concept	Daily average	Hourly average	Daily average	Hourly average
Benchmark	Mean reverting around windspeed mean			
Yearly average	log windspeeds & seasonal division log windspeeds & seasonal subtraction windspeeds & seasonal division windspeeds & seasonal subtraction			
Consecutive regressions	YQMWD YQMW ⋮ WD D	YQMWDH YQMWD ⋮ DH H	YQMWD YQMW ⋮ WD D	YQMWDH YQMWD ⋮ DH H

Table B.1: Overview of possible models to model daily or hourly average wind speed.

We look at all possible models that can be used, and reconstruct wind speeds using the OU-process parameter approximation with both methods. All models are compared and we look at

which one of the created distributions fits the original distribution best. This is done by using the Kolmogorov-Smirnov test for two samples. Using K-S tests and comparing the p-values of the different models with respect to the original wind speed distribution. We reconstruct a new series of wind speeds, 50 times the size of the original sample. We do this 10 times, to see whether the p-value per run differ a lot or not. Note that some of the average p-values may be slightly different that presented in Section 4.6, this is because different MATLAB files were used and the output is still affected to randomness.

Best model for daily average wind speeds

First we look into the comparison of all models for modeling the daily average wind speed. The results of this comparison are shown in Table B.2.
The first conclusion that we draw here is that the parameters of the process are better approximated using the OLS regression than the MLE. Furthermore, we see that removing the quarterly averages only makes the model worse. Apart from the quarterly averages, the rest of of the models seem pretty alike. The best 5 models are highlighted yellow.

Best model for hourly average wind speeds

Secondly we look into the comparison of all models for modeling the hourly average wind speed. The results of this comparison are showed in Table B.3. Since the quarterly seasonality had such a bad influence on the results when modeling daily average wind speed, we choose not to include this seasonality when testing for hourly wind speeds, as this saves us almost have of the CPU time, which is a considerable amount (6 hours!).
We now see that removing the yearly, quarterly and monthly trends has a bad influence on the reconstructed wind data. Moreover, we conclude that the transformation of wind data to log-wind data also has a negative effect on the reconstruction of wind data. Only six models can be considered to reconstruct wind speeds well, the mean reverting model, the yearly average deseasonalizing methods, and the consecutive regressions models that remove daily, hourly or daily and hourly trends.

	Distribution					Weekly differences			
	OLS		MLE			OLS		MLE	
Model	mean	std	mean	std		mean	std	mean	std
meanrev	0.0605	0.0025	0.0731	0.0014		0.0275	0.0008	0.0646	0.0011
logasub	0.0558	0.0019	0.0786	0.0014		0.0429	0.0009	0.0794	0.0014
normdiv	0.0476	0.0017	0.0696	0.0011		0.0155	0.0011	0.0573	0.0017
logadiv	0.0638	0.0017	0.0828	0.0018		0.0439	0.0009	0.0805	0.0011
normsub	0.0604	0.0023	0.0746	0.002		0.0205	0.0012	0.0604	0.002
yqmwd	0.2092	0.0016	0.1905	0.0018		0.0552	0.0014	0.0823	0.0015
yqmw	0.2128	0.0017	0.1938	0.0017		0.0558	0.0014	0.0825	0.0014
yqm d	0.2052	0.0019	0.1874	0.0022		0.035	0.0024	0.0722	0.0015
yqm	0.2099	0.0013	0.192	0.0012		0.0361	0.0014	0.0723	0.0011
yq wd	0.2018	0.0021	0.1836	0.0022		0.0366	0.0007	0.0727	0.0017
yq w	0.2067	0.0009	0.1875	0.0011		0.039	0.0016	0.0724	0.0016
yq d	0.1995	0.0014	0.1844	0.0019		0.0289	0.0014	0.068	0.0016
yq	0.2047	0.0031	0.1864	0.001		0.031	0.0016	0.0692	0.0006
y mwd	0.0912	0.0016	0.1045	0.0011		0.0374	0.0009	0.0711	0.0012
y mw	0.0943	0.0019	0.1037	0.0027		0.0377	0.0011	0.0706	0.0009
y m d	0.0816	0.0016	0.0972	0.0026		0.0232	0.0022	0.0649	0.0016
y m	0.0836	0.0022	0.0966	0.0016		0.0238	0.0022	0.0632	0.0008
y wd	0.0586	0.002	0.0842	0.0014		0.0239	0.0009	0.0645	0.0015
y w	0.0583	0.0014	0.0835	0.0024		0.0257	0.001	0.0644	0.0012
y d	0.0544	0.0021	0.0778	0.0016		0.0166	0.001	0.0599	0.0009
y	0.0549	0.0027	0.0738	0.0016		0.0262	0.0019	0.0644	0.0009
qmwd	0.1977	0.0013	0.1805	0.0015		0.0521	0.0012	0.0807	0.0018
qmw	0.2017	0.0016	0.1829	0.0016		0.0534	0.0017	0.0804	0.001
qm d	0.1936	0.0017	0.1769	0.0012		0.0336	0.0019	0.0708	0.001
qm	0.199	0.002	0.1816	0.002		0.0373	0.0011	0.0717	0.0013
q wd	0.1834	0.0023	0.1716	0.0014		0.0368	0.002	0.0723	0.0012
q w	0.1878	0.0025	0.1751	0.0015		0.0384	0.0012	0.0727	0.0011
q d	0.1826	0.0013	0.1707	0.0014		0.0295	0.0011	0.0677	0.0013
q	0.1861	0.002	0.1732	0.0013		0.0323	0.0015	0.0694	0.0013
mwd	0.0741	0.002	0.0934	0.0017		0.0309	0.0019	0.0683	0.001
mw	0.0752	0.001	0.0945	0.0011		0.0318	0.0015	0.0687	0.0008
m d	0.0643	0.0013	0.0872	0.0015		0.0189	0.0013	0.0614	0.001
m	0.0676	0.0016	0.0866	0.0013		0.0208	0.0013	0.0615	0.0014
wd	0.055	0.0015	0.085	0.0015		0.0214	0.0012	0.0656	0.0006
w	0.0579	0.0023	0.0831	0.0011		0.0219	0.001	0.0655	0.0014
d	0.0584	0.0042	0.0761	0.0017		0.0175	0.0014	0.0603	0.0013

Table B.2: Mean and standard deviation of the p-values per daily average wind speed model, using OLS and MLE.

	Distribution					Weekly differences			
	Euler OLS		MLE			Euler OLS		MLE	
Model	mean	std	mean	std		mean	std	mean	std
meanr	0.0648		0.0651			0.0575		0.0579	
lgsub	0.1205		0.1206			0.1632		0.1752	
nmdiv	0.0527		0.0499			0.0584		0.0597	
lgdiv	0.1305		0.1329			0.1696		0.1823	
nmsub	0.0653		0.0597			0.0574		0.0585	
ymwdh	0,4061		0,4037			0.0713		0.073	
ymwd	0,4078		0,4064			0.0689		0.0709	
ymw h	0,4059		0,405			0.0689		0.0709	
ymw	0,4084		0,4087			0.067		0.0701	
ym dh	0,3881		0,3856			0.058		0.0605	
ym d	0,3903		0,3874			0.0569		0.0593	
ym h	0,39		0,3863			0.0591		0.0596	
ym	0,3913		0,3905			0.0572		0.0587	
y wdh	0,3037		0,3034			0.0615		0.0628	
y wd	0,3077		0,3058			0.0603		0.062	
y w h	0,3037		0.2992			0.0614		0.0621	
y w	0,3053		0,3028			0.0609		0.0611	
y dh	0.1211		0.1215			0.0575		0.0586	
y d	0.1264		0.1256			0.0569		0.0573	
y h	0.1043		0.105			0.0567		0.0583	
y	0.1035		0.1118			0.0568		0.057	
mwdh	0,3811		0,3803			0.0678		0.0698	
mwd	0,3829		0,3815			0.0659		0.068	
mw h	0,3836		0,3803			0.0657		0.0678	
mw	0,3855		0,3844			0.0644		0.0672	
m dh	0,3521		0,3514			0.0584		0.0591	
m d	0,3573		0,3548			0.0569		0.0578	
m h	0,3548		0,3512			0.0582		0.0587	
m	0,3568		0,3561			0.0574		0.0575	
wdh	0.213		0.2128			0.0584		0.0595	
wd	0.2189		0.214			0.0581		0.0576	
w h	0.2012		0.198			0.0578		0.0589	
w	0.2045		0.2038			0.058		0.0578	
dh	0.0657		0.0681			0.0571		0.0585	
d	0.0655		0.0633			0.0563		0.0573	
h	0.0619		0.0662			0.0566		0.0577	

Table B.3: The p-values per hourly average wind speed model, using MLE and Euler OLS.

Appendix C

COS-method for Weibull

As was said in 5, the Weibull distribution can be approximated using the COS-method by means of the characteristic function of the Weibull distribution and the characteristic function of the log-Weibull distribution. Using the log-Weibull distribution is more accurate and more stable, but it is possible to use the characteristic function of the Weibull distribution. In this appendix we will show how the derivations are done and what the results are in terms approximation of the distribution and of the prices of several options with underlying being Weibull distributed at maturity.

C.1 Approximation of the Weibull distribution

Again we first approximate the probability density function, to see whether the COS-method using the characteristic function of the Weibull distribution results into a good estimate. We assume this is possible for fitting parameters i.e. the proper combination of k and λ. For well chosen parameters, this function decays to 0 rapidly, as x goes to ∞. Also, $f(x)$ is an entire function (as it is a product of entire functions), we expect exponential convergence of the cosine expansion of $f(x)$. Therefore we expect accurate approximations. The main difference in methodology compared to Section 5.2.4 is that we have a different characteristic function, and we will not make a transform to the log-domain. The derivation of the characteristic function is a nontrivial one, and for now I will just assume that the characteristic function found by Muraleedharan [60], is the characteristic function. The derivation will look as follows:

$$\begin{aligned}
\phi(\omega) &= \int_{\mathbb{R}} e^{i\omega x} f(x) \mathrm{d}x \\
&= \int_0^{\infty} e^{i\omega x} \frac{k}{\lambda} (\frac{x}{\lambda})^{k-1} e^{-(\frac{x}{\lambda})^k} \mathrm{d}x \\
&\vdots \\
&= \sum_{n=0}^{\infty} \frac{(i\omega)^n \lambda^n}{n!} \Gamma(1 + \frac{n}{k}). \\
&= 1 + \sum_{n=0}^{\infty} \left(i \cdot \frac{j\pi}{b-a} \lambda \right)^{n+1} \frac{1}{n!k} \Gamma(\frac{n+1}{k})
\end{aligned}$$

This sum will tend to infinite as n tends to infinity, however $\phi(\omega)$ appears convergent at first.

This can best be seen when plotting the values for F_j where F_j is written as:

$$F_j \quad = \quad \frac{2}{b-a}\text{Re}\left\{\phi\left(\frac{j\pi}{b-a}\right)\exp\left(-i\frac{ja\pi}{b-a}\right)\right\}.$$

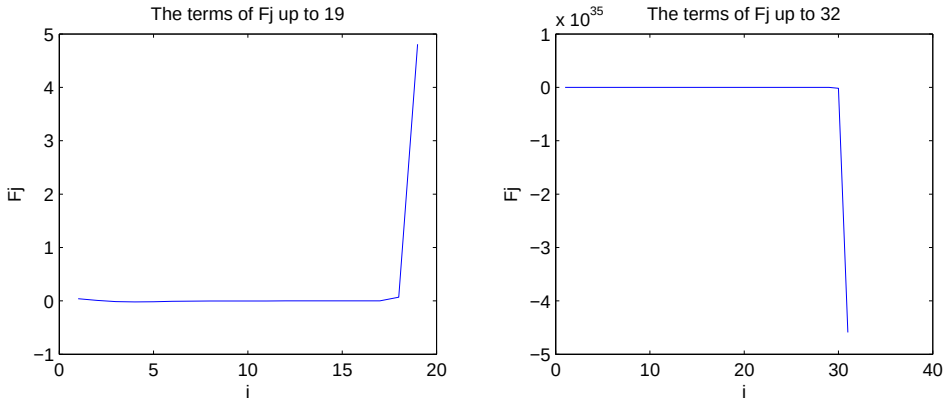

Figure C.1: Exploding behavior of F_j in negative or positive direction as j attains larger values.

Figure C.1 shows on the left side the behavior of F_j up to $j = 19$, on the right side j runs until 32. It displays the explosion of the terms of F_j, but it also shows some near to zero terms before exploding. This implies that truncating the characteristic function could still give good estimates when using the COS-method. We truncate as follows:

$$\phi(\omega) \quad \approx \quad 1 + \sum_{n=0}^{m}\left(i\cdot\frac{j\pi}{b-a}\lambda\right)^{n+1}\frac{1}{n!k}\Gamma(\frac{n+1}{k}),$$

where the value of m depends on λ and k and can be computed in MATLAB. Similar steps as were done in Section 5.2.4 and in [54], will yield an approximation of the probability density function written as:

$$f_2(x) = \sum_{j=0}^{N-1}{}'F_j\cdot\cos\left(j\pi\frac{x-a}{b-a}\right). \tag{C.1}$$

We see in the case study, that the errors coming in with this truncations, are rather small as the values of our approximation are close to the 'true' values of $f(x)$. This implies that even if a characteristic function is not stable, by using truncation still satisfiable estimates can be attained.

C.2 European options

Also, options with a Weibull distributed underlying can be priced using the COS-method with the characteristic function of the Weibull distribution. The steps taken are very similar to those in Section 5.2.4, but we do not make a transfer to the log domain. We again focus on European options (these options can only be exercised at maturity). Going through similar steps as in Section 5.2.4, we find the approximation $v_3(t_0, x)$:

$$
\begin{aligned}
v_3(t_0,x) &= e^{-r\Delta t}\sum_{k=0}^{N-1}{}'F_k(x)V_k \qquad \text{with } F_k = \mathrm{Re}\left\{\phi\left(\frac{k\pi}{b-a};x\right)\exp\left(-i\frac{k\pi a}{b-a}\right)\right\} \\
&= e^{-r\Delta t}\frac{2}{b-a}\sum_{k=0}^{N-1}{}'\mathrm{Re}\left\{\phi\left(\frac{k\pi}{b-a};x\right)\exp\left(-i\frac{k\pi a}{b-a}\right)\right\}V_k
\end{aligned}
$$

C.2.1 Expressions for V_k for plain vanilla options

The expressions for V_k will change slightly in comparison to Section 5.2.4, since we are not transferring to the log-domain. For plain vanilla options, with underlying y and strike price K we know that we have the following payoffs:

$$
\begin{aligned}
V_k^{\text{Call}} &= \int_a^b V(T,y)\cos\left(\frac{y-a}{b-a}k\pi\right)dy \\
&= \int_a^b (\alpha(y-K))^+\cos\left(\frac{y-a}{b-a}k\pi\right)dy \\
&= \chi(K,b) - K\psi(K,b),
\end{aligned}
$$

where $\chi(c,d)$ and $\psi(c,d)$ are also slightly different. Derivations of the new integrals are done below in (C.2) and (C.3). The derivation of V_k^{Put} be similar to the derivation above, and results in:

$$
V_k^{\text{Put}} = -\chi(a,K) + K\psi(a,K).
$$

To evaluate these integrals $\chi(c,d)$ and $\psi(c,d)$, we use integration by parts. Full derivation can be found in C.5.

$$
\begin{aligned}
\chi(K,b) &= \int_K^b y\cos\left(\frac{y-a}{b-a}k\pi\right)dy \\
&\quad -\frac{K}{\frac{k\pi}{b-a}}\sin\left(\frac{K-a}{b-a}k\pi\right) - \frac{1}{\frac{k\pi}{b-a}^2}\cos\left(\frac{K-a}{b-a}k\pi\right)
\end{aligned} \tag{C.2}
$$

However, when $k=0$, then the integral is even easier:

$$
\int_c^d y dy = \frac{1}{2}(c^2-d^2)
$$

For the second part we find the following if $k \neq 0$:

$$
\begin{aligned}
\psi(K,b) &= \int_K^b \cos\left(\frac{y-a}{b-a}k\pi\right)dy \\
&= \frac{1}{\frac{y-a}{b-a}}\sin\left(\frac{y-a}{b-a}k\pi\right)\Big|_K^d \\
&= \frac{b-a}{k\pi}\left(\sin\left(\frac{d-a}{b-a}k\pi\right) - \sin\left(\frac{c-a}{b-a}k\pi\right)\right)
\end{aligned} \tag{C.3}
$$

However, if $k = 0$, then we find

$$\begin{aligned} \psi(K, b) &= \int_K^b dy \\ &= b - K \end{aligned}$$

C.3 Case study; Weibull(2.25,9)

In this section we shortly review the results for one case study. To estimate scale parameter (k) and shape parameters (λ), we fit the Weibull distribution on the data set of wind speeds of the K13 wind site, in the North sea using MLE in MATLAB. Here, k is equal to 2.25, and λ equals 9. In short, this would be the Weibull(2.25,9) distribution. First, we approximate several points of the Weibull distribution. The results of this approximation are compared to the values of the Weibull distribution, as computed from MATLAB. Next we approximate the values of some plain vanilla options. These results are compared to the results of the Monte Carlo method, and a numerical method (Trapezoidal rule). We will look at the values for the options, as well as at the time it took to reach to the answer.

C.3.1 Weibull distribution

We will approximate $f(x)$ at 11 points, i.e. 0 up to 20 with step size 2. We will look at the absolute value of the maximum error between the density function and the COS-method approximation. E.g. (error $= |f(x) - f_2(x)|$). We use two MATLAB function files to determine a, b and m, using a fixed N. We find the results as displayed in Table C.1.

N	4	8	16
error	0.064644	0.0161	0.0061
cpu time (sec.)	0.0003	0.0006	0.0012

Table C.1: Maximum error when recovering $f(x)$ from $\phi(x)$ by Fourier-cosine expansion.

We see that for $N = 16$ the value comes close at what we're looking for. However, if N increases above 16, the characteristic function will become unstable, and the error will grow extremely large.

C.3.2 Options

Computing the European option prices with the COS-method, is similar to computing the values of the Weibull distribution. This time, a payoff function is included, as was shown above. As an example, we took $N = 2^6$, and let a, b and m be computed by MATLAB. Furthermore, we took strike prices $K = [1, 6, 11, 16, 21]$
If we look at the errors, per N, the amount of terms of the series, and take one strike price $K = 6$, we compute the following table of absolute and relative errors:
We conclude that we obtain satisfiable values with the COS-method for Weibull(2.25,9). However, using the characteristic function of the log-Weibull distribution is this case is preferable. However, if for a distribution both the characteristic function of the distribution, and the log-distribution are unstable it can be considered to use truncation of one of the characteristic functions.

	K	1	6	11	16	21	26
Call	MC	6.8357	2.5814	0.5061	0.0444	0.0015	0
	Num	6.8357	2.5806	0.5065	0.0441	0.0015	0
	COS	6.836	2.5811	0.5068	0.0444	0.0017	0.0001
Put	MC	0.0021	0.6484	3.4761	7.9143	12.7722	17.6717
	Num	0.0021	0.6481	3.4749	7.9136	12.772	17.6715
	COS	0.0037	0.6499	3.4766	7.9151	12.7734	17.6728

Table C.2: Prices of options as calculated with different techniques with different strike prices.

	N	4	8	16	32
Abs	Call	0.1073	0.2246	0.0019	0.0005
	Put	0.5881	0.4514	0.0149	0.0018
Rel	Call	0.0416	0.0870	0.0008	0.0002
	Put	0.9075	0.6966	0.0229	0.0027

Table C.3: Absolute and relative errors of the COS-method for an option with strike 6 and underlying Weibull distributed

C.4 Characteristic function of log-Weibull distribution

In Section 5.2.4, we use the characteristic function of the log-Weibull distribution. By definition the characteristic function of the log-Weibull distribution is:

$$\begin{aligned}\phi_Y(\omega) &= \mathbb{E}\left[e^{i\omega\log(x)}\right] \\ &= \int_0^\infty e^{i\omega\log(x)}\frac{k}{\lambda}\left(\frac{x}{\lambda}\right)^{k-1}e^{-\left(\frac{x}{\lambda}\right)^k}\mathrm{d}x.\end{aligned}$$

Using the transformations

$$y = \left(\frac{x}{\lambda}\right)^k \Leftrightarrow \mathrm{d}y = k\frac{x^{k-1}}{\lambda^k}\mathrm{d}x,$$

we then find:

$$\begin{aligned}\phi_Y(\omega) &= \int_0^\infty e^{i\omega(\frac{1}{k}\log(y)+\log(\lambda))}e^{-y}\mathrm{d}y \\ &= \int_0^\infty e^{i\omega(\frac{1}{k}\log(y)+\log(\lambda))}e^{-y}\mathrm{d}y \\ &= \lambda^{i\omega}\int_0^\infty y^{\frac{i\omega}{k}}e^{-y}\mathrm{d}y \\ &= \lambda^{i\omega}\Gamma\left(1+\frac{i\omega}{k}\right).\end{aligned}$$

Where the last equality holds per definition of the Gamma function.

C.5 Integration by parts for characteristic function of the Weibull distribution

Using integration by parts, we find for the first part that

$$\begin{aligned}\int_c^d y\cos(ay)dy &= y\frac{1}{a}\sin(ay)\Big|_c^d - \int_c^d \frac{1}{a}\sin(ay)dy \\ &= y\frac{1}{a}\sin(ay)\Big|_c^d - \frac{1}{a^2}\int_c^d \cos(ay)dy \\ &= \frac{d}{a}\sin(ad) + \frac{1}{a^2}\cos(ad) - \frac{c}{a}\sin(ac) - \frac{1}{a^2}\cos(ac)\end{aligned}$$

The second part is a lot easier

$$\begin{aligned}\int_c^d K\cos(ay)dy &= K\int_c^d \cos(ay)dy \\ &= \frac{K}{a}\sin(ay)\Big|_c^d \\ &= \frac{K}{a}(\sin(ac) - \sin(ad))\end{aligned}$$

C.6 Closed-form solution Weibull options

C.6.1 Closed-form solution for European options

The derivations for the closed-form solutions to European options with Weibull underlying are easily calculated. We define T to be the time to maturity, r the risk-free interest rate, x is the wind speed at t_0 and y is the wind speed at maturity, K the reference wind speed, furthermore we consider a Weibull distribution with parameters k and λ. For a call, with strike K, we find:

$$\begin{aligned}v^C(t_0,x) &= e^{-rT}\int_{-\infty}^{\infty}(S-K)^+\frac{k}{\lambda}\left(\frac{y}{\lambda}\right)^{k-1}\exp\left(-\left(\frac{y}{\lambda}\right)^k\right)\mathrm{d}y \\ &= e^{-rT}\int_{\left(\frac{K}{\lambda}\right)^k}^{\infty}(\lambda z^{\frac{1}{k}} - K)\exp(-z)\,\mathrm{d}z.\end{aligned}$$

By substitution of $\left(\frac{y}{\lambda}\right)^k = z$.

$$\begin{aligned}v^C(t_0,x) &= e^{-rT}\int_{\left(\frac{K}{\lambda}\right)^k}^{\infty}(\lambda z^{\frac{1}{k}} - K)\exp(-z)\,\mathrm{d}z \\ &= e^{-rT}\lambda\int_{\left(\frac{K}{\lambda}\right)^k}^{\infty} z^{\frac{1}{k}}\exp(-z)\,\mathrm{d}z - e^{-rT}K\int_{\left(\frac{K}{\lambda}\right)^k}^{\infty}\exp(-z)\,\mathrm{d}z \\ &= e^{-rT}\lambda\Gamma\left(1+\frac{1}{k},\left(\frac{K}{\lambda}\right)^k\right) - e^{-rT}K\exp(-\left(\frac{K}{\lambda}\right)^k),\end{aligned}$$

where $\Gamma(a, b)$ is the incomplete Gamma function, from b to infinite. Similar derivations yield the following expression for the Weibull put option:

$$\begin{aligned} v^P(t_0, x) &= e^{-rT}\left[K\int_0^{\left(\frac{K}{\lambda}\right)^k} \exp(-z)\mathrm{d}z - \lambda\int_0^{\left(\frac{K}{\lambda}\right)^k} z^{\frac{1}{k}}\exp(-z)\mathrm{d}z\right] \\ &= e^{-rT}\left[K\left(1-\exp\left(-\left(\frac{K}{\lambda}\right)^k\right)\right) - \lambda\gamma\left(1+\frac{1}{k}, \left(\frac{K}{\lambda}\right)^k\right),\right] \end{aligned}$$

where $\gamma(a, b)$ is the incomplete Gamma function from 0 to b.

C.6.2 Closed-form solution for cash-or-nothing options

The derivations of closed-form solutions to cash-or-nothing options having Weibull distributed underlying are similar to the derivations that were done to compute the values of European options. We define T to be the time to maturity, r the risk-free interest rate, x is the wind speed at t_0 and y is the wind speed at maturity, K the reference wind speed, B the possible payoff and furthermore we consider a Weibull distribution with parameters k and λ. The price of a call and a put cash-or-nothing option are defined as:

$$\begin{aligned} v^{conc}(t_0, x) &= e^{-rT}B\int_{\left(\frac{K}{\lambda}\right)^k}^{\infty} \exp(-z)\,\mathrm{d}z \\ &= e^{-rT}B\exp\left(-\left(\frac{K}{\lambda}\right)^k\right) \quad \text{and} \\ v^{conp}(t_0, x) &= e^{-rT}B\int_0^{\left(\frac{K}{\lambda}\right)^k} \exp(-z)\,\mathrm{d}z \\ &= e^{-rT}B\left(1-\exp\left(-\left(\frac{K}{\lambda}\right)^k\right)\right) \end{aligned}$$

Bibliography

[1] Michael Hanley. Hedging the force of nature. *Risk Professional*, 1:21–25, 1999.

[2] D. Kurowicka & A. Hanea. Risk analysis lecture slides. As from BlackBoard, 2013.

[3] Antonis K Alexandridis and Achilleas D Zapranis. *Weather Derivatives: Modeling and Pricing Weather-Related Risk*. Springer, 2013.

[4] Yuji Yamada. Simultaneous optimization for wind derivatives based on prediction errors. In *American Control Conference, 2008*, pages 350–355. IEEE, 2008.

[5] Antoine Leroy. Design and valuation of wind derivatives. *White Papers, Solvay Business School*, 2004.

[6] A. Smits & J. Ettema J.W. Verkaik. Wind climate assessment of the netherlands 2003. Technical report, Royal Netherlands Meteorological Institute (KNMI), 2003.

[7] Jon Wiernga. Representative roughness parameters for homogeneous terrain. *Boundary-Layer Meteorology*, 63(4):323–363, 1993.

[8] W. Bierbooms. Offshore wind climate lecture slides. As from TU Delft website, 2012.

[9] Gertie Geertsema. Personal conversation.

[10] Robert Vautard, Julien Cattiaux, Pascal Yiou, Jean-Noël Thépaut, and Philippe Ciais. Northern hemisphere atmospheric stilling partly attributed to an increase in surface roughness. *Nature Geoscience*, 3(11):756–761, 2010.

[11] Alexander MR Bakker and Bart JJM van den Hurk. Estimation of persistence and trends in geostrophic wind speed for the assessment of wind energy yields in northwest europe. *Climate dynamics*, 39(3-4):767–782, 2012.

[12] Mukund R Patel. *Wind and solar power systems: design, analysis, and operation*. CRC press, 2005.

[13] Gary L Johnson. *Wind energy systems*. Prentice-Hall Englewood Cliffs (NJ), 1985.

[14] Tony Burton, Nick Jenkins, David Sharpe, and Ervin Bossanyi. *Wind energy handbook*. John Wiley & Sons, 2011.

[15] A. Betz. Das maximum der theoretisch mglichen ausnutzung des windes durch windmotoren. *Zeitschrift fr das gesamte Turbinenwesen*, 20, 1920.

[16] Frank R Eldridge. Wind machines. Technical report, Mitre Corp., McLean, Va.(USA), 1975.

[17] D. Scanlin & B. Summerville. Final report, task j: Western north carolina renewable energy initiative. Technical report, Appalachian State University, 2007.

[18] Jens Boening. Phone call.

[19] Fred Espen Benth and Jūrate Šaltytė Benth. *Modeling and Pricing in Financial Markets for Weather Derivatives*, volume 17. World Scientific Publishing Company, 2012.

[20] D Watkins. Us futures exchange to list wind derivatives - risk.net. `http://www.risk.net/risk-magazine/feature/1518097/us-futures-exchange-list-wind-derivatives`. Accessed January 11th, 2013.

[21] Volume 27 bulletin #032 usfe nordix financial wind index contracts. `http://www.clearingcorp.com/bulletins/2007/bulletins/b27-032.html`. Accessed December 21th, 2012.

[22] Charles Piszczor. Phone call.

[23] Annual market update 2011. Technical report, GWEC, 2011.

[24] B. Oduntan, R. & Schauble. Using customized weather derivatives to hedge earnings volatility in energy markets. As presented at the Second Conference on Weather, Climate and the New Energy Economy.

[25] Jerry de Leeuw. Several personal conversations.

[26] John Polasek. Personal conversation at a conference.

[27] Desmond Higham. *An introduction to financial option valuation: mathematics, stochastics and computation*, volume 13. Cambridge University Press, 2004.

[28] N. Molloy. Who should pay for wind power risk? `http://www.risk.net/energy-risk/feature/2106756/pay-wind-power`. Accessed February 2nd, 2013.

[29] J.P. Coelingh. Wind and power derivatives in project financing. As presented at EWEC Milano, 2007.

[30] Hélyette Geman. Insurance and weather derivatives: from exotic options to exotic underlyings. 1999.

[31] Anders Brix, Stephen Jewson, and Christine Ziehmann. Weather derivative modelling and valuation: a statistical perspective. *Climate Risk and the Weather Market. Risk Books, London*, pages 127–150, 2002.

[32] Lalarukh Kamal and Yasmin Zahra Jafri. Time series models to simulate and forecast hourly averaged wind speed in quetta, pakistan. *Solar Energy*, 61(1):23–32, 1997.

[33] Jose Luis Torres, Almudena Garcia, Marian De Blas, and Adolfo De Francisco. Forecast of hourly average wind speed with arma models in navarre (spain). *Solar Energy*, 79(1):65–77, 2005.

[34] Rafael Zárate-Miñano, Marian Anghel, and Federico Milano. Continuous wind speed models based on stochastic differential equations. *Applied Energy*, 104:42–49, 2013.

[35] Julio J Lucia and Eduardo S Schwartz. Electricity prices and power derivatives: Evidence from the nordic power exchange. *Review of Derivatives Research*, 5(1):5–50, 2002.

[36] Frank J Massey Jr. The kolmogorov-smirnov test for goodness of fit. *Journal of the American statistical Association*, 46(253):68–78, 1951.

[37] Ross B Corotis, Arden B Sigl, and Joel Klein. Probability models of wind velocity magnitude and persistence. *Solar Energy*, 20(6):483–493, 1978.

[38] Jay Devore. *Probability & Statistics for Engineering and the Sciences*. CengageBrain. com, 2012.

[39] FM Dekking C Kraaikamp and HP Lopuhaä LE Meester. A modern introduction to probability and statistics, 2005.

[40] Arno Brand. Various personal conversations.

[41] George E Uhlenbeck and Leonard Salomon Ornstein. On the theory of the brownian motion. *Physical review*, 36(5):823, 1930.

[42] Dorje C Brody, Joanna Syroka, and Mihail Zervos. Dynamical pricing of weather derivatives. *Quantitative Finance*, 2(3):189–198, 2002.

[43] Rüdiger Seydel. *Tools for computational finance*. Springer, 2012.

[44] Carlos M Jarque and Anil K Bera. A test for normality of observations and regression residuals. *International Statistical Review/Revue Internationale de Statistique*, pages 163–172, 1987.

[45] Cornelis Vuik, P Van Beek, F Vermolen, and J Van Kan. *Numerical Methods for Ordinary differential equations*. VSSD, 2007.

[46] Mingxin Xu. Risk measure pricing and hedging in incomplete markets. *Annals of Finance*, 2(1):51–71, 2006.

[47] Fred Espen Benth. On arbitrage-free pricing of weather derivatives based on fractional brownian motion. *Applied Mathematical Finance*, 10(4):303–324, 2003.

[48] Fred Espen Benth and Jūratė šaltytė Benth. The volatility of temperature and pricing of weather derivatives. *Quantitative Finance*, 7(5):553–561, 2007.

[49] Hélène Hamisultane. Which method for pricing weather derivatives? 2008.

[50] Steven E Shreve. *Stochastic calculus for finance II, Continuous Time Models*, volume 2. Springer New York, 2003.

[51] B Zhang and CW Oosterlee. Efficient pricing of asian options under lévy processes based on fourier cosine expansions part i: European-style products. 2011.

[52] Robert Savickas. A simple option-pricing formula. *Financial Review*, 37(2):207–226, 2002.

[53] Robert Alexander Adams and Christopher Essex. *Calculus: a complete course*, volume 6. Addison-Wesley Don Mills, Ontario, 2006.

[54] Fukang Fang and Cornelis Willebrordus Oosterlee. *On an option pricing method based on Fourier-Cosine series expansions*. Delft University of Technology, 2008.

[55] B Zhang LA Grzelak CW Oosterlee. Efficient pricing of commodity options with early-exercise under the ornstein–uhlenbeck process. 2011.

[56] Ken-iti Sato. *Lévy processes and infinitely divisible distributions*. Cambridge university press, 1999.

[57] Fred W Steutel and Klaas Van Harn. *Infinite divisibility of probability distributions on the real line*. CRC Press, 2003.

[58] Christiaan Heij, Paul De Boer, Philip Hans Franses, Teun Kloek, Herman K Van Dijk, et al. *Econometric methods with applications in business and economics*. Oxford University Press, 2004.

[59] Jun Yu. Bias in the estimation of the mean reversion parameter in continuous time models. *Journal of Econometrics*, 169(1):114–122, 2012.

[60] G Muraleedharan, N Unnikrishnan Nair, and PG Kurup. Application of weibull model for redefined significant wave height distributions. *Proceedings of the Indian Academy of Sciences-Earth and Planetary Sciences*, 108(3):149–153, 1999.